ACQUISITION SCHEMES FOR BURST MODE DIRECT SEQUENCE SPREAD SPECTRUM PACKET RADIO

by

Desmond Wai Ming Yan

B.A.Sc. Simon Fraser University, 1992

A THESIS SUBMITTED IN PARTIAL FULFILLMENT
OF THE REQUIREMENTS FOR THE DEGREE OF
MASTER OF APPLIED SCIENCE
in the School
of
Engineering Science

SIMON FRASER UNIVERSITY
September 1994

APPROVAL

Name: Desmond Wai Ming Yan

Degree: Master of Applied Science

Title of thesis : Acquisition Schemes for Burst Mode Direct Sequence Spread Spectrum Packet Radio

Dr. J. Cavers
Direrctor, School of Engineering Science, SFU

Examining Committee:

Dr. P. Ho
Associate Professor, Engineering Science, SFU
Senior Supervisor

Dr. J. Cavers
Professor, Engineering Science, SFU
Internal Supervisor

Dr. J. Vaisey
Assistant Professor, Engineering Science, SFU
Examiner

Date Approved: September 21, 1994

PARTIAL COPYRIGHT LICENSE

I hereby grant to Simon Fraser University the right to lend my thesis, project or extended essay (the title of which is shown below) to users of the Simon Fraser University Library, and to make partial or single copies only for such users or in response to a request from the library of any other university, or other educational institution, on its own behalf or for one of its users. I further agree that permission for multiple copying of this work for scholarly purposes may be granted by me or the Dean of Graduate Studies. It is understood that copying or publication of this work for financial gain shall not be allowed without my written permission.

Title of Thesis/Project/Extended Essay

"Acquisition Schemes for Burst Mode Direct Sequence Spread Spectrum Packet Radio"

Author:

(signature)

Desmond YAN
(name)

August 24, 1994
(date)

Abstract

Code Division Multiple Access (CDMA) is a promising technology for future digital cellular and personal communications. Some of the nice features in CDMA include (1) anti-multipath, (2) higher system capacity than TDMA and FDMA, and (3) its flexibility in providing bandwidth on demand. To despread the pseudo noise (PN) code and thus understand the message sent, PN code synchronization is necessary a priori. As a matter of fact, the throughput of a packet mode CDMA system is directly related to the performance of its synchronization algorithm. PN code synchronization is usually performed in two stages: *acquisition* and *tracking*. The former aims to find a coarse alignment between the incoming signal and the local PN code replica, while the latter fine adjusts the phase. In this thesis, we will consider the PN code acquisition problem. Particularly, we propose two new acquisition algorithms: the *On-Off Keying Assisted Acquisition Scheme* and the *Differentially Encoded Barker Sequence Acquisition Scheme*. The preamble in the first method follows an on-off pattern and the algorithm performs a Markov search. The second method, on the other hand, uses DPSK to encode a Barker sequence as the preamble. The algorithm looks for the Barker sequence to declare acquisition. We have also introduced a windowing technique in both methods which we found effective in overcoming the partial correlation effect. The two proposed schemes are compared with some existing ones in the literature like the coincidence detector or simple Markov search, and we find that our algorithms outperform the others both under AWGN and frequency selective fading channels.

Acknowledgements

I would like to thank my supervisor, Dr. Paul Ho, for his guidance throughout my study, and also Dr. J. Cavers for his invaluable ideas. Besides, I would like to thank Dr. J. Vaisey who have spent his precious time in reading and revising my thesis. Last, I would like to thank Dr. J. Mark for his generosity and kindness during my stay at the University of Waterloo. Many thanks is also directed to the National Science and Engineering Research Council of Canada and Canadian Institute for Telecommunications Research for their financial support.

Contents

List of Tables

List of Figures

List of Abbreviations

ACQ	Acquire state
AWGN	Additive White Gaussian Noise
BPSK	Binary Phase Shift Keying
CDMA	Code Division Multiple Access
CFAR	Constant False Alarm Rate
CSMA	Carrier Sense Multiple Access
DPSK	Differentially coherent Phase Shift Keying
DS	Direct Sequence
FA	False Alarm
FDMA	Frequency Division Multiple Access
FH	Frequency Hopping
NRZ	Non-Return to Zero
PN	Pseudorandom Noise
PSK	Phase Shift Keying
RARASE	Recursion-Aided Rapid Acquisition Sequential Estimation
RPCR	Relative Power Control Rate
SPRT	Sequential Probability Ratio Test
SWI	Syn-Worthiness Indicator
TDMA	Time Division Multiple Access

Chapter 1

Introduction

During the past two decades, the amount of mobile communication has increased significantly, which poses a challenging problem to the telecommunications industry because of the tremendous bandwidth required. Various characteristics of spread spectrum communication such as processing gain or lower data rate during silent periods have demonstrated its increased capacity compared to (Frequency Division Multiple Access) FDMA or (Time Division Multiple Access) TDMA used respectively for the first and the second generation mobile cellular. Spread spectrum communication is therefore considered as a potential candidate for the underlying technique for third generation cellular radio, and field trials have already been done by company like Qualcomm [1].

In spread spectrum communication, the power spectrum of the transmitted signal is spreaded out before transmission, making it indistinguishable from additive white Gaussian noise. This attractive property makes it possible to overlay new applications on the bandwidth already assigned to others, as suggested in [10]. At the receiver side, the reverse process takes place and the original signal is recovered. Moreover, the ability of spread spectrum communications to provide frequency diversity makes it particularly suitable for a frequency selective fading channel, which is typical in

mobile communication environment.

Code Division Multiple Access (CDMA) is a modulation and multiple access scheme based on spread spectrum communication. The word "Code Division" comes from the fact that we use different spreading codes to distinguish one user from another. In this chapter, we will cover the basics in spread spectrum communication to lay a background for coming chapters.

1.1 Spread Spectrum Communications

Two types of spread-spectrum techniques are in wide use: the *direct sequence* (DS) and *frequency hop* (FH) spread spectrum. In DS system, a narrowband data signal is modulated first by a high rate pseudorandom code sequence before the carrier modulation. The pseudorandom code modulation spreads out the power spectrum of the original signal, and makes it indistinguishable from AWGN (Additive White Gaussian Noise). A frequency hop spread spectrum system, on the other hand, is accomplished by using a pseudorandom code to select different carrier frequency. The resulting carrier frequency rapidly switches over a very large number of values spread over a very wide range, on which (hopping frequency) the data is modulated. Our focus in this thesis is the direct sequence system. For readers interested in a frequency hopping configuration, they are suggested to refer to [2] for a detailed discussion.

1.1.1 Direct Sequence Spread Spectrum Systems

We will demonstrate the DS system with a square $\pm$ NRZ (Non Return to Zero) pulses. A typical configuration in spread spectrum communication is shown in figure 1.1. The only difference between this configuration and a system not employing spread spectrum is the multiplication of the PN (pseudorandom noise) code $PN(t)$ before transmission and before demodulation on the receiver side. Figure 1.2 shows an

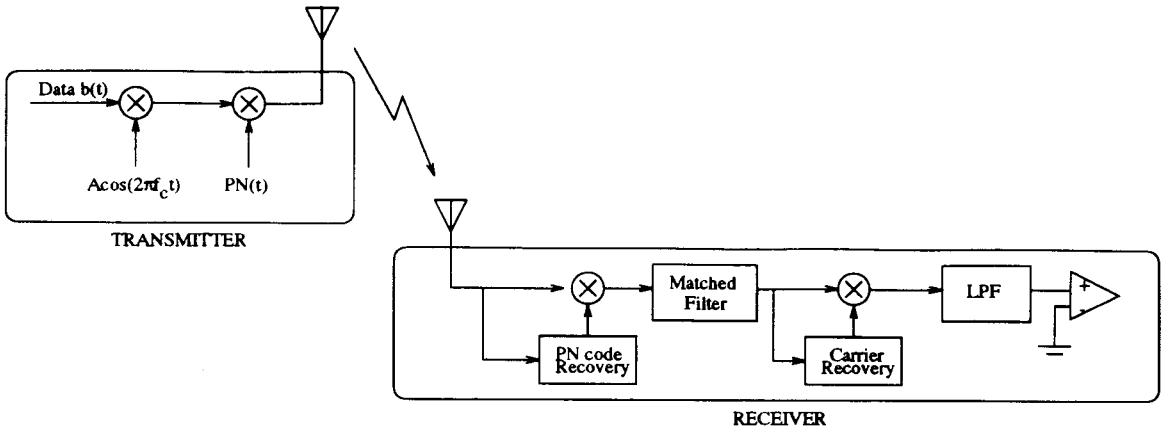

Figure 1.1: Direct Sequence Spread Spectrum Configuration.

example of a data stream $b(t)$ multiplied by a PN code which is four times faster than the data rate. Although we demonstrate a four times faster pseudorandom noise sequence in the figure, in real applications, the PN code should be orders of magnitude faster than the data rate to acquire the spreading effect. Each symbol of the PN code is called a chip, and $\frac{1}{T_c}$ is called the chip rate. Suppose we use a carrier magnitude of A and a carrier frequency of f_c, the resulting transmitted signal will be given by

$$s(t) = Ab(t)PN(t)\cos(2\pi f_c t). \tag{1.1}$$

If we multiply equation (1.1) with $PN(t)$ at the receiver, we will get

$$\begin{aligned} r(t) &= s(t) \times PN(t) \\ &= PN(t)^2 \times Ab(t)\cos(2\pi f_c t) \\ &= Ab(t)\cos(2\pi f_c t), \end{aligned} \tag{1.2}$$

since $PN(t)^2 = 1$. The multiplication of data sequence $b(t)$ with $PN(t)$ is a sequence with the same period T_c as the PN code. The resultant signal $b(t)PN(t)$ therefore has an approximate bandwidth of $\sim \frac{2}{T_c}$Hz in contrast to a value of $\sim \frac{2}{T_b}$Hz of the original data sequence $b(t)$, where T_b is a bit duration. Since T_c is orders of magnitude smaller than T_b, the resulting signal occupies a much wider bandwidth (spread spectrum). The signal bandwidth is spread out to an extend that it is hidden under the AWGN. As a result, unintended user does not ever detect its existence. Even knowing the existence of signal, decoding is still impossible without knowing the particular PN

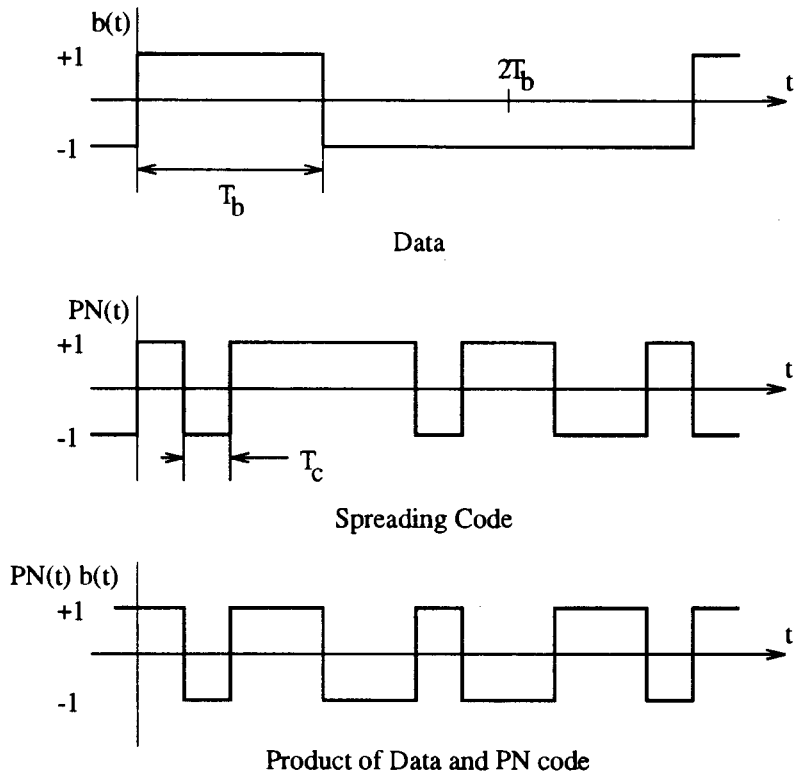

Figure 1.2: Example of PN code Spreading.

code. At the same time, the despreading process at the receiver will spread any jammer in the incoming signal. These two facts account mainly for the popularity of using spread spectrum in military applications.

1.1.2 Pseudorandom Noise Sequence

Either a DS or a FH spread spectrum system requires a pseudorandom code to spread and despread the signal at the transmitter and the receiver respectively. The sequence must have two desirable characteristics: i) they must be easy to generate, and ii) they must appear to be random in nature with good autocorrelation and cross-correlation properties. The first feature lowers the software and hardware processing power required, while a good autocorrelation is necessary in acquisition problem and good cross-correlation is important in the multiple access scheme to lower interference from other users.

To despread the PN code, we need to multiply it with a local replica which is in alignment (synchronization) with the incoming signal. In order to achieve PN code synchronization, we rely on the autocorrelation property. A perfect PN code is one with cyclic autocorrelation:

$$R(\tau) = \begin{cases} \mathcal{L} & \tau = 0, \mathcal{L}, 2\mathcal{L}, ... \\ 0 & otherwise, \end{cases} \tag{1.3}$$

where $\mathcal{L}$ is the PN sequence length. With this autocorrelation function, the correlation output of the incoming signal and the local replica will give a high value when they are in synchronization. If $R(\tau) \neq 0$ for some value $\tau \neq 0$, for example, it has a high value at $j \neq 0$, this position may cause the acquisition algorithm to treat j as the correct synchronization. Although demodulation based on the wrong index j is still possible, as shown in figure 1.3, the performance is much degraded because $R(j) < R(0)$, that is, we have a lower SNR. The cross-correlation property between one PN code and another is particularly important for the multiple access scheme, where different users use different PN code. The ideal situation occurs when the cross-correlation always has a value of 0, in which case no interference exists from other users sharing the

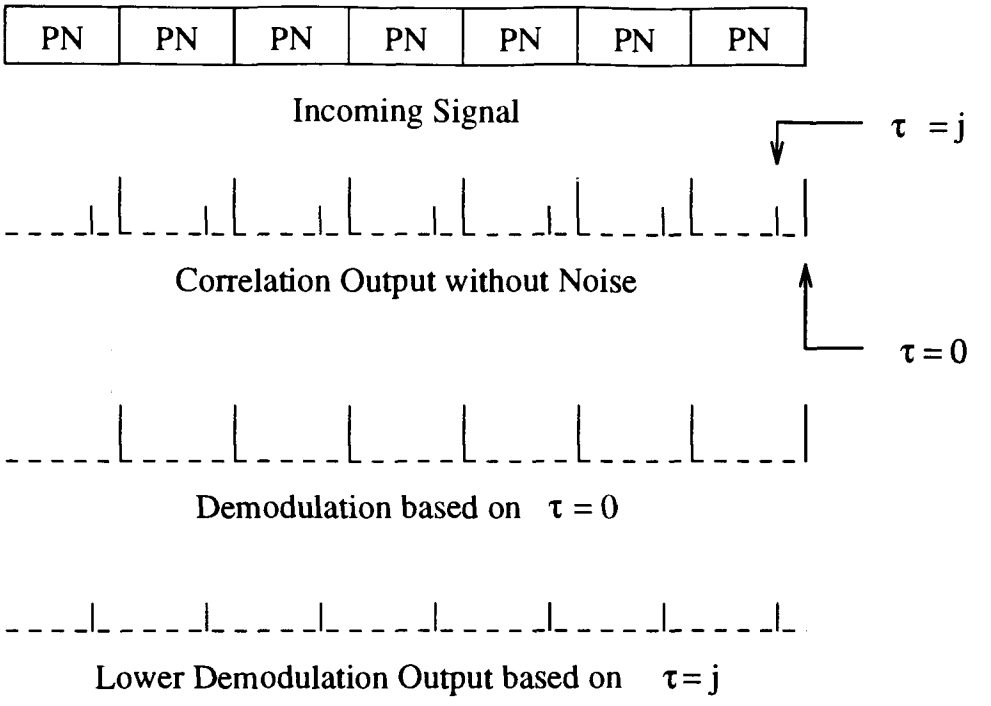

Figure 1.3: Demodulation based on Wrong Acquisition Position.

same bandwidth. The PN codes are said to be orthogonal to each other. Poor cross-correlation results in increased interference, and in the worst case, causes the receiver to treat other person's signal as its own.

One very commonly used PN code is the Maximal-length linear feedback shift register sequence (M-sequence). It is easy to generate and has good autocorrelation property. A number of other PN sequences are available [41], although they are not as common as the M-sequence. We also use M-sequence in our study and it will be covered in the following section.

M-sequence

A M-sequence is generated with a linear feedback shift register as shown in figure 1.4. The coefficients $a_0, a_1, \cdots, a_r$ are either 1 or 0. Contents in the registers are modulo-two added and fed back to the register. This configuration is general in producing so

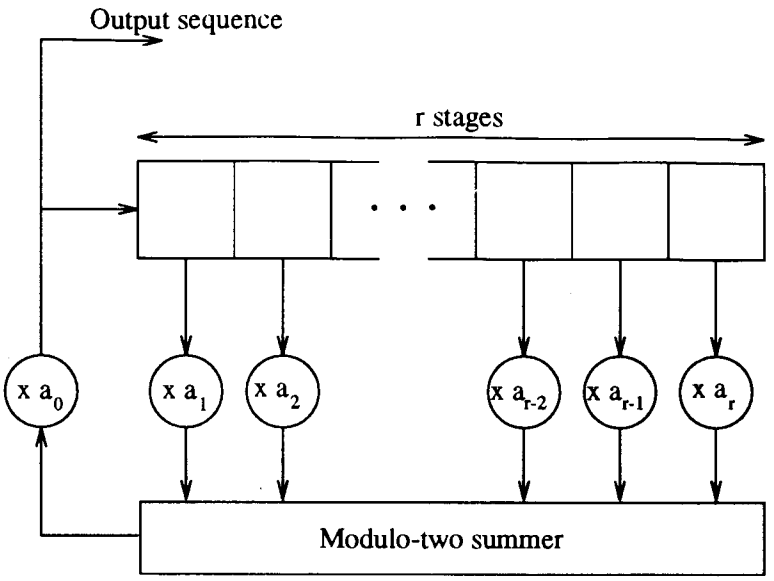

Figure 1.4: M-sequence Generation with a Linear Feedback Shift Register.

called linear feedback shift sequence. With particular selections of the tap coefficients, however, the sequence so generated will contain all possible states except for the all-zero one – an M-sequence. Table 1.1 shows examples of connection coefficients for M-sequence generation. The length of an M-sequence is $\mathcal{L} = 2^r - 1$ where r is the

Register Length	Connection coefficients in Octal notation
2	[7]
3	[13]
4	[23]
5	[45],[75],[67]
6	[103],[147],[155]
7	[203],[211],[217],[235],[367] $\cdots$
8	[435],[453],[537],[545],[551] $\cdots$

Table 1.1: Connection Coefficients for Maximal-Length Shift Register Generators.

register length. M-sequences can be shown to have the following properties [9, 37]:

1. There are 2^{r-1} ones and $2^{r-1} - 1$ zeros.

2. A run of length m chips of the same sign will occur about $\frac{l}{2^m}$ times in a sequence of l chips.

3. The M-sequence has the autocorrelation function

$$R(\tau) = \begin{cases} \mathcal{L} & \tau = 0, \mathcal{L}, 2\mathcal{L}, ... \\ -1 & otherwise. \end{cases} \tag{1.4}$$

4. The cross correlation of any two sequences $PN_i(t)$ and $PN_j(t+\tau)$ will be small.

We have to note that autocorrelation is defined on a cyclic basic, that is, it is a multiplication between a local PN code with a continuous repetition of itself, offset by τ. During acquisition, the situation is different. We are facing with an abrupt change from no signal to having a signal. The partial overlap (or partial correlation) plays an important part[1], and as stated in [41], the partial correlation sometimes poses a limit on the system's performance.

1.2 Mobile Communication Environment

To appreciate the benefits of CDMA for mobile radio applications, we will start by introducing a typical mobile communication environment.

When a base station emits a signal, the signal will go over a number of different paths before reaching the mobile station. Different paths may be due to various reflectors around the mobile station, as shown in figure 1.5. If a single pulse is sent, the received signal is a train of pulses with different delays, each of them corresponds to one path. The spread in time is called the multipath spread. Lets denote $s(t)$ as the transmitted signal,

$$s(t) = \mathrm{Re}[u(t)e^{j2\pi f_c t}], \tag{1.5}$$

[1]We will cover the topic of partial correlation in more details when we are dealing with our proposed mechanisms.

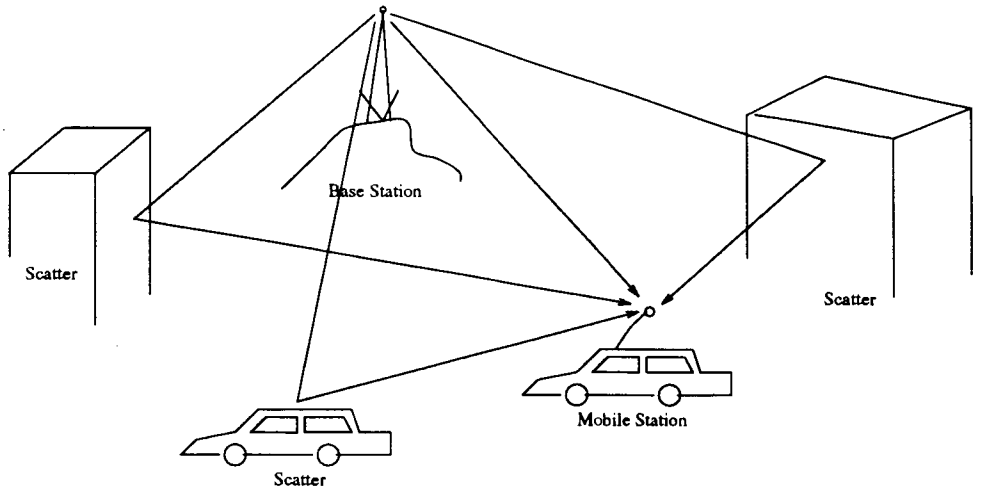

Figure 1.5: Multiple Reflections of Transmitted Signal.

where $u(t)$ is the baseband signal, and f_c is the carrier frequency. When there are multiple propagation paths, we receive the signal

$$\begin{aligned} x(t) &= \sum_i \alpha_i(t) s[t - \tau_i(t)] \\ &= \mathrm{Re}\left(\left\{ \sum_i \alpha_i(t) e^{-j2\pi f_c \tau_i(t)} u[t - \tau_i(t)] \right\} e^{j2\pi f_c t} \right). \end{aligned} \tag{1.6}$$

$\alpha_i(t)$ is the attenuation factor for signal received on ith path and τ_i is the corresponding propagation delay. We can see from equation 1.6 that the equivalent lowpass received signal is

$$r(t) = \sum_i \alpha_i(t) e^{-j2\pi f_c \tau_i(t)} u[t - \tau_i(t)]. \tag{1.7}$$

Consider the transmission of an unmodulated carrier, that is $u(t) = 1$, the received signal becomes

$$r(t) = \sum_i \alpha_i(t) e^{-j2\pi f_c \tau_i(t)}. \tag{1.8}$$

Although very wide range of $\alpha_i(t)$ is required to cause significant changes in the in received signal, a change in $\tau_i(t)$ by $\frac{1}{f_c}$ will result in a phase change of 2π. Various vectors may add destructively to cause a deep fade, or constructively to make $r(t)$ large. When there are a large number of paths, the Central Limit Theorem can be applied and $r(t)$ becomes a complex-valued Gaussian random process in the t variable.

It was found that a minimum of 6 paths is enough for getting a complex-valued Gaussian random process [2]. When the impulse response of the channel is modeled as a complex-Gaussian random variable, the envelope will be Rayleigh distributed – a Rayleigh fading channel.

One very important parameter in a fading channel is the *coherence bandwidth* (Δf_c), which is defined as the minimum frequency separation between two frequency components that will be subject to the same fading effect. Depending on the bandwidth of the signal used, we can distinguish two situations:

Flat Fading When the transmitted signal bandwidth W is smaller than Δf_c, for example in a narrowband system, each component is subject to the same fading effect, and the channel impulse response can be expressed as

$$I(t) = \alpha(t)e^{-j\phi(t)}, \tag{1.9}$$

where $\alpha(t)$ is the envelope with $\phi(t)$ being the phase. The envelope $\alpha(t)$ is Rayleigh-distributed for any fixed value of t and $\phi(t)$ is uniformly distributed over the interval $(-\pi, \pi)$.

Frequency Selective Fading If W is greater than Δf_c, different components are subject to different fading effects and it is possible to isolate the different components. The channel impulse response can be modeled as a tapped-delay line [2] as shown in figure 1.6. Each $c_i(t)$ is a zero mean complex-valued stationary Gaussian random process. The length of the tap delay line L_s equals $T_s W + 1$, where T_s is the multipath spread. The channel impulse response is

$$I(t) = \sum_{n=1}^{L_s} c_n(t)\delta(t - \frac{n}{W}). \tag{1.10}$$

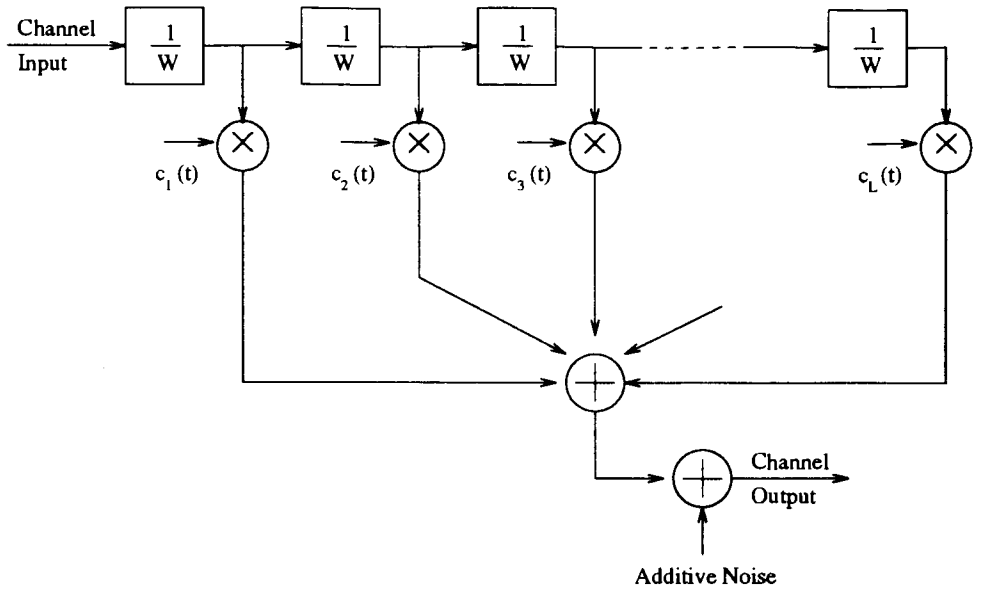

Figure 1.6: Tapped-delay Model for a Frequency Selective Channel.

1.3 Code Division Multiple Access

In order to accommodate various users in the same bandwidth, a mechanism is necessary to separate one user from another. For first generation of cellular networks where the system is analog, frequency division multiple access (FDMA) is used. The allocated bandwidth is divided into smaller trunks each of them being assigned to one user. Another possibility is the time division multiple access (TDMA) scheme like the one in the European GSM. Under TDMA, the transmission is divided into frames each consists of a number of time slots. Each user will be assigned with one time slot in the frame. For users requiring larger bandwidth, he/she can be assigned more than one slot. Thus, TDMA provides some flexibility in bandwidth allocation. A mixture of FDMA and TDMA is possible, by which we divide the allocated bandwidth into different channels and on each of them we use TDMA.

Code Division Multiple Access (CDMA) is a multiple access scheme relying on spread spectrum communication where each user transmits in the same bandwidth. Each user gets a different PN code in order to distinguish one from another. Since no coordination among different users is intended, the access scheme is asynchronous in

nature. As in TDMA, a mixture of CDMA and FDMA is possible, where the bandwidth is divided into trunks each of which is a separate CDMA system. Researchers generally refer to a system when all users share the same wide bandwidth as a wideband CDMA system, while a combination of FDMA and CDMA as a narrowband CDMA. In this section, we will explain some characteristics of CDMA which makes it a more suitable candidate than the others.

1.3.1 Soft HandOff

A cellular network relies on frequency reuse phenomena with the covered area divided into different regions called cells. A hexagonal cell structure is usually adopted, as shown in figure 1.7. We assign a frequency band A for the center cell in the figure,

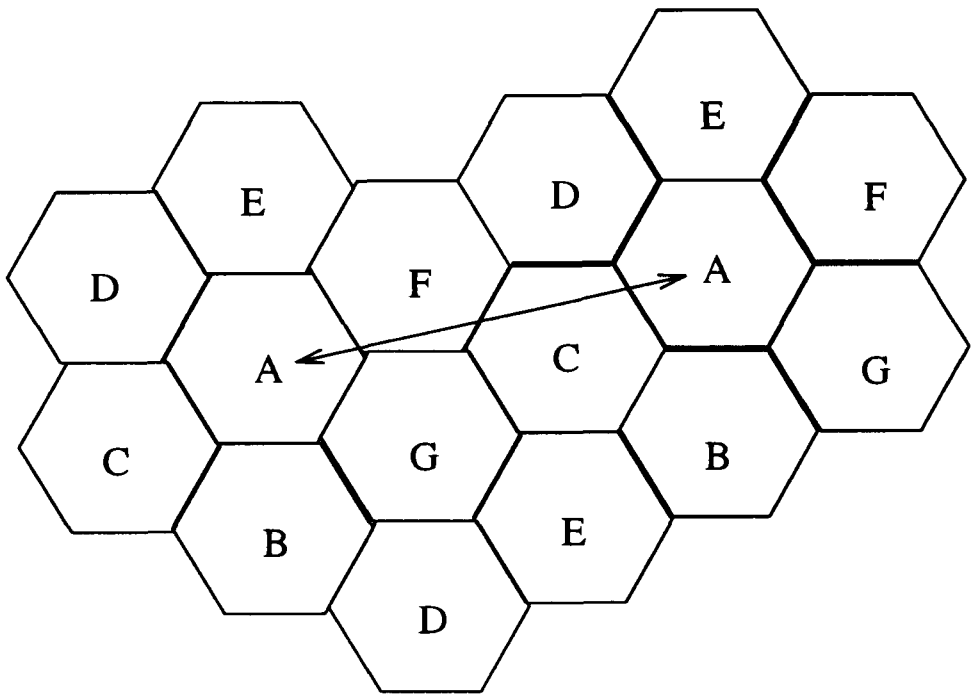

Figure 1.7: Hexagonal Cell Layout.

while those surrounding it use different bands. The same frequency band A can be reused in a cell far enough from it, so that interference between cells using the same

band is acceptable.

When a mobile comes close to the boundary between two cells, say from cell A to cell B, the mobile has to switch frequency from A to B. A practical approach in frequency switching is to switch when signal from B is lower than that from A. However, before it has actually entered cell B (transition from A to B), the signal from A may become weaker than B temporarily because of shadowing, fading, etc. When this happens, the mobile will switch to frequency B prematuredly. Some time later, the signal from A may become stronger again, causing another switching. This "Ping-Pong" effect will cause dropping of the call.

In a CDMA cellular system, the same frequency bandwidth is used in every cell. No switching of frequencies is necessary. A mobile in cell transition can receive signals from both cells at the same time until the link from new cell B is firmly established; this is called "soft handoff". The probability of dropping a call during transition is greatly reduced. This make-before-break mechanism is more reliable compared to the break-before-make scheme in FDMA or TDMA.

1.3.2 Increased Capacity compared with FDMA and TDMA

Lets denote the intended received signal power as S, and the interference as S_i. The value of S and S_i are given by $R \cdot E_b$ and $W \cdot N_0$ respectively, where R is the data rate, E_b is signal energy per bit, W is the spreaded code bandwidth, and N_0 is the interference power spectral density. The signal power to interference ratio is given by

$$\frac{S}{S_i} = \frac{R \cdot E_b}{W \cdot N_0}. \tag{1.11}$$

In a multiple access system using CDMA, the interference S_i comes from two sources: from other users, and the AWGN. S_i is therefore given by $[(N-1)S + \eta]$, with N being the total number of users in the system, and η is the background noise. Putting the expression for S_i into equation (1.11) and rearranging, we have

$$N = 1 + \frac{W/R}{E_b/N_0} - \frac{\eta}{S}. \tag{1.12}$$

The ratio E_b/N_0 is an important parameter for reliable transmission. It has been shown that with error-correcting codes and interleaving, a SNR of 7dB is sufficient [11]. W/R is generally referred as the "processing gain", and we can see from the equation that capacity increases with this parameter.

Studies have shown that normal telephone conversation consists of alternate active and silent periods, and active period occupies only 35% of time. When FDMA or TDMA is used, the channel bandwidth is still reserved and wasted during silent periods, which is not the case for CDMA. With voice activity detection circuits, we can lower the data rate (or stop the data transmission) for silent periods, which in turn will result in lower interference to other users. Due to the statistical distribution of silent periods, we can allow on average about $\frac{1}{0.35} \sim 3$ times the number of users as given in equation (1.12).

1.3.3 Soft Capacity Limit

Every cellular phone user probably has experienced getting a rejection message during rush time at noon. The number of maximum users allowed in a FDMA or a TDMA system is fixed. When the capacity limit is reached, a new-comer will be rejected. Such a limit does not exist in CDMA. The interference increases gradually with increasing number of users in the system, resulting in gradual degradation in performance. At rush hours, the interference will be higher temporarily and there will be an increased bit error rate which is acceptable for urgent users, while others may hang-up and try their calls later. Rather than being dominated by the system, the user is now in control of his access to the network. This flexibility is more favorable from the user point of view.

1.3.4 Statistical Multiplexing

The evolution of communications is so dynamic with the possibility of tremendous increase in mobile computing stations in the future which not only require telephone conversations, but also fax, file transfer or even video. The CDMA scheme is asynchronous in nature, which means that each user can transmit at any time he/she likes. Moreover, there is no restriction on the data rates they use because each user's transmission appears as noise to others, independent of transmission rate. This means that the CDMA scheme provides statistical multiplexing naturally and different types of traffic can be mixed under the same bandwidth. This CDMA feature makes engineering issues for future expansion easier.

1.3.5 Frequency Diversity

As mentioned before, in a wideband system such as CDMA, we can isolate different path components. Each of these paths will be an independent Rayleigh fading process. When several fading processes are added together, the deep fade of one will usually be compensated by the others. As a result, the fading effect is reduced and this phenomenon is called frequency diversity.

1.3.6 Privacy

With PN code multiplication, only users knowing the particular PN sequence can decode the corresponding signal. In this way, encryption is performed naturally without any additional efforts.

1.4 Acquisition Problem

We have demonstrated that in spread spectrum communications, it is essential to decode the received signal with a local PN code multiplication which is in synchronization. The problem of PN code synchronization is usually performed in two steps: *acquisition* and *tracking*. The former aims to find a coarse alignment while the latter does the actual fine adjustment.

The focus of this thesis is the acquisition part of PN code synchronization in the reverse link, that is from mobile to base station. Particularly, we will propose two new schemes for the acquisition in a packet radio environment. Through simulation studies, we find that the new methods outperform the conventional ones.

1.5 Outline of the Thesis

The organization of this thesis is as follows:

Chapter two gives more detailed information on the acquisition problem and reviews previous research results on the topic.

Chapter three presents our first proposed scheme – on-off keying assisted scheme, which superimposes an on-off pattern on the preamble. Together with a windowing technique, simulation results show that this method outperforms the conventional ones under both a flat fading and a frequency selective fading channel. In addition, an upper bound analysis for the various method will be provided.

Chapter four is materials on the other scheme based on a Barker sequence encoded preamble section using DPSK. Simulations on a frequency selective channel shows comparable performance with the on-off keying scheme. Thus, it is also superior than the conventional ones.

In chapter five, we put considerations into the effect of power control on the

acquisition algorithm. We argue that only open-loop power control is possible during the preamble section. Simulation results on a AWGN channel (perfect power control) are presented, which show that our schemes are still better than the conventional ones. Having proved the two extremes of AWGN and a frequency selective fading channel, it is possible to conclude that our schemes are better in all real situations.

Lastly, we draw our conclusions in chapter seven.

Chapter 2

Literature Overview

The acquisition problem involves searching through an uncertainty region and determines the position which corresponds to synchronization. An intrinsic element in any PN code acquisition system is a correlator which finds the correlation between the incoming signal and a local replica of the particular PN code. When the two PN codes are in synchronization (the local and the incoming one), the correlator output will become high enough to exceed a threshold which is set usually by the constant false alarm rate (CFAR) [13].

Various acquisition algorithms exist [12, 33] and they can be classified in different ways: coherent vs noncoherent, by correlator type (active integrator, SAW convolver, digital matched filter), by verification algorithm (single dwell, multiple dwell, sequential detector ...), etc. If coherent detection is used, the receiver must be capable of determining good estimates of the carrier phase and frequency shift brought by propagation delay or Doppler effect. This estimation, although not absolutely impossible, is very difficult in practice. In reality, despreading usually takes place ahead of carrier synchronization, and non-coherent acquisition is much more popular and natural.

The acquisition design bears a strong relation with the available technology. Back

to the World War II when everything was still analog, an active[1] integrator/correlator would be the only choice available. However, with the advance of technology, a digital matched filter [15] or SAW convolver [22] provides alternatives for which different verification procedures may be more appropriate. We believe that digital matched filter will become dominant in the near future because of its simplicity, decreasing price and more advanced VLSI design which makes longer matched filter possible. In this chapter, we will give an overview on previous research on the PN acquisition. We will still confirm ourselves to DS systems, although a direct analogy with the FH system exists.

2.1 Serial Search with Active Integrator

The simplest acquisition scheme is the sliding correlator as shown in figure 2.1 [20, 34]. The input signal is first multiplied with the local PN code, passed through the

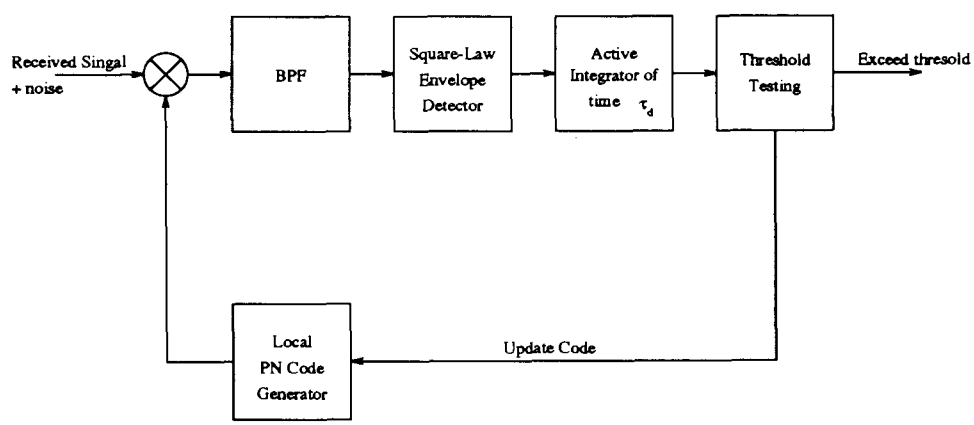

Figure 2.1: Sliding Correlator with Single Dwell Time.

bandpass filter, square law detector and then the active integrator. The correlation time τ_d of the integrator is called *dwell time*. If two signals are in synchronization,

[1]For an active integrator, the local PN code is advanced with the incoming signal during correlation/integration, which is in contrast to a passive matched filter where the local PN code is fixed.

the integrator output will become high, for which we test against a threshold. When the threshold is crossed, the corresponding PN code position will be treated as the correct acquisition. If not, the local PN code will be advanced by an amount Δ, where Δ is usually equal to half a chip[2]. This value of Δ allows the pull-in range of the tracking process following PN code acquisition, while maintaining a fast search. Each new PN code position generated is called a *cell.* Depending on the uncertainty region, the number of cells that needed to be checked varies. With no prior knowledge about the PN phase, the uncertainty region is the whole PN code, and the number of cells searched equals $\frac{\mathcal{L}}{\Delta}$, where $\mathcal{L}$ is the PN length in number of chips. The acquisition algorithm therefore involves searching through the cells in the uncertainty region to find the correct one. The threshold τ in the testing circuit is set usually by the Neyman Pearson statistics [13] to ensure a constant false alarm rate (CFAR).

Although it is stated in [12] that we can replace the threshold testing with the maximum-likelihood algorithm, it is erroneous. Conceptually, with the maximum-likelihood algorithm, the receiver correlates the incoming signal with all the possible positions of local PN code and store the results. The maximum among the generated results will be treated as the acquisition. The fallacy overlooked in [12] which will make the maximum likelihood algorithm unpractical is the fact that they do not consider the situation when actually there is no signal present. When only AWGN is in the incoming signal, the maximum-likelihood algorithm will continuously declare acquisition at a rate of $\frac{1}{\tau_d}$ because it simply picks the maximum. A threshold testing mechanism is therefore essential in any acquisition algorithm. One modification that makes the maximum likelihood algorithm workable is to choose the maximum that also exceeds the threshold. Another difficulty exists because the algorithm has to check through all the PN positions. When the PN code is very long (the case in real life), the time spent for the search will be too long. Therefore, it is applicable only in a parallel configuration such as those described in [16, 17] with a high price of hardware required.

[2]Although we have stated here that the local PN code is advanced by Δ, the actual advancement should be $\tau_d + \Delta$ to compensate for the integration time τ_d.

2.2 Parallel Search with Active Correlator

The decision output rate of the sliding correlator equals $\frac{1}{\tau_d}$ because of the integration time and the acquisition time is $v\tau_d$, where v is a random variable. One direct way to speed up the acquisition time is to increase the search rate by utilizing more than one correlator, resulting in a parallel configuration, as shown in figure 2.2. The largest one

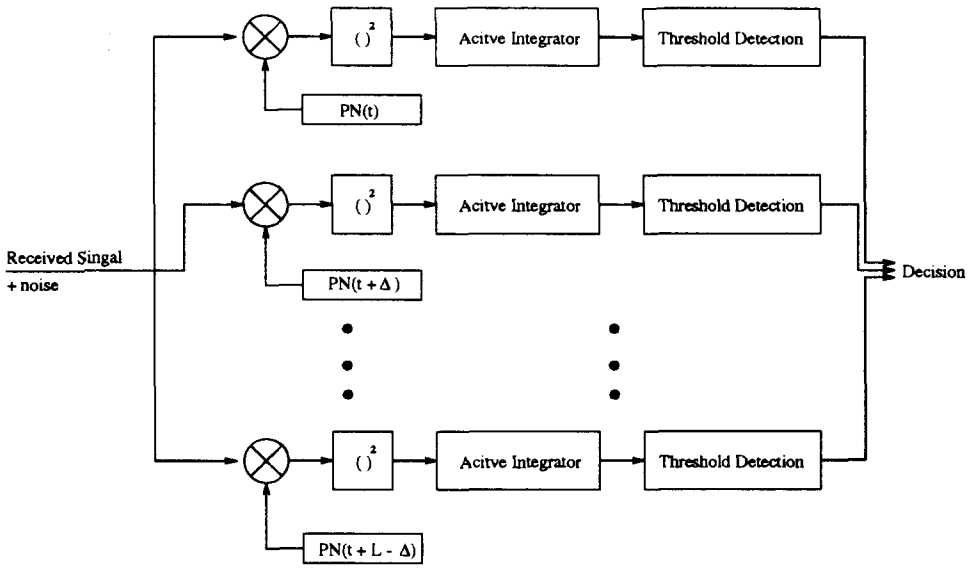

Figure 2.2: Parallel Acquisition Configuration.

that crosses the threshold will be a potential candidate with correct acquisition. Figure 2.2 shows a fully parallel implementation, where the number of active correlators equals $\frac{\mathcal{L}}{\Delta}$, where $\mathcal{L}$ is the PN code length in number of chips. The scheme searches all the cells at the same time, with a price paid for the significant amount of hardware required. To lower the hardware requirements, a partial parallel configuration will be used, with the number of correlators being smaller than $\frac{\mathcal{L}}{\Delta}$. The trade-off is the search speed against hardware requirement.

2.3 Sequential Detection

Ward [6] has demonstrated that a sequential probability ratio test (SPRT) is the most efficient method for obtaining a decision under two hypotheses. The nature of the acquisition system makes it equivalent to the situation of testing two hypotheses: H_0 : *No signal present*, and H_1 : *Signal present*. Thus a number of acquisition schemes based on the SPRT are proposed [4, 5].

Lets consider a particular sequential implementation as shown in figure 2.3. The

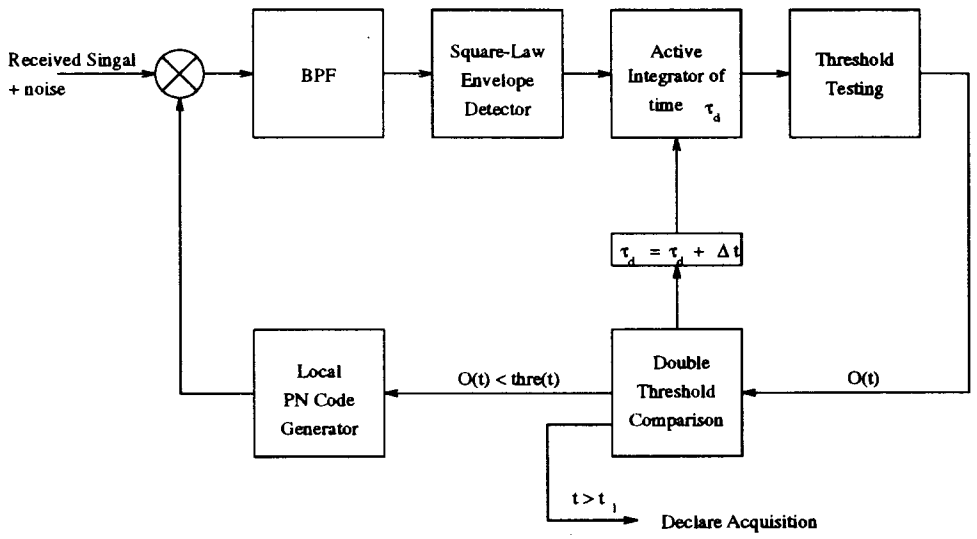

Figure 2.3: Sequential Detection.

output of the active correlator will increase continuously and depending on whether signal is present or not, we will get two situations as shown in figure 2.4. The detection algorithm works as follows: For a particular cell under testing, the correlator output is monitored until either it falls below a threshold $\eta(t)$ or a time-limit τ_0 is reached. The former case rejects the current cell, while the latter declares acquisition. The beauty of this scheme, when compared to the serial search, is that cells not corresponding to true acquisition (most of the cases) are dismissed earlier than the serial search time τ_d. The higher the magnitude of the threshold, the faster the output for the noise-only condition to dip below it. However, a higher threshold also implies a higher chance of the integrator output for signal plus noise case to fall below the threshold.

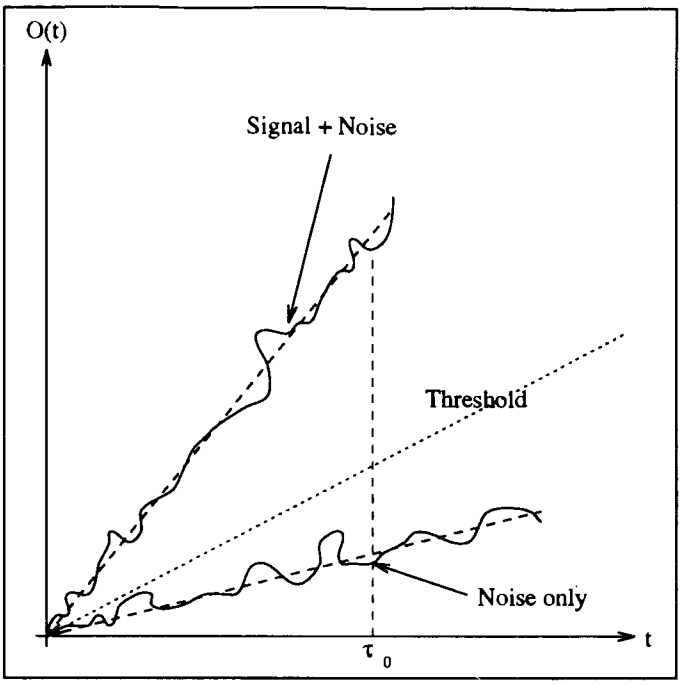

Figure 2.4: Sequential Detection Output.

Thus, a compromise threshold value must be chosen which allows fast dismissal of false synchronization positions, but still allows the integrator output for the true synchronization staying above the threshold.

2.4 Matched Filter

Even in a fully-parallel configuration as shown in figure 2.2, the decision output rate is restricted to $\frac{1}{\tau_d}$. One may argue to increase the search rate by decreasing τ_d. However, restriction exists on the lower limit of τ_d, as too low a value of τ_d will cause unacceptable low detection probability. Fortunately, a matched filter (contrast to active correlator) can perform operations in real time and it examines one cell per T_c, in contrast to one cell per τ_d. Especially with the advance of VLSI technology, long digital matched filters are now available, which is used to be a limitation in the

digital matched filter approach. Figure 2.5 shows a configuration of digital matched filter. Incoming signal is sampled at a rate of $\frac{\Delta}{T_c}$ and shifted into the register. The

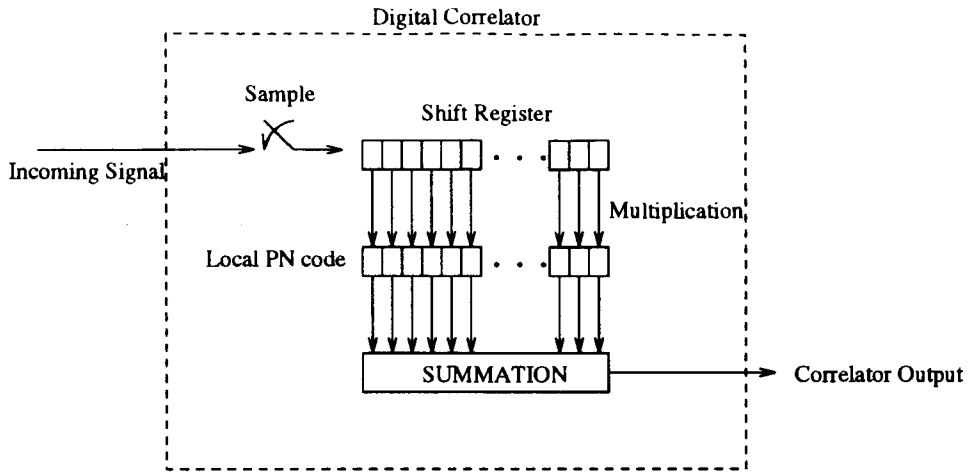

Figure 2.5: Digital Matched Filter.

modulo-two summation circuit sums up register contents and provides output also at a rate of $\frac{\Delta}{T_c}$. The application of matched filter also features the serial [15] or the parallel [16, 17] cofigurations.

2.4.1 Verification Algorithm

The methods discussed in the above section are based on a single threshold testing, which may not be reliable in real situations. Usually, a verification stage follows to improve the performance. A very common verification algorithm is the one used in [16, 17]. A number M of additional correlations with the same length are collected after the initial threshold crossing. If N out of the M also show threshold crossings, then acquisition is declared. Otherwise, the algorithm looks for the initial crossing again.

Other verification algorithms exist such as the search strategies as shown in figure 2.6a [19] and figure 2.6b [42].

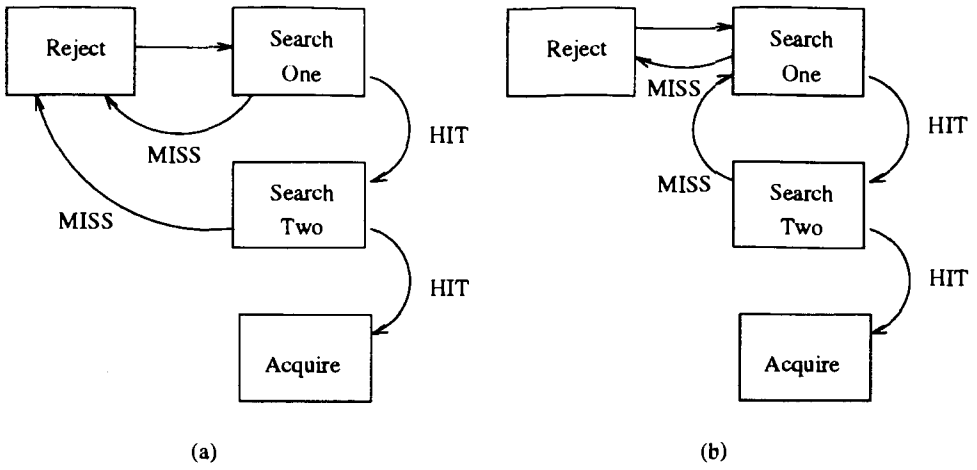

Figure 2.6: Two Search Strategies for Verification.

All the above verification algorithms discussed in this section is categorized as fixed mulitple-dwell system where more than one correlation of time τ_d is performed. Moreover, instead of using fixed value of τ_d for each dwell, one may use a different value, resulting in so called variable, mulitple-dwell algorithms [19, 20].

Another interesting acquisition scheme is proposed by Rappaport and Schilling [35] as shown in figure 2.7, which uses a passive matched filter as the initial crossing detection, while a bank of active correlators for verification. When a threshold crossing

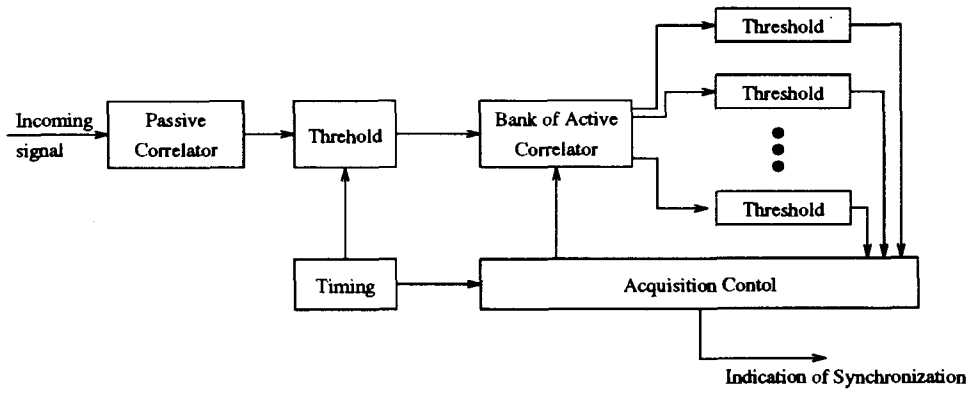

Figure 2.7: Two-Level Acquisition Scheme proposed by Rappaport and Schilling.

is detected in the passive correlator, one of the idle active correlators (if one exists)

will engage in this PN phase position. If the active correlator output also exceeds the second threshold, then acquisition is declared.

2.5 Estimation Based Acquisition Schemes

Another scheme which was first proposed by Ward [7] is based on the fact that we can generate the corresponding M-sequence once we know r values in the shift register correctly, with known connection coefficients. A modified version came out about one decade later, which was given the acronym RARASE (Recursion-Aided Rapid Acquisition Sequential Estimation), as shown in figure 2.8. A five-stage M-sequence

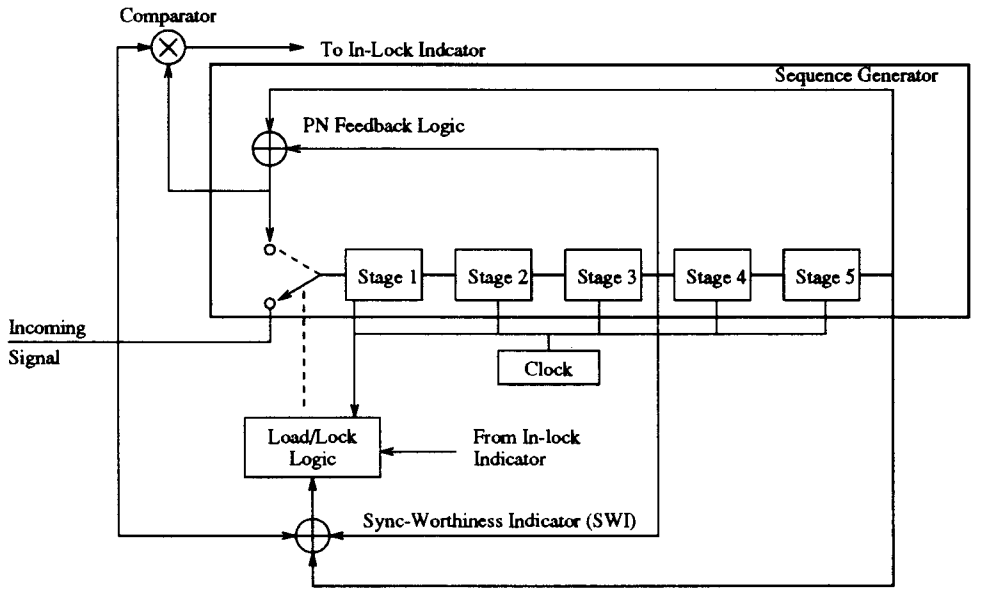

Figure 2.8: Recursion-Aided Rapid Acquisition Sequential Estimation.

generator identical to the one in the transmitter feedbacks the output to produce estimate of next state according to the current register contents. The estimate and the actual received signal are compared in the Sync-Worthiness Indicator (SWI). Once three consecutive agreements is detected, the load/track logic will raise the switch to the upper position. A trial track and in-lock correlation is then performed while the

shift register continues to produce a replica of the incoming sequence with initial phase corresponding to the contents of the shift register when the switch was raised. If a not-in-lock decision is made at the end of trial period, the switch is lowered and the process is repeated.

Since this method relies heavily on accurate estimates of incoming states, it has the drawback of being highly vulnerable to noise and interference signals. Moreover, the estimation process consists of a simple demodulation and hard-limiting detection of the signal in the same way as detecting any PSK signal, which implicitly requires carrier synchronization. This scheme therefore is coherent and thus is of limited use in most spread-spectrum applications [12].

2.6 Performance Analysis

Performance measures must be defined in order to evaluate different acquisition methods designed. The *acquisition time* becomes the obvious candidate because it is highly desirable to obtain acquisition at the shortest time possible. Various techniques for evaluating the acquisition time or the variance of the acquisition time have been investigated such as the signal flow graph/Markov chain [14, 15, 16, 17, 18, 19], or probabilistic evaluations [21, 23, 24]. Due to the random nature of the acquisition problem, the signal flow graph (Markov chain) method matches directly with the problem and is dominantly used for analysis. Here, we will present the unified approach provided by Polydoros and Weber [14] which is applicable to systems with predetermined and fixed dwell times [3]. This analysis is presented here because of its general applicability.

The flow graph for the acquisition technique is shown in figure 2.9. A minimum number of states to model the process is used, namely $v+2$. Out of the $v+2$ states, $v-1$ corresponds to cells not synchronized, while one state corresponds to the state

[3]The restriction is based on the desire to utilize the discrete Markov nature of the imbedded process to allow the application of the flow graph technique.

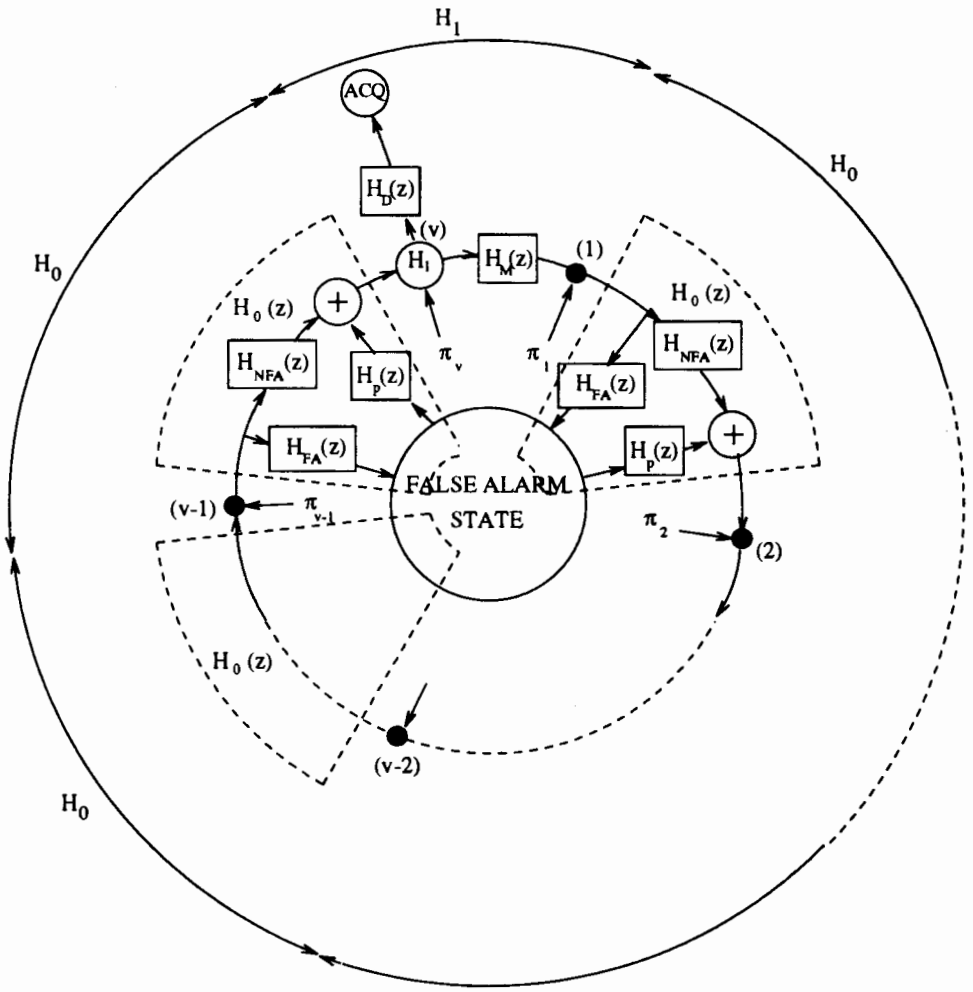

Figure 2.9: Unified Approach in Serial Search Code Acquisition.

when signal is present. The remaining two states are the false alarm (FA) state and the correct acquisition (ACQ) state. Note that the acquisition state can be reached only from the v-th state, whereas the false alarm state can be directly reached from any of the $v-1$ states corresponding to offset cells. The value of $\pi_j\{j=1,2,...,v\}$ is the probability of entering state j. Without any *prior* information about the relative position of code, $\pi_j = \frac{1}{v}$. $H_{(\cdot)}(z)$ represents the generalized gain which characterizes all possible ways by which the process can move along that branch. Various gains are designated as follows:

$$\begin{aligned} H_D(z) &= \text{gain for verification of detection,} \\ H_M(z) &= \text{gain for missed verification of detection,} \\ H_{FA}(z) &= \text{gain for false alarm,} \\ H_{NFA}(z) &= \text{gain for no false alarm,} \\ H_p(z) &= \text{gain for penalty after false alarm occurrence.} \end{aligned}$$

We can move from state j to state $j+1$ either directly (without false alarm), or passing through the false alarm state first. $H_0(z)$ is therefore given by

$$H_0(z) = H_{NFA}(z) + H_{FA}(z)H_p(z). \tag{2.1}$$

With signal flow graph reduction techniques, it can be shown that the moment generating function $U(z)$ is [14]

$$U(z) = \frac{H_D(z)}{1 - H_M(z)H_0^{v-1}(z)} \sum_{j=1}^{v} \pi_j H_0^{v-1}(z). \tag{2.2}$$

And uniform distribution of π_j implies

$$U(z) = \frac{1}{v} \frac{H_D(z)}{1 - H_M(z)H_0^{v-1}(z)} H_0^{v-1}(z). \tag{2.3}$$

In theory, by filling out expressions for various $H_{(\cdot)}(z)$, we can use the generating function to find the corresponding first moment (acquisition time), second moment (variance of acquisition time), ... However, finding the corresponding expressions may be a very difficult task and approximations must be made [12].

2.7 Research Objective

We have seen in this chapter that a whole variety and combination of schemes exist for PN code acquisition. With such a broad scope, considering all possibilities seems to be impossible. In order to narrow our study, we first decide to use a digital matched filter as the correlator structure. We believe that the digital filter will become the mainstream in the near future with the evolution towards digital cellular radio network, and the availability of very high chip rate spread-spectrum processor, for example, the *PA-100* by *UNISYS* has a maximum rate of 32 Mcps (Mega chips per second), and possible to generate a code length of up to 2^{16} chips long[3].

The unified approach mentioned in the previous section is able to give an expression for the acquisition time in terms of the dwell time τ_d, detection probability P_D, and false alarm rate P_{fa}. In fact, the majority of previous research is directed towards the analysis of various schemes. In a packet radio system, on the other hand, the preamble length is fixed, and the acquisition time may not be an appropriate measure. We will use the throughput as a performance measure instead.

We will emphasize on the uplink, that is, transmission from the mobile to the base station. In the uplink, different users will be assigned different PN codes. The base station will use the corresponding PN code to decode a particular user's message. The downlink problem is simpler in nature because a broadcast type of scheme will be sufficient.

To summarize, our research aims to design a good acquisition scheme in a packet radio cellular network. Besides, we assume that we are dealing with a frequency selective channel where no interleaving or coding is performed (both interleaving and coding is impossible during acquisition when we have not established any link yet). The result is receiving a preamble section which is subject to fading, and the fading effect is highly correlated between symbols.

Chapter 3

On-Off Keying Assisted Acquisition Scheme

As we have mentioned in Chapter 2, previous researchers are more interested in the formulation of the acquisition time distribution with different correlator structures such as matched filters and SAW devices, or correlator arrangements (serial, parallel)[16]-[22]. This approach probably derives from the nature of early spread spectrum communications, where communcation starts only after synchronization is obtained. However, in a packet radio system, the preamble length is fixed and the acquisition time may not be an appropriate measure. We believe that throughput is a more desirable measure of performance. In our study of the two different schemes we propose, we use a fixed blocking probability (P_b, probability of finding the receiver busy when a packet arrives) criterion, in contrast to the constant false alarm rate. Based on a Poisson distribution of false alarm arrival, we derive equations for P_b for various methods and use them to set the thresholds accordingly. In this way, the throughput is given by

$$Throughput = (1 - P_b) \times P_d,$$

where P_d is the detection probability. The best acquisition method is therefore the one that can maximize the throughput. Although it would be nice to pick system paramters that maximize the throughput. However, such an approach is mathematically intractable. On the other hand, designing based on a fixed blocking probability enables us to derive the threshold analytically. If simulation time is not a problem, we can then generate performance curves for different blocking probablity and for each channel SNR, the one with the best throughput would be picked as the optimal design. In this chapter, we will consider one of the two schemes we propose, *the on-off keying assisted acquisition method*, which utilizes on-off keying during the preamble section. One difficulty in spread spectrum communication's acquisition is the partial correlation effect which may cause high correlation output, thus giving false alarm. In order to combat this effect, we introduce a windowing technique which we find useful in overcoming the difficulty. With simulation studies, we find that the on-off scheme, together with the windowing technique, outperforms the other existing ones in both a flat fading and a frequency selective fading channels.

3.1 Packet Format

In a mobile radio packet system, data is sent in packets, with the beginning of each packet being a fixed length of preamble used for synchronization. If synchronization is not acquired during the preamble, the corresponding packet will be lost. Figure 3.1 shows the packet data format where the preamble consists of L symbols. We simply represent the remaining section of a packet (beside the preamble) as "Data" as it is not the focus of this thesis. This portion may contain a header for locating the start of actual data, or other overhead. We have made the assumption here that the length of each symbol equals one PN code. There are two desirable features in a CDMA packet radio system:

High Throughput A lost packet will require retransmissions (e.g. file transfer), or loss of information (e.g. voice, radio) – another price. Thus, we would like to ensure

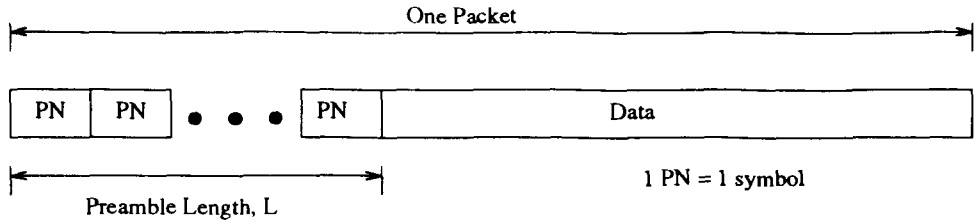

Figure 3.1: Packet Data Format.

a minimum required throughput.

Robustness Since the signal will be subject to fading, shadowing and varying SNR, a robust system is needed to operate under different channel signal to noise ratio (SNR).

In other words, a good acquisition system is able to achieve high detection probability P_d under varying SNR, given a particular blocking probability P_b desired. Our system also tries to achieve the above two goals.

3.2 Flat Fading Channel Model

Assuming BPSK used for the modulation of data, the transmitted DS-SS signal is

$$s(t) = A \cdot b(t) \cdot PN(t) \cdot \cos(\omega_c t + \theta), \tag{3.1}$$

where

$$\begin{aligned} A &= \text{amplitude of carrier,} \\ b(t) &= \text{data, } \{-1, 1\}, \\ \omega_c &= \text{carrier frequency,} \\ PN(t) &= \text{PN sequence of the intended receiver,} \\ \theta &= \text{phase offset.} \end{aligned}$$

In a Rayleigh fading channel with a maximum doppler frequency of f_D, the received signal is

$$r(t) = A \cdot g(t) \cdot b(t) \cdot PN(t)\cos[\omega_c t + \theta + \phi(t)] + n_W(t), \tag{3.2}$$

where $g(t)$ is the Rayleigh fading envelope, $\phi(t)$ is a uniformly distributed random phase, and $n_W(t)$ is the channel's additive white Gaussian noise (AWGN). It is assumed that $g(t)$ has a mean square value of $2\sigma_g^2$ and the AWGN has a two-sided power spectral density of $N_0/2$. The received signal is assumed to be first brought down to baseband before correlation and despreading takes place; see figure 3.2. The resultant

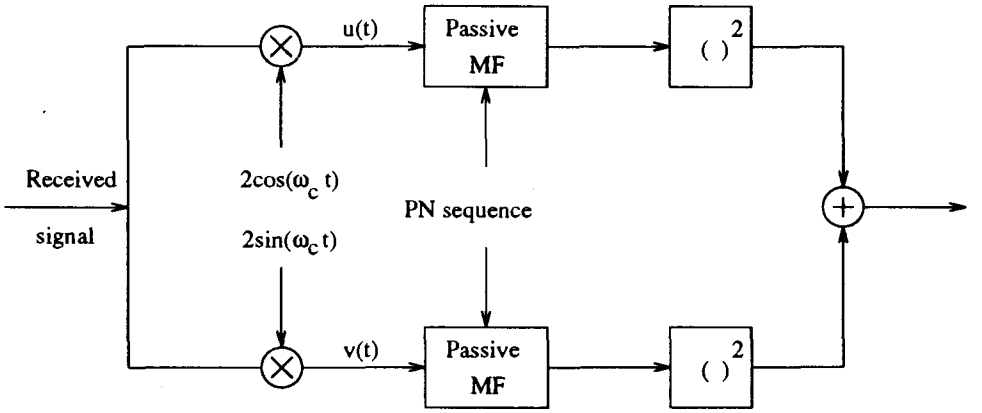

Figure 3.2: Noncoherent Detector Structure

complex baseband signal can be written as

$$w(t) = u(t) + j \cdot v(t), \tag{3.3}$$

where

$$\begin{aligned} u(t) &= Ax(t)PN(t)b(t) + n_I(t), \\ v(t) &= Ay(t)PN(t)b(t) + n_Q(t), \end{aligned}$$

and

$$\begin{aligned} x(t) &= g(t)\cos[\phi(t) + \theta], \\ y(t) &= g(t)\sin[\phi(t) + \theta], \end{aligned}$$

are two independent zero mean Gaussian processes that represent fading; while $n_I(t)$ and $n_Q(t)$ are the equivalent low-pass AWGN. For typical mobile radio channel, both $x(t)$ and $y(t)$ have an autocorrelation function of

$$\rho(\tau) = \overline{x(t) \cdot x(t+\tau)} = \overline{y(t) \cdot y(t+\tau)} = \sigma_g^2 \cdot J_0(2\pi f_D \tau), \tag{3.4}$$

where $J_0(\cdot)$ is the zero order Bessel function and as mentioned before, f_D is the doppler frequency. On the other hand, the power spectral density of the low-pass AWGN, $n_I(t)$ and $n_Q(t)$, are both N_0.

When the local PN sequence is in synchronization with the transmitted one, the output of the energy detector is

$$E_1 = \left| \int_0^T w(t) PN(t) dt \right|^2 = a_{1x}^2 + a_{1y}^2, \tag{3.5}$$

where

$$\begin{aligned} a_{1x} &= A \int_0^T x(t)dt + \int_0^T n_I(t) PN(t) dt, \\ a_{1y} &= A \int_0^T y(t)dt + \int_0^T n_Q(t) PN(t) dt, \end{aligned}$$

and T is the length of the PN sequence, which also equals one symbol duration. Assuming fading is slow enough that it is constant over one symbol duration, then both a_{1x} and a_{1y} are zero mean Gaussian random variables with a variance of

$$\sigma_1^2 = A^2 \sigma_g^2 T^2 + N_0 T. \tag{3.6}$$

This implies E_1 is exponentially distributed with a *pdf* of

$$p(E_1) = \frac{1}{2\sigma_1^2} e^{-\frac{E_1}{2\sigma_1^2}}. \tag{3.7}$$

On the other hand when the transmitted and local PN waveforms are not in synchronization, or when there is no signal present, the received signal energy is

$$E_0 = a_{0x}^2 + a_{0y}^2, \tag{3.8}$$

where

$$\begin{aligned} a_{0x} &= \int_0^T n_I(t) PN(t) dt, \\ a_{0y} &= \int_0^T n_Q(t) PN(t) dt, \end{aligned}$$

are both zero mean Gaussian random variables with a variance of $\sigma_0^2 = N_0 T$.

The term E_0 itself is exponential with a *pdf* of

$$p(E_0) = \frac{1}{2\sigma_0^2} e^{-\frac{E_0}{2\sigma_0^2}}. \tag{3.9}$$

From the *pdf* in equation (3.9), we can select the appropriate thresholds for a given false alarm rate, which in turn is determined by the desired blocking probability, P_b. In summary, the acquisition problem can be formulated as testing the two hypotheses.

$$H_1 : \quad E_1 = a_{1x}^2 + a_{1y}^2$$
$$H_0 : \quad E_0 = a_{0x}^2 + a_{0y}^2$$

3.3 On-Off Keying Assisted DS/SS Acquisition System

Traditional methods for the acquisition of the PN code requires a transmission of a stream of bits 1 to the receiver, and the difference among different schemes lies merely in the verification stage, for example, a coincidence detector or Markov Chain search.

In the On-Off Keying Assisted DS/SS Acquisition System, we not only recommend a new verification stage, but also a new synchronization pattern which works together with the verification procedure to give better performance. Instead of sending a series of bits 1, the preamble section follows an on-off pattern. The power varying capability is necessary in any CDMA system to overcome the far-near problem, thus this scheme appears to impose no additional hardware requirements. For simplicity, lets assume that the length of a single "on" state equals one PN sequence length[1]. Figure 3.3 shows an overall view of the new acquisition system, assuming a correlator length of one PN sequence. Since an on-off scheme is adopted, we can double the

[1]The length of the "on" state is not necessarily equal to one PN sequence. Rather, it can be multiple of the PN length.

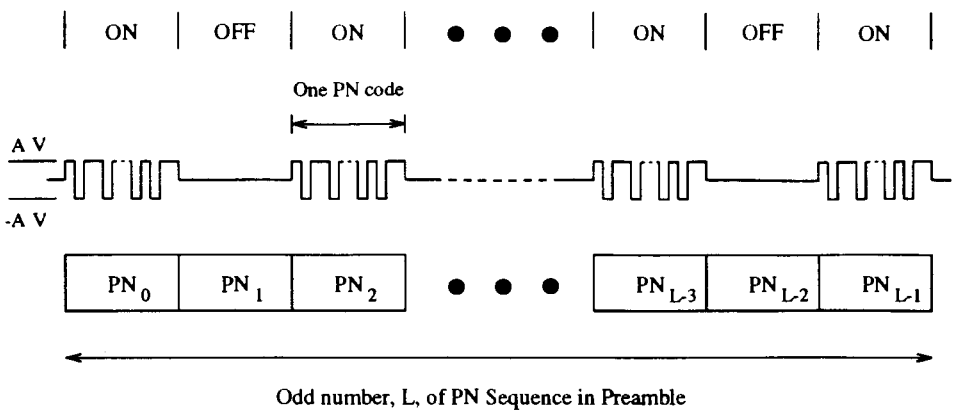

Figure 3.3: On-Off pattern in Preamble

power during the "on" state, while still maintaining the same average power as in other schemes[2]. Given a particular P_b required, we can calculate the corresponding false alarm rate, P_{fa}, which in turn can be found by Markov chain (discussed in next section) analytically. From the P_{fa}, thresholds for the "on" and "off" states are defined, say τ_1 and τ_0 respectively. For the receiver, who does not know whether the current pulse sent is "on" or "off", keeps on tracking threshold τ_1 in the first place. Once the first threshold is detected, the algorithm continuously looks for alternate τ_0 and τ_1 for the second, third bits ... until either acquisition is reached or the search being terminated as the number of state transitions exceeds the preamble length L (explained in later sections). Figure 3.4 shows the search strategy used. The τ_1 or τ_0 in

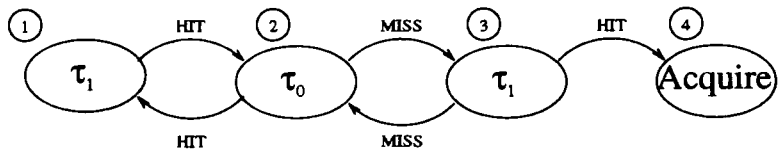

Figure 3.4: On-Off Keying Assisted Search Strategy

each node indicates the current threshold in each state. A **HIT** represents correlator output exceeding the threshold, while the **MISS** is the opposite. Note that a **MISS** (not a **HIT**) will cause a transition from state 2 to state 3 because falling below the

[2]A discussion on extending the on-off pattern to on-off-off-on... pattern is covered in the conclusion section of this chapter.

threshold means a high probability for the presence of noise.

Intuitively speaking, the benefits of this method are two-fold: first, a higher power in the "on" state increases its resistance to Rayleigh fading – subject to the same fading effect, a higher power implies a greater probability of crossing the corresponding threshold; second, the "off" state which now consists of only AWGN, is not subject to any fading.

3.3.1 Probability of False Alarm

Probability of false alarm is the probability of declaring acquisition when there is actually no signal. A false alarm occurs when we pass both the first threshold crossing and the verification procedure. We will use the Markov chain approach to find P_{fa}. Figure 3.5 shows the Markov chain model. In the figure, P_{00} denotes the probability of crossing τ_0 and P_{01} is the probability of crossing τ_1, by the presence of noise. Furthermore, a reject state is introduced because returning to state 1 will not cause a false alarm. Note that each state in figure 3.5 is marked as "off" because a false alarm is caused by noise only. We implement an additional mechanism in our acquisition:

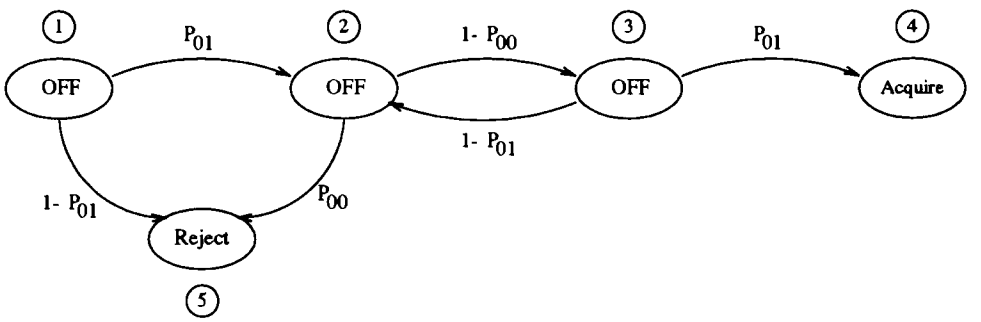

Figure 3.5: On-Off Keying

a counter is kept for the number of transitions since the first τ_1 threshold crossing. This counter will be increased by one for each additional transition and the search will terminate if the counter exceeds L. In other words, we limit the maximum number of searches to L. The mechanism is able to lower the total number of combinations

to reach false alarm, thus producing a lower false alarm rate, given particular τ_1 and τ_0 values[3].

The transition probability matrix corresponding to figure 3.5 is given by

$$Q = \begin{bmatrix} 0 & P_{01} & 0 & 0 & (1-P_{01}) \\ 0 & 0 & (1-P_{00}) & 0 & P_{00} \\ 0 & (1-P_{01}) & 0 & P_{01} & 0 \\ 0 & 0 & 0 & 1 & 0 \\ 0 & 0 & 0 & 0 & 1 \end{bmatrix}. \tag{3.10}$$

The probability of false alarm is

$$P_{fa} = Q^L_{(1,4)}. \tag{3.11}$$

Subscript $(1,4)$ in the above equation denotes the first row, fourth column element in the matrix Q raised to power L.

3.3.2 Blocking Probability

To derive the blocking probability, we use a similar approach as those in [23, 24]. The time frame is partitioned in alternate periods of busy and idle, denoted by B and A respectively in figure 3.6. We assume that the busy time caused by an actual packet

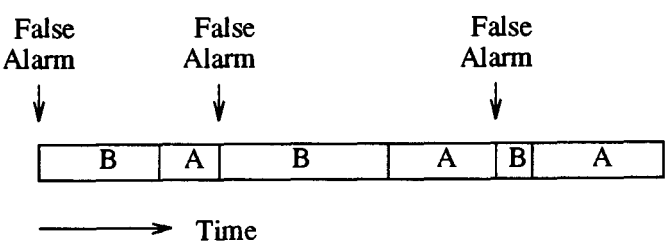

Figure 3.6: Time Pattern for False Alarm

[3]When the preamble length is set to L, there is no reason to search for more than L symbols..

coming is negliable, which translates to the situation for low traffic load. Over a long period of time, the blocking probability is simply given by

$$P_b = \frac{\bar{B}}{\bar{B} + \bar{A}}, \tag{3.12}$$

where

$$\begin{aligned} \bar{A} &= \text{expected idle period,} \\ \bar{B} &= \text{expected receiver busy time due to false alarm.} \end{aligned}$$

The idle period $\bar{A}$ is defined as the time from the end of one busy period to the arrival of next false alarm. Denoting P_{fa} as the overall false alarm probability (false alarm after verification), the expected busy time is

$$\begin{aligned} \bar{B} &= \left\{ P_{fa}[(L-1)+L_D] + (1-P_{fa}) \left[\frac{\sum_{i=2;i+2}^{L-1} P_{01}P_{00}[(1-P_{00})(1-P_{01})]^{\frac{i-2}{2}} \cdot (i-1)}{\sum_{i=2;i+2}^{L-1} P_{01}P_{00}[(1-P_{00})(1-P_{01})]^{\frac{i-2}{2}}} \right] \right\} \times T \\ &= \left\{ P_{fa}[(L-1)+L_D] + (1-P_{fa}) \left[\frac{\sum_{j=1}^{(L-1)/2} P_{01}P_{00}[(1-P_{00})(1-P_{01})]^{j-1} \cdot (2j-1)}{\sum_{j=1}^{(L-1)/2} P_{01}P_{00}[(1-P_{00})(1-P_{01})]^{j-1}} \right] \right\} \times T, \end{aligned} \tag{3.13}$$

where L is the preamble length, P_D is the data length, and T is one symbol (bit) duration. When a false alarm occurs, the receiver will try to decode the whole packet, thus making it busy for a period of $[(L-1)+L_D]$ symbols. We use a value of $L-1$ instead of L here because of the digital matched filter assumption, in which case the incoming signal is continuously shifted into the register and the receiver is busy only for the verification stage, $L-1$ symbol (bit) long.

The second term in equation (3.13) accounts for various possible busy time periods for the receiver to reach the "Reject" state when the verification procedure is not passed. Referring back to figure 3.5, we can reach state 5 from 1 by following the routes, 125, 12325, 1232325, 123232325 ...(each number represents the corresponding state passed), so the summation term in the numerator gives the total probability of false alarm; while $(i-1)$ gives the busy time associated with a particular route. The upper limit in the summation is $L-1$ because of the restriction we put on the maximum number of transitions. Equation (3.13) can be simplified (see Appendix A)

by using series expansion to obtain[4]

$$\bar{B} = \left\{ P_{fa}[(L-1) + L_D] + (1 - P_{fa}) \left[1 + \frac{2x}{1-x} - \frac{(L-1)x^{(L-1)/2}}{1 - x^{(L-1)/2}} \right] \right\} \times T, \quad (3.14)$$

where

$$x = (1 - P_{00})(1 - P_{01}).$$

The expected false alarm inter-arrival time $\bar{A}$, on the other hand, can be obtained based on a Poisson distribution, assuming that we have a probability P_{01} of crossing threshold τ_1 once every T_c seconds, and given by equation

$$\bar{A} = \frac{T_c}{P_{01}}, \qquad T_c \text{ is one chip duration.} \quad (3.15)$$

Having chosen the desired value of P_{00} (τ_0 is fixed), and with a particular value of blocking probability P_b, the value of P_fa is found from which we calculate τ_1.

In a packet radio system, a false alarm will cause the receiver busy, thus making it incapable of detecting any packet coming during the busy time – a penalty price. The constant false alarm rate criterion (CFAR) used traditionally has assumed implicitly a constant penalty price for a false alarm, which may not be true in real situations. As seen from those expressions for the blocking probability, it accounts for not only the packet decoding time with a false alarm, but also for various other busy periods possible when failing the verification; therefore, the fixed blocking probability is a more appropriate criterion in the packet radio environment.

3.4 Other Techniques for Comparison

To put our results in perspective, we will compare our algorithm with the following methods: the coincidence detector, and two other techniques relying on additional threshold testings. These techniques are chosen because they belong to the multiple, fixed-dwell category, same as the on-off keying technique proposed, and they are common techniques employed in real applications.

[4]Note that $1 + x + x^2 + \cdots + x^n = \frac{1-x^{n+1}}{1-x}$.

3.4.1 Coincidence Detector

The concept of coincidence detector originates from radar detection [25, 26]. After the first threshold crossing, N additional correlations of the same length are done. If M out of the N additional tests exceed the threshold, acquisition is declared. Let τ be the threshold and P_0 be the probability of a threshold crossing caused by white Gaussian noise. The probability of false alarm follows a binomial distribution and is given by

$$P_{fa} = P_0 \cdot \sum_{i=M}^{N} C_i^N P_0^i (1 - P_0)^{N-i}, \tag{3.16}$$

where $C_i^N = \frac{N!}{i!(N-i)!}$. The first P_0 is the probability of first threshold crossing and the later part is the probability of passing the majority test (M out of N). The blocking probability is again given by the equation

$$P_b = \frac{\bar{B}}{\bar{B} + \bar{A}}. \tag{3.17}$$

However, in this case, the receiver will be busy for a constant period of $(L-1)$ symbols once the first threshold is crossed, thus giving the value of $\bar{B}$ as

$$\bar{B} = \{P_{fa}[(L-1) + L_D] + (1 - P_{fa})(L-1)\} \times T, \tag{3.18}$$

and the value of $\bar{A}$ is $\frac{T_c}{P_0}$.

3.4.2 Other Searches

The other two search techniques we used in the comparison are shown in figure 3.7a and figure 3.7b. These are the strategies taken from [18] and [19] respectively[5]. The main difference between the two is that one loops back to "search two" from "search three" when a **MISS** occurs, while the other will restart the algorithm again (back to "search one"). Our new search algorithm is similar to the first search (figure 3.7a), except that: i) We look for an alternate pattern (τ_0 and τ_1) after the first threshold crossing, ii) The transmitted signal follows an on-off pattern, iii) We limit the maximum transitions to L.

[5]We extend the search stage by one for comparison purposes.

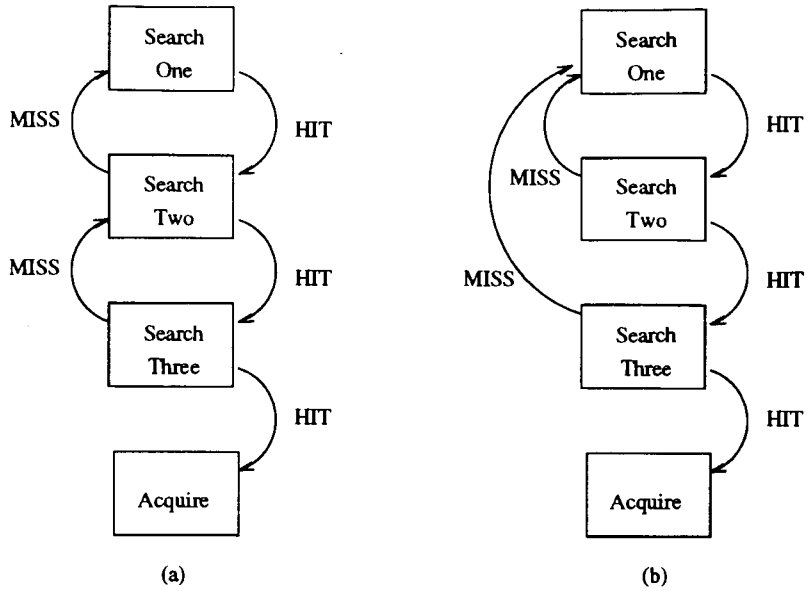

Figure 3.7: Two Search Techniques for Comparisons

The discrete Markov chain technique has been applied to analyze the first search [18], and analytic results exist for the second [19]. We have found that the original methods do not perform satisfactorily when infinite number of transitions are allowed in the search which causes high P_{fa}. Therefore, the maximum number of transitions is also limited to L, as in our On-Off Keying Assisted system. We will use similar arguments as those in the on-off keying scheme to obtain their blocking probabilities. Denoting P as the probability of crossing the threshold by noise, we have the following equations for the search in figure 3.7a:

First Search

$$
\begin{aligned}
P_b &= \frac{\bar{B}}{\bar{B} + \frac{T_c}{P}}, \\
\bar{B} &= \left\{ P_{fa}[(L-1) + L_D] + (1 - P_{fa}) \frac{\sum_{i=2,i+2}^{L-1} [P(1-P)]^{i/2} \cdot (i-1)}{\sum_{i=2,i+2}^{L-1} [P(1-P)]^{i/2}} \right\} \times T \\
&= \left\{ P_{fa}[(L-1) + L_D] + (1 - P_{fa}) \left[\frac{2(1 - x^{(L+1)/2})}{(1 - x^{(L-1)/2})(1-x)} - \frac{(L+1)x^{(L-1)/2}}{1 - x^{(L-1)/2}} - 1 \right] \right\} \times T,
\end{aligned}
\tag{3.19}
$$

where $x = P(1-P)$.

Second Search For the second search, we have

$$\begin{aligned} P_b &= \frac{\bar{B}}{\bar{B} + \frac{T_c}{P}}, \\ \bar{B} &= \left\{ P_{fa}[(L-1) + L_D] + (1 - P_{fa}) \frac{\sum_{i=2}^{3} (1-P) P^{i-1} \cdot (i-1)}{\sum_{i=2}^{3} (1-P) P^{i-1}} \right\} \times T \\ &= \left\{ P_{fa}[(L-1) + L_D] + (1 - P_{fa}) \frac{1+2P}{1+P} \right\} \times T. \end{aligned} \tag{3.20}$$

3.5 Frequency Selective Fading Channel

In the above discussions, we have considered the flat fading channel in which the coherence bandwidth is wider than the signal bandwidth, so that different frequency components are subject to the same fading effect. One nice feature of spread spectrum technique is that the signal bandwidth is wider than the coherence bandwidth and we can isolate different path components, and combine them in order to overcome the multipath effect [2, 29] – frequency diversity. In a frequency selective channel, the received signal can be written as

$$r(t) = \sum_{i=1}^{i=n} A g_i(t-\tau_i) b(t-\tau_i) PN(t-\tau_i) \cos[\omega_c(t-\tau_i) + \theta_i + \phi_i(t-\tau_i)] + n_W(t), \tag{3.21}$$

where

$$\begin{aligned} n &= \text{total number of resolved paths,} \\ A &= \text{amplitude of carrier,} \\ \tau_i &= \text{delay of signal from path } i, \\ g_i(t) &= \text{Rayleigh fading envelope for path } i, \\ b(t) &= \text{data, } \{-1, 1\}, \\ \omega_c &= \text{carrier frequency,} \\ PN(t) &= \text{PN sequence of the intended receiver,} \end{aligned}$$

θ_i = phase offset for path i,

ϕ_i = uniformly distributed random phase for path i,

$n_W(t)$ = channel's additive white Gaussian noise.

The summation sign accounts for various number of signal paths, and the flat fading channel is a special case where $n = 1$. Researchers have found that a RAKE receiver [2, 30] structure is efficient in combining energy collected from various paths. In the ideal situation, output from the RAKE receiver will be the same as if the signal has transversed only a single path.

3.5.1 RAKE Receiver Structure

A RAKE receiver structure which uses energy detection for acquisition is shown in figure 3.8. It consists of a tapped-delay line where the separation between every two taps is $\frac{1}{W}$, with W as the bandwidth of the transmitted signal. The length of the tapped-delay line is designed to cover the maximum delay spread of the received signal. A typical value of delay spread is $5-10\mu$s [31] in urban areas. The envelope output for each branch will still follow an exponential distribution. The RAKE receiver output, which is the sum of individual branches and thus a sum of exponential distributions, will follow a Gamma distribution.

Hardware Implementation

We propose to use a matched filter correlator structure, figure 3.9, which can be implemented solely in the digital domain. The incoming signal, after brought down to baseband, is sampled at a rate of Δ/T_c where Δ is the number of samples per chip. The sampled output are shifted into a register and being multiplied by the local PN sequence. The result is then summed and squared to give the in-phase component to be combined with the quadrature term (obtained by a similar correlator structure), producing the energy sum. Although in figure 3.8 we have explicitly drawn two correlators (in-phase and quadrature) for each tap position, we only need a total of

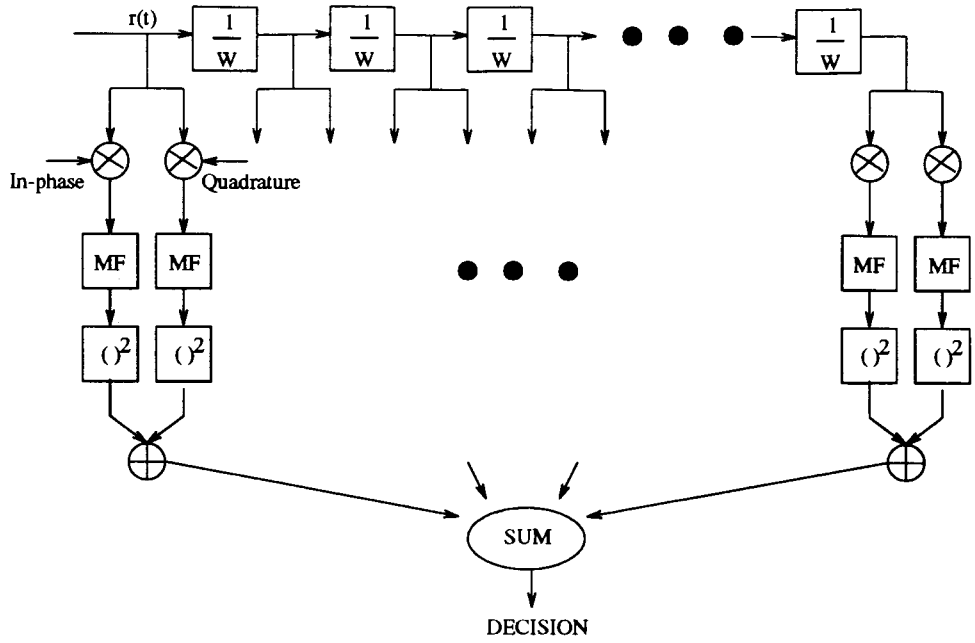

Figure 3.8: RAKE Receiver Structure.

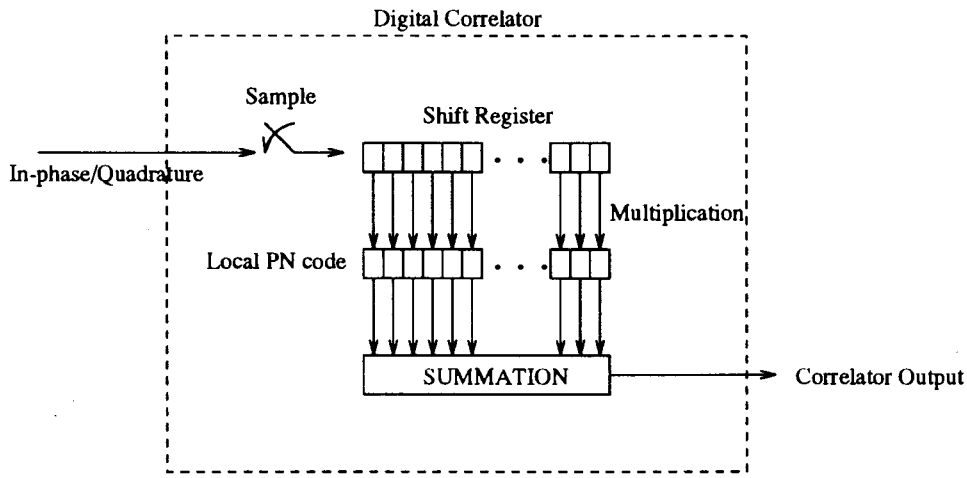

Figure 3.9: Digital Correlator Structure.

two correlators to implement the RAKE receiver structure when a digital matched filter is used. Figure 3.10 shows the hardware structure. The sum of output of the

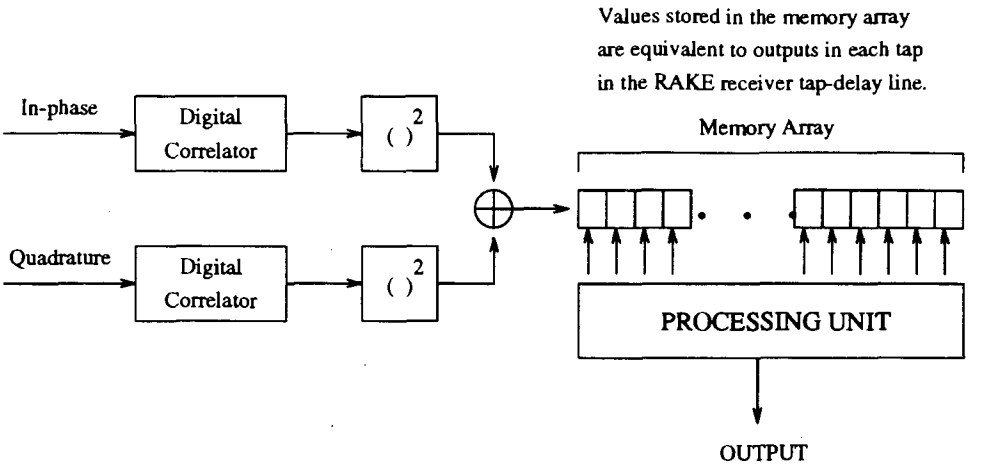

Figure 3.10: RAKE receiver Implemented with Digital Matched Filter.

correlators is shifted into an array of memory locations with length equals the tapped-delay line. In this way, each value in the array represents one correlator output as in figure 3.8, with the leftmost being the most recent one. The processor unit is responsible for summing up values in the memory array according to the particular RAKE receiver algorithm designed. This general hardware structure also provides flexibility in changing the actual acquisition algorithm – just by changing program in the processing unit.

3.5.2 RAKE Receiver Algorithm

We are going to describe our RAKE Receiver Algorithm in this section. Assume that the received signal consists of several path components. The correlator output will become high the first time when the signal from the shortest path arrives; this value is then shifted into the first memory location. The receiver algorithm works in two stages as follows, see figure 3.11: i.) the processing unit continuously monitors the value shifted into the first memory location. When this value exceeds a particular

threshold, $\tau_{preliminary}$, enough additional correlator outputs are collected (more samples collected) until the value originally in the first location has been shifted to the end location. Now, the memory array will contain all the different path components with the first ray located at the rightmost memory location, provided that the memory length is longer than the delay spread. ii.) The processing unit then selects the largest five correlation outputs from the array, sums them up and tests the value against another threshold which is set according to the scheme (on-off, coincidence ...) and the particular blocking probability required. Passing both stages declares acquisition of signal. If the second stage is not passed, we scan backwards from the last location to check if any correlation output exceeds $\tau_{preliminary}$ and repeat the second stage if necessary. If no such value exists, the algorithm restarts again in checking the first location continuously.

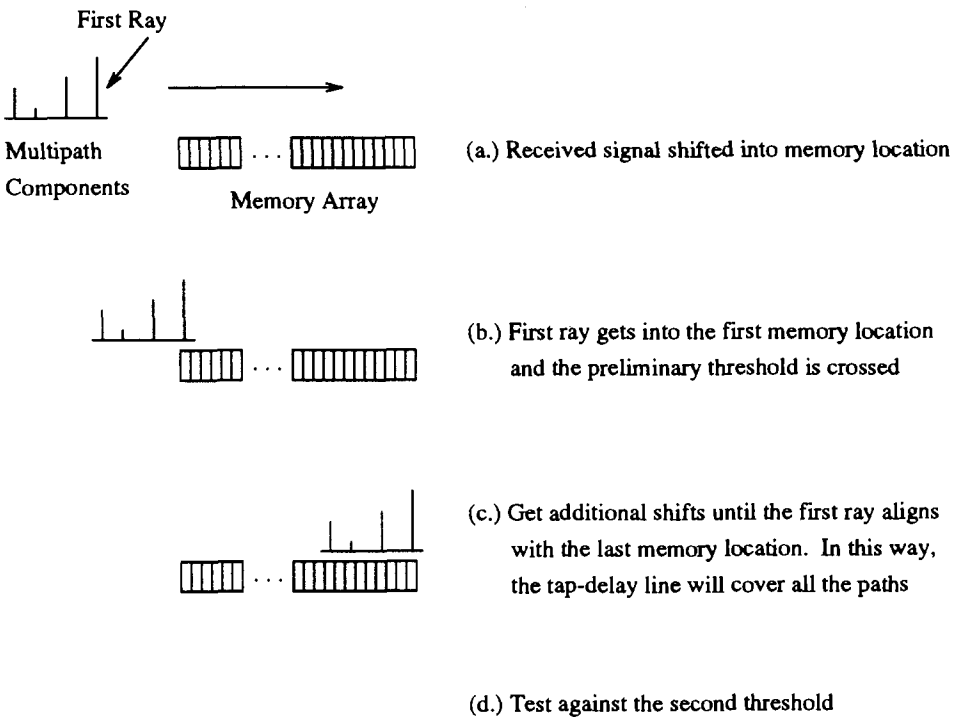

Figure 3.11: RAKE Receiver Algorithm.

In the above algorithm, the processing unit only selects the five largest components with a trade-off of neglecting the 6th, 7th... paths. However, when the channel has

only a few strong paths (most situations), most of the correlator outputs (values in memory array) will mainly consist of noise. Summing all the values will produce a low SNR, thus giving poorer performance [2].

The purpose of the first stage is to align the first ray to the last memory location, so that the RAKE receiver covers the whole delay spread, while the second stage does the actual threshold testing. Since the energy of the received signal is distributed among various paths, if we set the value of $\tau_{preliminary}$ too high, we may miss the first few rays when their carrying energy is low, as shown in figure 3.12a. On the other

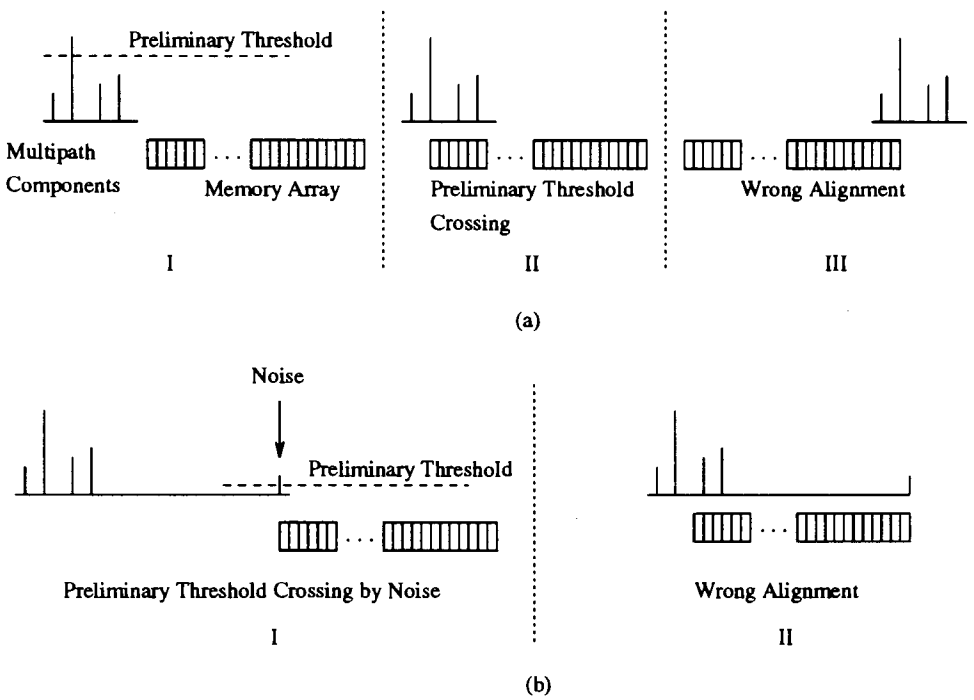

Figure 3.12: Wrong Alignment when $\tau_{prelimary}$ is (a) Too High, (b)Too Low.

hand, if $\tau_{preliminary}$ is too low, we may not be able to capture all the rays available, see figure 3.12b, as noise causes a lot of $\tau_{preliminary}$ crossings. A compromise is needed and we find that a $\tau_{preliminary}$ value of 10^{-3} gives satisfactory results in our simulation studies.

3.6 Problem of Partial Correlation with PN Sequence

In the experiments, we utilize the M-sequence of length 127 as our PN sequence which has very good cyclic autocorrelation properties. For energy detection, we are faced with an abrupt change from nothing to having a signal. Before the first symbol (first PN code) has been shifted entirely into the correlator, we have partial overlap between the incoming and the locally generated PN sequence – partial correlation. Figure 3.13 shows the correlator output for a train of bits 1 received which have passed through a two-ray channel without any noise. We can see from the figure that in a period of 1 symbol (bit) before the first match (high output), some additional noise caused by the partial correlation is found, which can be as high as 15% of the signal strength. This temporary increase in noise occurs within one symbol (bit) before the first ray

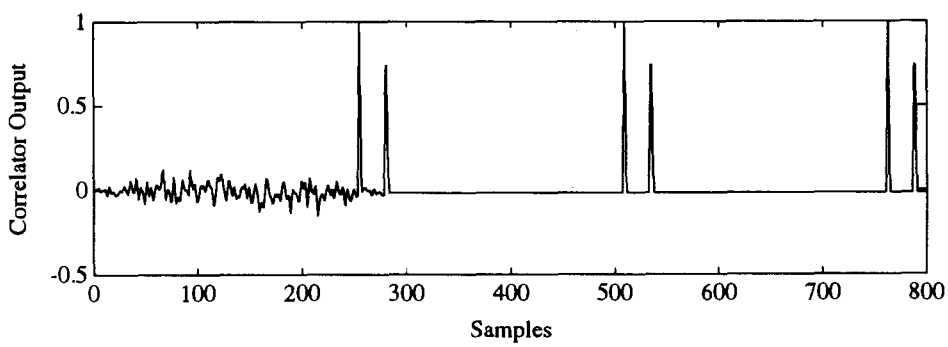

Figure 3.13: Partial Correlation.

and will cause the RAKE receiver to react incorrectly: one of the noise will exceed the $\tau_{preliminary}$ and be treated as the first ray. There is also a high probability of passing the second stage because 1) the sum of the squares of the partial correlations (RAKE receiver output) is already higher than the second threshold, and 2) if the $\tau_{preliminary}$ crossing occurs within one delay-spread before the actual first ray, then after shifting this crossing to the rightmost of the memory array, the RAKE receiver delay line still covers the actual rays, thus giving a high output than the second threshold. Therefore,

the partial correlation may cause wrong acquisition

The temporary noise increase due to partial correlation is proportional to the signal strength. As a result, the effect will be more prominent when SNR is high. In our experiments, we introduce a simple windowing technique to overcome this difficulty.

3.6.1 Windowing Technique

Let us denote the RAKE receiver output as a sequence of $[\cdots, O_{-2}, O_{-1}, O_0, O_1, O_2, \cdots]$ in which O_0 corresponds to the correct acquisition. Suppose $\tau_{preliminary}$ is crossed at index $-i$ and O_{-i} is also larger than τ. Instead of treating $-i$ as the correct acquisition, we will look forward to the outputs $[O_{-i+1}, \cdots, O_{-i+w}]$ and see if any of them is greater than O_{-i}. If O_k is the largest value in the window that satisfies $(O_k > O_{-i}, -i+1 \leq k \leq i+w)$, and the single correlator output at index k is greater than $\tau_{preliminary}$, then k will be treated as the correct acquisition.

The underlying working principle is as follows: The $\tau_{preliminary}$ crossing may be due to noise or partial correlation. In the former case, O_{-i} will be unlikely greater than τ, while in the latter case, the first ray will be within one symbol. As long as the value w is large enough, the window will cover the actual acquisition position and the corresponding RAKE output will be the largest because it sums up all the rays.

Next, we will explain why this windowing technique will be most effective in the on-off keying scheme. As mentioned before, we want the value of w to be large to give high probability covering the actual acquisition. Due to the length of the RAKE tapped-delay line, the maximum value of w is (1 symbol − tapped-delay line length). To see why this restriction exists, lets assume that a $\tau_{preliminary}$ crossing occurs at index -2 and we open up a window of size w from index -2, ie. $[O_{-2}, O_{-1}, O_0, \cdots, O_{-2+w}]$ where O_0 is the correct acquisition. Consider the last element in the window, O_{-2+w}. With the RAKE receiver structure, this output is contributed by correlator outputs from $(-2+w)$ to $(-2+w+$tap-delay line length$)$. If $(w \geq$ symbol - tap-delay line length$)$, the range $(-2+w)$ to $(-2+w+$tap-delay line length$)$ will contain rays from the second

symbol and may be greater than O_0 in which case we get incorrect acquisition. We claim here that the restriction on w is weaker in the on-off scheme because the second symbol in the preamble is an "off" stage containing only noise. As a conclusion, the value of w in the on-off situation may be set even greater than one symbol, as long as it is smaller than (2 symbols - tap-delay line length).

3.7 Simulation Results on Flat Fading Channel

In our simulations, we have used a fade rate of 100Hz, a PN code of length 127, and a data rate of 16kbit/s. The fade rate is typical for a moving mobile. The fading is assumed to stay constant during one symbol and the procedure of simulations is

1. Choose a particular blocking probability, P_b.
2. From the required P_b, find the required thresholds for each individual method.
3. Generate enough fading input data, for which we apply the different methods to find the percentage of successful acquisitions.

Figure 3.14 and figure 3.15 show simulation results for a blocking probability of 10^{-3} and 10^{-5} respectively. Note that the SNRs defined in the figures are those for the correlator output, not the received signal, and the preamble length is in bits.

We can make two observations from the results. First, the on-off assisted keying scheme always performs better than the others, regardless of the SNR. Second, increasing the preamble length will cause increase in throughput, except for the coincidence detection where the extra busy time encountered with increasing preamble length offsets the gain in longer coincidence period.

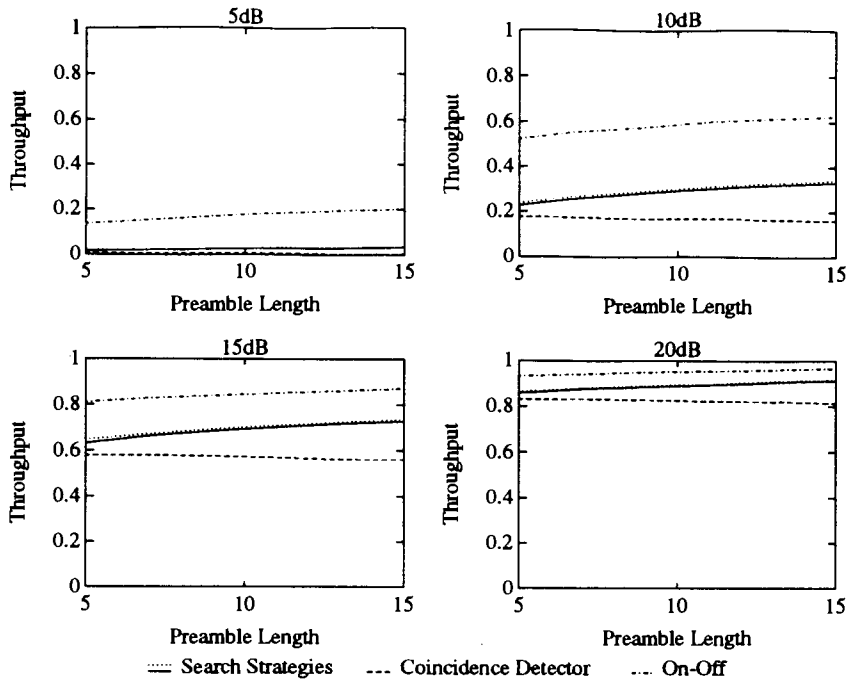

Figure 3.14: Simulation Results for a Blocking Probability of 10^{-3}.

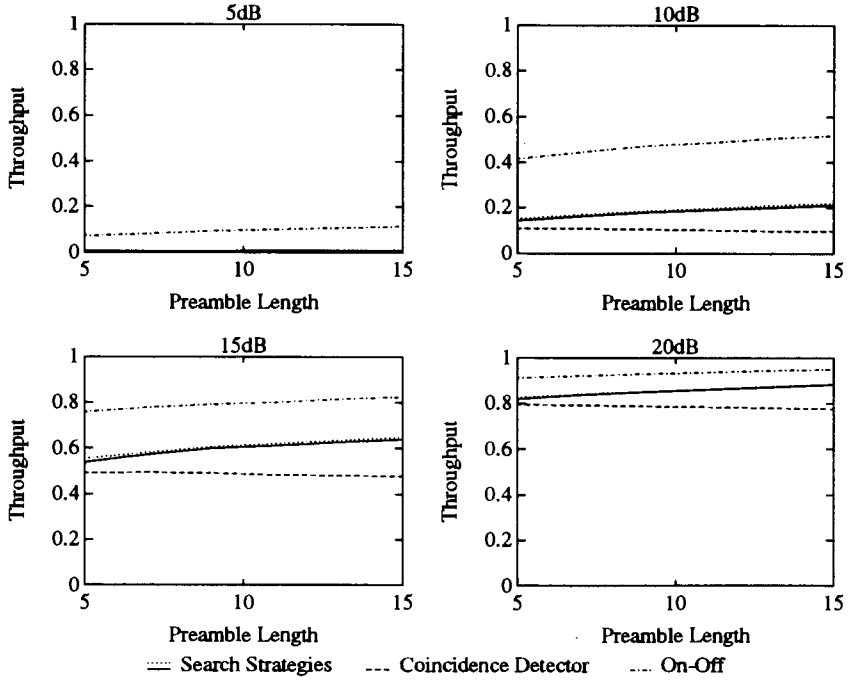

Figure 3.15: Simulation Results for a Blocking Probability of 10^{-5}.

3.8 Simulation Results for the Frequency Selective Channel

In our simulation studies, we use a two-ray frequency selective Rayleigh fading channel [32]. Three parameters are studied: 1.) various SNR, 2.) preamble length, and 3.) different distribution among the two rays. Parameters for simulations are: data rate of 16kbits/s, a fading frequency of 100Hz, PN length of 127, the propagation difference between two rays is 6μs, and a blocking probability of 10^{-5}. In each study, we fix other parameters except the one under investigation to see its effect.

Figure 3.16 shows the simulation results where only the SNR is changed. The preamble is fixed at 5 and the power is distributed equally among two rays. As one expects, the trend is increase in throughput with increasing SNR.

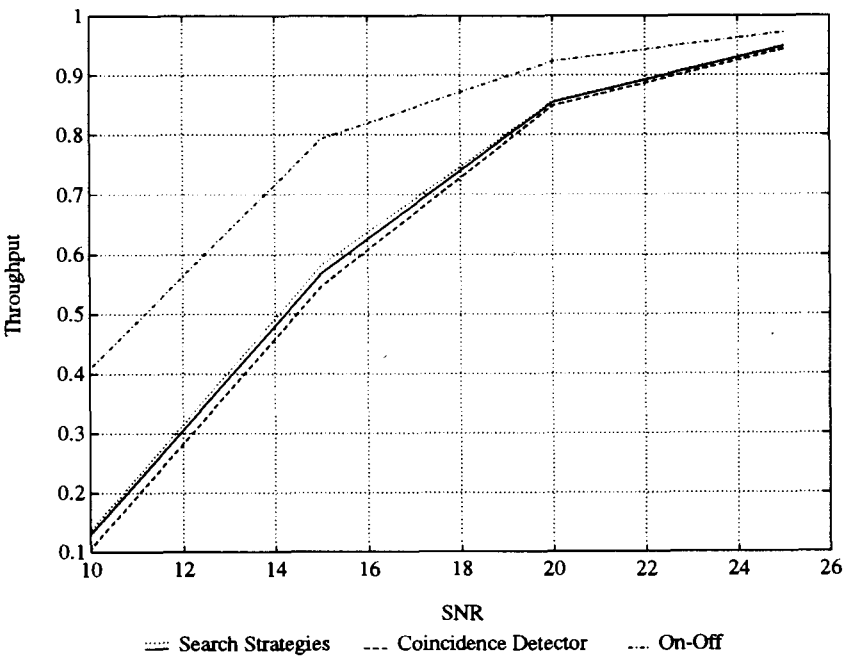

Figure 3.16: Simulation Results for: $P_b = 10^{-5}$, $L = 5$, Equal Power Distribution.

In the second study, we fix the SNR, while varying the preamble length. Figure 3.17 shows simulation results for two SNR values, 15dB and 20 dB. Generally speaking,

the throughput increases with increasing preamble length.

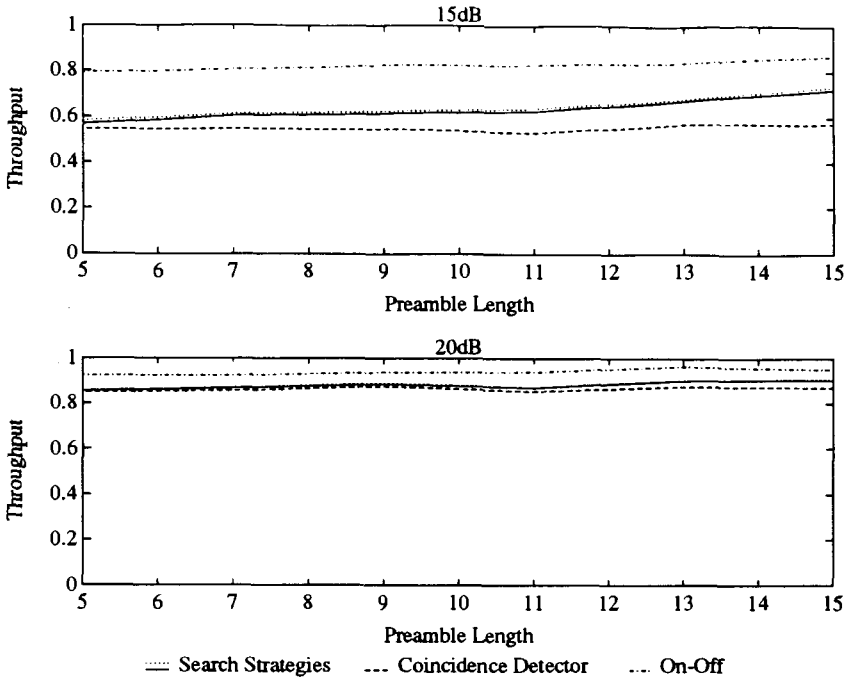

Figure 3.17: Simulation Results for: $P_b = 10^{-5}$, Equal Power Distribution.

At last, in figure 3.18, we perform simulations where we vary the distribution of energy among the two paths. The parameter is defined as the ratio of power of 1st ray to the 2nd ray.

Results show that the on-off scheme outperforms the others in all situations. Compared with the flat fading channel, we discover that the RAKE receiver can achieve similar throughput, given the same SNR. This implies that the RAKE receiver has actually performed its job of frequency diversity[6] and combining energy from all paths.

Occasionally, the algorithm will acquire on the second ray which causes a decrease in SNR when decoding the data since only energy from the second ray is obtained. In our study, we consider this situation as errors although in the real situations, locking on the second ray will only cause a lowering in SNR, result in higher bit error rate. However, results for the flat fading channel which are based on a single ray

[6]For example, if the SNR is 15dB, with equal distribution, each path will be 12dB. Without the RAKE receiver, we are tracking on only one ray of 12dB, which must be inferior to the flat fading channel of 15dB.

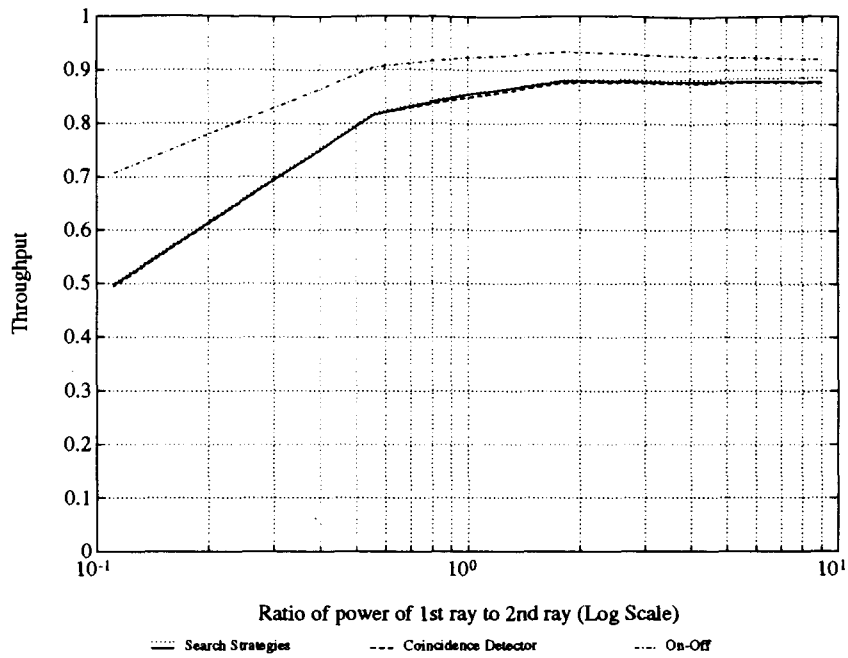

Figure 3.18: Simulation Results for: $P_b = 10^{-5}$, $L = 5$, Varying Power Distribution.

have already demonstrated that the on-off scheme will perform better than the others given the condition of missing the first one.

3.8.1 Simulations Results on a 3-Ray Frequency Selective Channel

To represents a more realistic situation, we performed additional simulations on the 3-ray channel suggested by [47]. Figure 3.19 shows simulation results for SNR equals 15dB and 20dB, with a power distribution of the three rays as (0dB,−3dB,−6dB) relative to the first ray. We can see that the results highly resembles results for a 2-ray model. This means that the RAKE receiver has performed its job of combining energy regardless of the actual distribution.

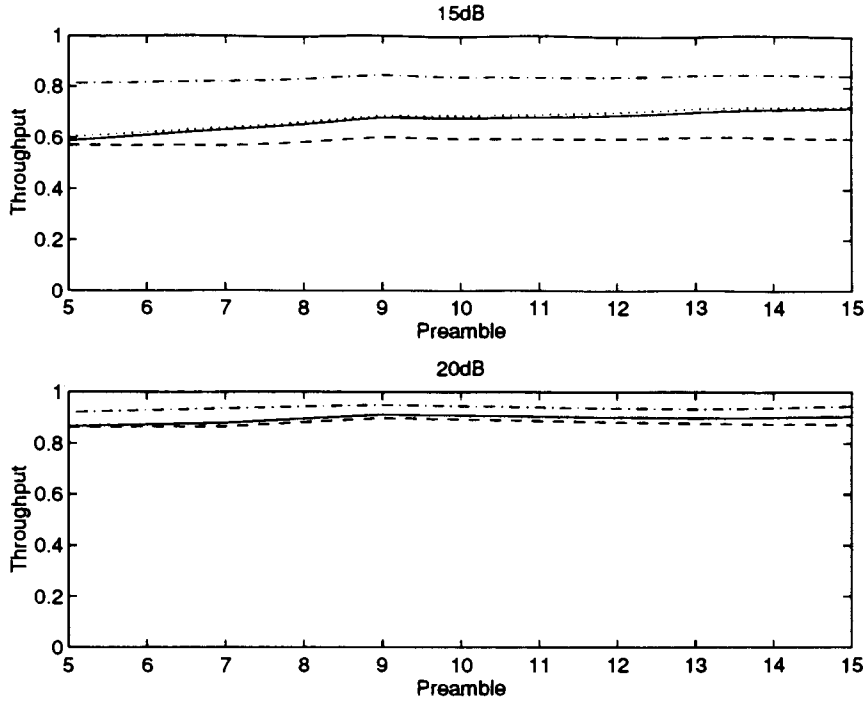

Figure 3.19: Simulation Results for a 3-ray Frequency Selective Channel.

3.9 Upper Bound Analysis

Although interleaving with coding is an effective way to combat fading, we cannot apply interleaving to the preamble section. Consequently, the preamble will consist of a train of highly correlated data symbols. Because of this high correlation among preamble symbols, exact expressions for various acquisition schemes are very difficult. Instead, we will provide analysis for the upper bound.

Our analysis is based on the outage probability and the fade duration distribution and we assume that no noise is present. The outage probability is the probability of the fading envelope to fall below a particular value. When no noise is present, the only reason for the correlator output not exceeding the threshold is because of a deep fade – the magnitude of the fading is so low that it makes the signal magnitude fall below the threshold τ set. There will be two situations in which we cannot achieve synchronization: when the whole preamble is inside a fade, or when part of the preamble is inside the fade such that the part outside is not long enough to pass

the search algorithm, as shown in figure 3.20.

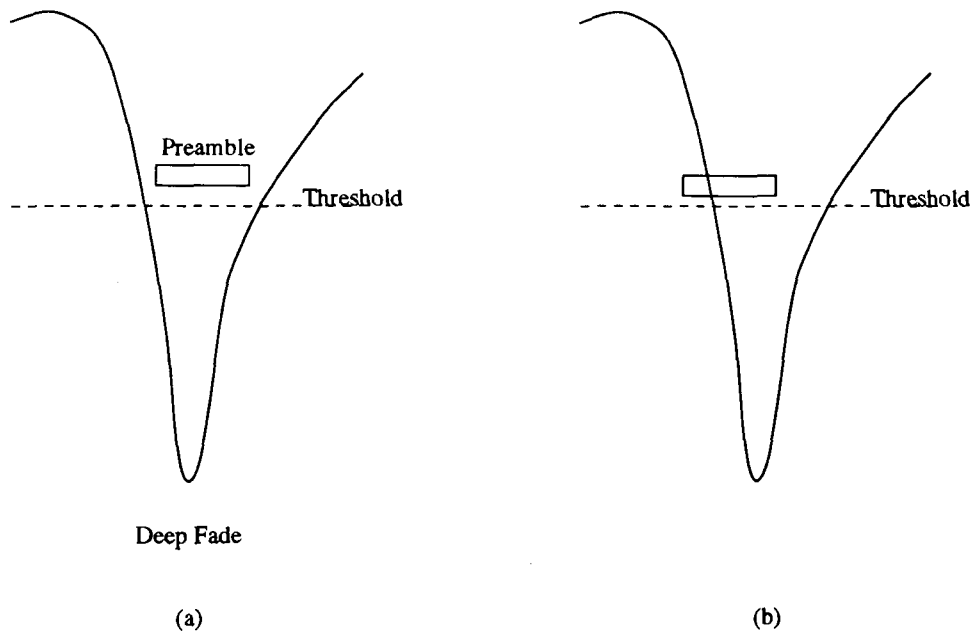

Figure 3.20: Situation not able to have PN Acquisition.

Lets define l as the fade duration, subscript o as outage and subscript m as a **MISS**. The probability of **MISS** is given by

$$P(m) = P_o(\tau) \times P(m|o), \tag{3.22}$$

where $P_o(\tau)$ is the outage probability at threshold value of τ, and $P(m|o)$ is the probability of **MISS** conditional on outage. The probability of outage $P_o(\tau)$ can be obtained by using the exponential distribution expression for the Rayleigh envelope. The value of $P(m|o)$ can be evaluated with the integration

$$\begin{aligned} P(m|o) &= \int_{l=0}^{\infty} P([m|o] \ \& \ l)dl \\ &= \int_{l=0}^{\infty} P(l)P([m|o]|l)dl. \end{aligned} \tag{3.23}$$

An expression for the fade duration has been derived in [44] for deep fade and given as

$$P(l) = \frac{2\bar{l}}{l} I_1\left(\frac{2\bar{l}^2}{\pi l^2}\right) \exp\left(-\frac{2\bar{l}^2}{\pi l^2}\right), \tag{3.24}$$

where $\bar{l}$ is the average fade duration at threshold τ. The value of $\bar{l}$ is simply given by

$$\bar{l} = P_o(\tau) \times \frac{1}{f_D}, \tag{3.25}$$

where f_D is the doppler frequency. The validity of equation 3.25 comes from the fact that the average fade duration plus the average non-fade duration must equal one fade cycle duration. The remaining unknown is the expression of $P([m|o]|l)$.

For the on-off keying technique or the Markov searches, as long as more than three bits are situated outside the fade, we can achieve acquisition. Lets mark the third bit as the point of interest and consider the situation when the fade duration is 7 bits long, ie. $l = 7$ and a preamble length of 7. As shown in figure 3.21, there are 5 positions where we will not be able to have acquisition. In general, the number of positions for a fade duration l and a preamble of length L is $l - L + 5$.

We therefore have the following equation

$$P([m|o]|l) = \begin{cases} \frac{l-L+5}{l} & l \geq L-4 \\ 0 & l < L-4 \end{cases} \tag{3.26}$$

Knowing all the equations for the unknown variables, we can use numerical integration to find the probability of **MISS** in equation (3.22). Undoubtedly, we still need the blocking probability and false alarm rate equations to find out the threshold τ. Similar techniques can be applied to find the upper bound of the coincidence detector.

Figure 3.22 shows the simulation results with the corresponding upper bound shown with points, at a blocking probability of 10^{-5} in a flat fading channel. We can observe that the bound becomes more loose as the SNR is decreased which is expected as our analysis does not include any noise effect and the discrepancy increases with decreasing SNR. Although the upper bound is based on a flat fading channel, it is also true for a frequency selective fading channel because the performance of which is below the corresponding flat fading channel.

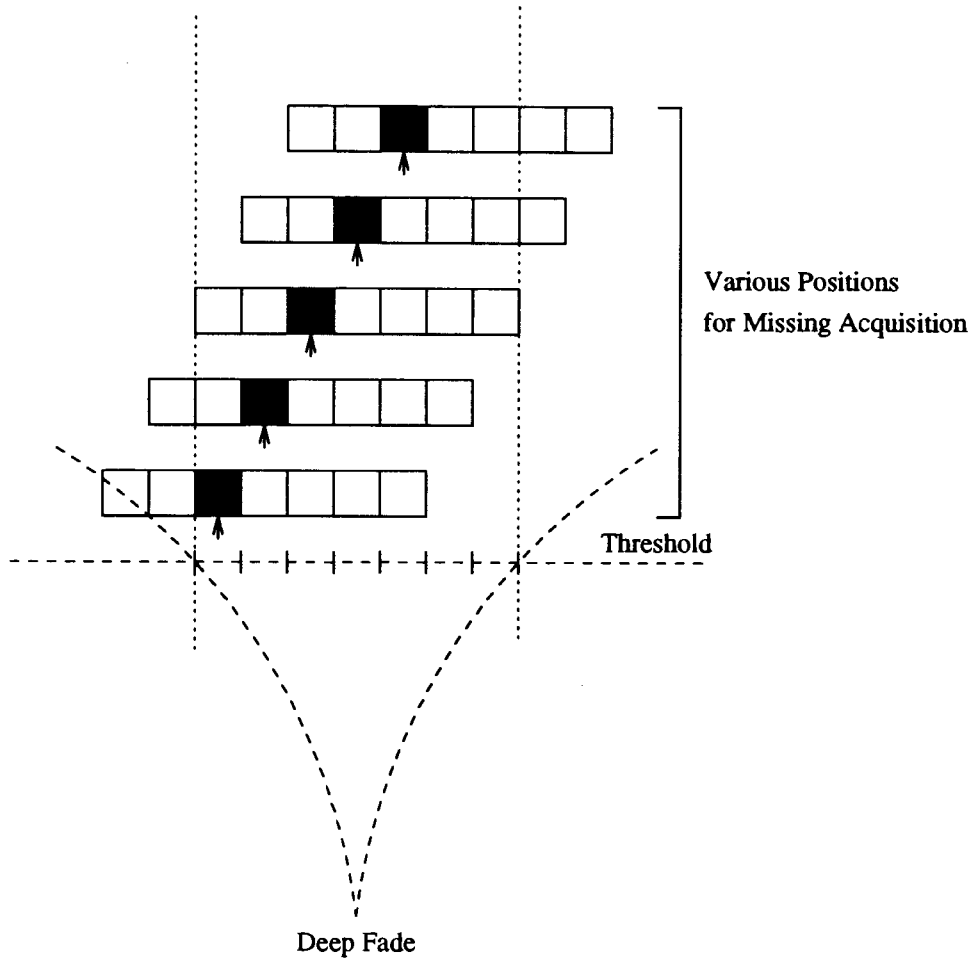

Figure 3.21: Situation for Preamble length of 7 and Fade duration of 7.

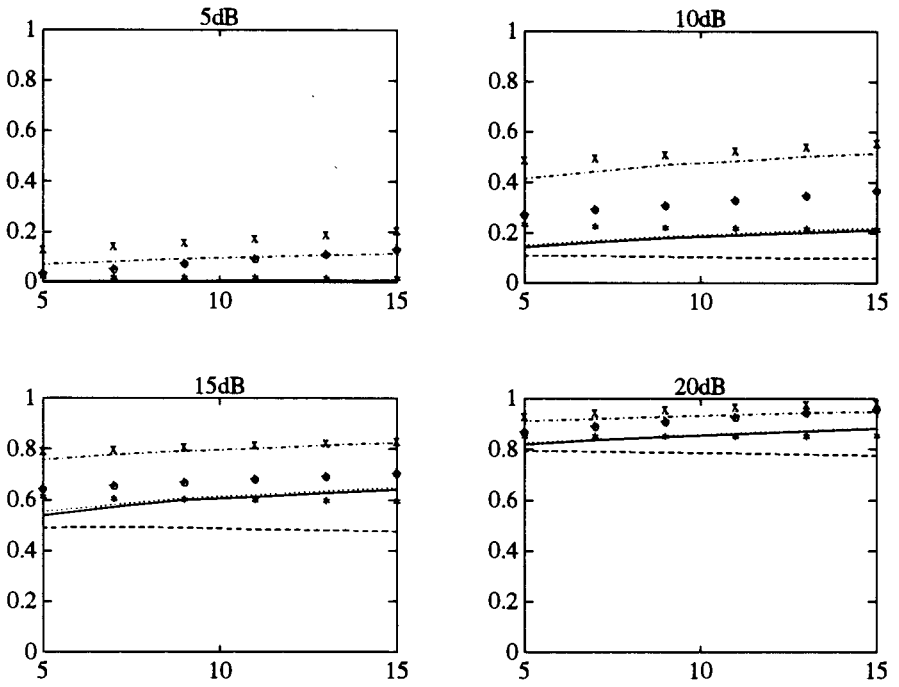

Figure 3.22: Upper Bound Result for a Flat Fading Channel.

3.10 Conclusions

In previous section, we have proposed a hardware structure for the RAKE receiver structure for the acquisition. However, the story of PN code synchronization does not end here. Following the acquisition stage will be the tracking stage where either a delay lock loop or a dither-tau loop is used. With the information provided by the RAKE algorithm about various rays' positions, an individual tracking unit is necessary for each path located. In our case, since the largest five rays are collected, we need additional four correlators (the original one can be used to track on one ray). This gives another reason to keep the total number of paths summed to be small – reducing hardware. Depending on the actual environment, a number smaller than five may be appropriate.

One thing that can be observed from the simulation results of the flat fading and the frequency selective fading channels is that the throughput does not increase significantly with the preamble length. Actually, simulations of preamble length of 35 and 65 in 20dB case have been done and the highest throughput obtained is only 0.96. This observation bears a significant effect on high level system design consideration. Since the preamble poses an overhead on the packet, it may be necessary to use a high SNR in the preamble section, rather than using a long preamble length, as the latter does not improve the throughput much. However, after the preamble section, the SNR of the actual data in the packet can be lowered to a bear minimum necessary for reliable transmission. The power varying ability, as mentioned before, is one feature of the CDMA scheme and imposes no additional hardware requirement.

On may consider the possiblility of extending the on-off pattern, for example, making the pattern as on-off-off-on.... In this way, the power of the "on" state will be tripled and the performance may become better. Following the same logic, one may conclude that the best method is one that has energy all concentrated on the first bit of the preamble, while the others are all "off" states. However, there are two reasons to prevent us from doing so. First, the partial correlation effect will become stronger and stronger as the power is increased. Second, a large number of "off" states have to be passed if we miss the first "on" bit, before we get to the next "on" state.

In this chapter, we have designed a new acquisition scheme which utilizes on-off keying during the preamble section to achieve better performance. As acquisition usually proceeds before the carrier tracking process, energy detection (square law detector) is assumed which does not need any carrier phase information. Another commonly used modulation scheme which does not require carrier synchronization is *differential detection* where data is differentially encoded/decoded. In the next chapter, we will consider a new scheme which utilizes differential detection to eliminate the carrier tracking requirement. The new differential acquisition technique can give comparable performance as the on-off keying technique described in this chapter.

Chapter 4

Barker Sequence Acquisition Scheme

Differentially coherent Phase Shift Keying (DPSK) is a modulation scheme where we transmit the difference in phase between the current symbol and the previous one. Due to the differential encoding process, the demodulation relies only on the phase difference to determine the actual symbol received. No carrier phase information is needed as long as the phase offset introduced by the transmission medium is the same for the current and the previous symbol (medium characteristics change slowly compared to data rate). This modulation scheme is particularly useful in a slow fading channel [2] to combat the random unknown carrier phase caused by fading.

The characteristic of not requiring any carrier tracking also makes DPSK a suitable candidate for the acquisition process in spread spectrum communication, where acquisition occurs before carrier tracking. Moreover, while we are unable to distinguish between a symbol of 1 and -1 in energy detection (both squares to 1), we can detect the values of data sent in DPSK. The additional information provided by DPSK can be used for frame synchronization. In this Chapter, we propose a new

acquisition method employing DPSK which can acquire both PN sequence and frame synchronization at the same time. In the new scheme, instead of using a bit streams of 1s as the preamble, a Barker sequence of length 7 is utilized. This Barker sequence is encoded by DPSK and then multiplied by the PN code before transmission. At the receiver side, we try to locate this Barker sequence to declare acquisition. The price for getting both PN code and frame synchronization at the same time is the extra hardware required. Simulation studies have revealed that this method provides comparable performance as the on-off keying technique described in previous chapter, and outperforms other conventional methods.

4.1 Differential Coherent Phase Shift Keying

To elaborate on the working principle of DPSK, assume that the received signal is first brought down to baseband, passed through a matched filter and then sampled at a time interval of T where T is the data rate. At the nth signaling interval, the output is given by

$$V_n = g_n A e^{j(\theta_n - \phi_n)} + N_n, \tag{4.1}$$

where A is the amplitude of the carrier, g_n is the magnitude of the fading process at instant n, θ_n is the phase transmitted, and N_n is AWGN. ϕ_n is any phase uncertainty introduced by the fading process. We use a decision variable U_n given by

$$\begin{aligned} U_n &= V_n V_{n-1}^* \\ &= [g_n A e^{j(\theta_n - \phi_n)} + N_n][g_{n-1} A e^{j(\theta_{n-1} - \phi_{n-1})} + N_{n-1}]^*. \end{aligned} \tag{4.2}$$

When the fading process is slow compared to the data rate $(1/T)$, $g_n \sim g_{n-1}$ and $\phi_n \sim \phi_{n-1}$. Equation 4.2 becomes

$$U_n = g_n^2 A^2 e^{j(\theta_n - \theta_{n-1})} + g_n A N_{n-1}^* e^{j(\theta_n - \phi_n)} + g_{n-1}^* A N_n e^{-j(\theta_{n-1} - \phi_{n-1})} + N_n N_{n-1}^*. \tag{4.3}$$

Without the noise, the phase decision variable is $\theta_n - \theta_{n-1}$, which means that U_n is independent of the carrier phase. The decoding process lies in comparing phases of adjacent received symbols.

4.1.1 Binary DPSK

When we use a two-point constellation, the corresponding DPSK is called binary DPSK. The transmitted signal is the same as in BPSK except that we encode the binary source sequence into a differential binary sequence first. Suppose $a_k\{1,0\}$ is the original data sequence, the differential sequence is given by

$$b_k = a_k \oplus b_{k-1}, \tag{4.4}$$

where the symbol $\oplus$ denotes modulo-2 operation. Lets look at the example shown in Table 4.1. Here, the input sequence a_k is differentially encoded into sequence b_k, where a symbol of 0 is transmitted with phase π and 1 as phase 0.

Input sequence (a_k)	1	1	0	0	1	0	0	1	1	
Encoded sequency (b_k)	1	0	1	1	1	0	0	0	1	0
Transmitted Phase	0	π	0	0	0	π	π	π	0	π
Output sequence ($\hat{a}_k$)	1	1	0	0	1	0	0	1	1	

Table 4.1: Differential Encoding and Decoding

4.2 Barker Sequence

A Barker sequence or a Barker code is a very small set of binary sequences with outstanding full-length and partial-length autocorrelation [37]. Denote the autocorrelation as $R(\tau)$ of a Barker code of length $\mathcal{N}$, $R(\tau)$ has a peak value of $\mathcal{N}$ at $\tau = 0$, and low values otherwise. Due to its good auto-correlation property (high peak at $\tau = 0$, and low otherwise), a Barker code can serve for synchronization, for example, in satellite communications. An example of the autocorrelation of a Barker sequence of length 7 is shown in figure 4.1.

The total number of Barker sequences is limited. It has been proved that no Barker codes of odd length greater than 13 exist, and that if any others of even length

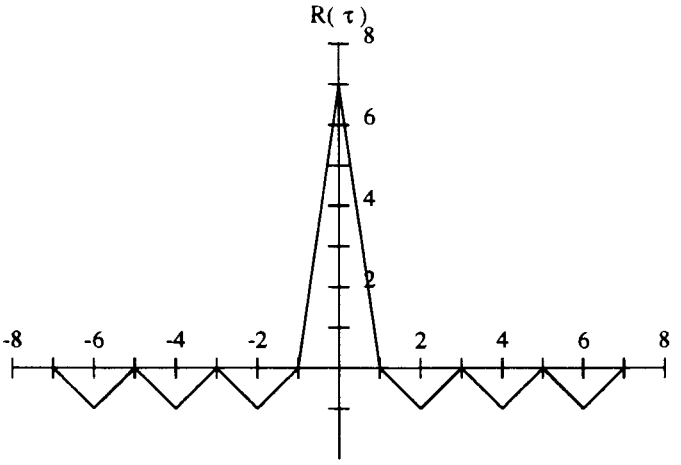

Figure 4.1: Barker Code Autocorrelation.

exists, the length must be the square of an integer [37]. To use the Barker sequence for synchronization purpose, we continuously monitor the correlation between signal after despreading and differential decoding, and the local Barker sequence. When the output becomes high, synchronization is declared. The mechanism is similar to a PN code despreading process. Actually, a Barker code can serve as a PN sequence[1], but its short length (< 13) prevents its use in spread spectrum communication. As a result, the main use of Barker code lies in frame synchronization – to detect the boundary of frame.

4.3 Acquisition Scheme using Differentially Encoded Barker Sequence

One preliminary requirement of spread spectrum acquisition is that we do not have carrier synchronization before acquisition [12]. An energy detector is a device which does not require carrier phase information. However, it also cannot differentiate a

[1] Barker codes of length 3 or 7 are maximal sequences also!

symbol of 1 or -1 because of the squaring process. On the other hand, if we use DPSK, we can obtain valuable information on the symbols sent. In our proposed method here, we take advantage of this DPSK characteristic and encode a Barker sequence in the preamble, so that we can obtain both chip and frame synchronization at the same time.

We use a Barker sequence of length 7, that is 0001101. This Barker sequence is particularly favorable for our application because the autocorrelation has a value of either 0 or -1 when $\tau \neq 0$ (this issue will become more clear when we describe the algorithm). In order to encode the Barker sequence with DPSK, we have to add an extra bit at the beginning to serve as a phase reference purpose. The preamble length then becomes 8 bits long. The preamble sequence 10001101, is differentially encoded to 11110110 and sent using BPSK. The new preamble, after concatenation with useful data, will be spreaded with the PN code, and then modulated with the carrier for transmission, as shown in figure 4.2.

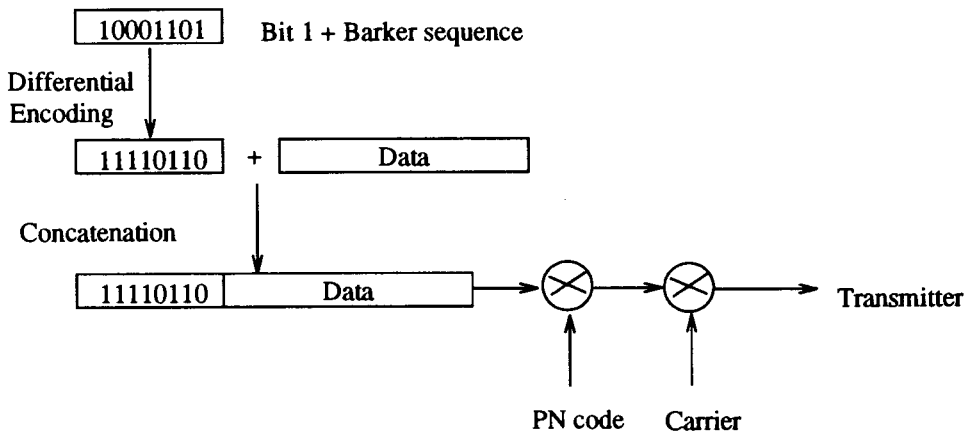

Figure 4.2: Transmission of Acquisition Scheme using Differentially Encoded Barker Sequence.

4.3.1 Receiver Hardware Implementation

The structure of the demodulator is similar to the one used for the on-off keying scheme with minor modifications, as shown in figure 4.3. There are two levels of correlation, one for the PN code despreading and one for the Barker Sequence, performed separately by the decoder and the processing unit respectively. The extra hardware required are the differential decoder, and a longer memory array capable for storing outputs of length 7 symbols long. The incoming signal is sampled at

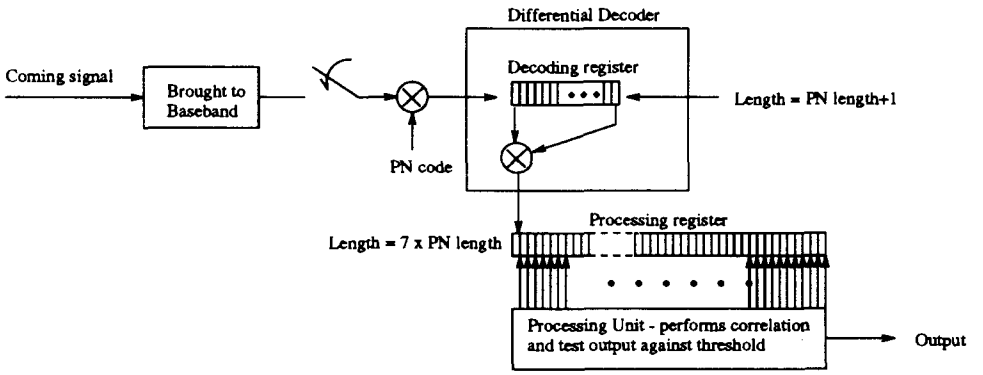

Figure 4.3: Hardware Implementation for Acquisition Scheme using Differentially Encoded Barker Sequence.

a rate of $\frac{\Delta}{T_c}$, and the outputs are shifted into a register where they are multiplied with the local PN code for despreading. As shown in figure 4.3, the outputs of the correlator are shifted into the decoding register with length = PN code length + 1, used for storing values for differential decoding. The length of the register required is one longer than the PN code because we need to multiply one sample with another, located exactly one PN code earlier. The decoder will forward outputs to the processing register where Barker sequence correlation is done. This register has a length equal to (Barker sequence Length $\times$ PN length). When the whole preamble has been differentially decoded, the processing shift register will contain a pattern that follows the Barker sequence. For example, the values in the register are as shown in figure 4.4. The register can be divided into 7 segments, each with length equals one PN code and corresponds to one bit in the Barker sequence. By multiplying each segment with the corresponding bit in the Barker sequence, we sum up the results to

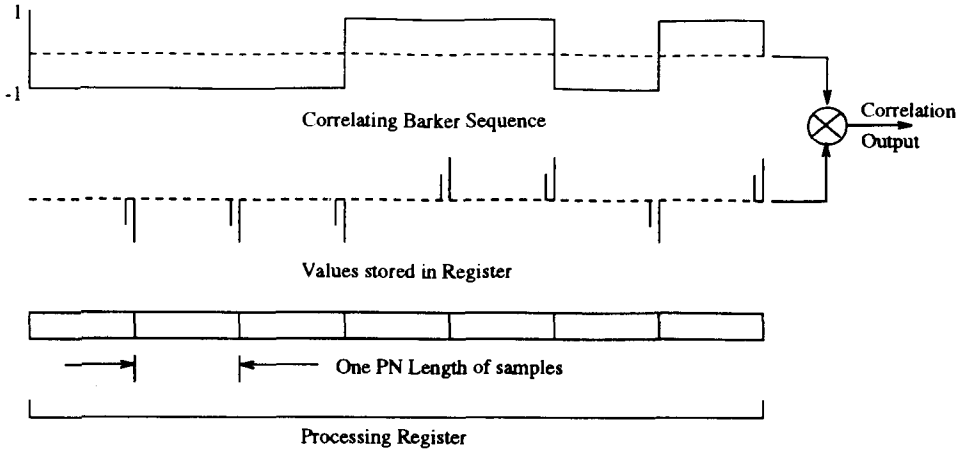

Figure 4.4: Encoder Outputs following the Barker Sequence

get the correlation output. This operation requires (7 × PN length) multiplications. The summation process captures energy for various path and performs the RAKE receiver's operation. In reality, we don't need to perform correlation for the whole register. For example, in a flat fading channel, only the first location in each segment contains the incoming signal's power. We only need to capture energy in this position and it requires a minimum of 7 multiplications. To obtain satisfactory results in a frequency selective fading channel, we require (7 × delay spread[2]) multiplications, as shown in figure 4.5. This saves processing power required and at the same time, keeps the noise level lower. In our experiment, we sum up 30 locations(taps)[3] for each segment. The output of the correlation is compared with a threshold determined by the false alarm rate desired. We have assumed the use of a digital matched filter in the hardware implementation, which we believe is the only matched filter possible in this situation. If we use an active integrator instead, the integration time will be 7 symbols long to get one output. The time delay between each output will be too long to make it practical in real situations.

We elaborate on the role of the Barker sequence by considering the situation when a Barker sequence is not used. Lets assume that we use a bit stream of 1s for the

[2]The delay spread is in samples.

[3]We sum up 30 instead of 5 taps as in the on-off keying technique because of the more prominent partial correlation effect explained in coming sections. Summing up more taps makes the threshold higher which helps to cover up partial correlation.

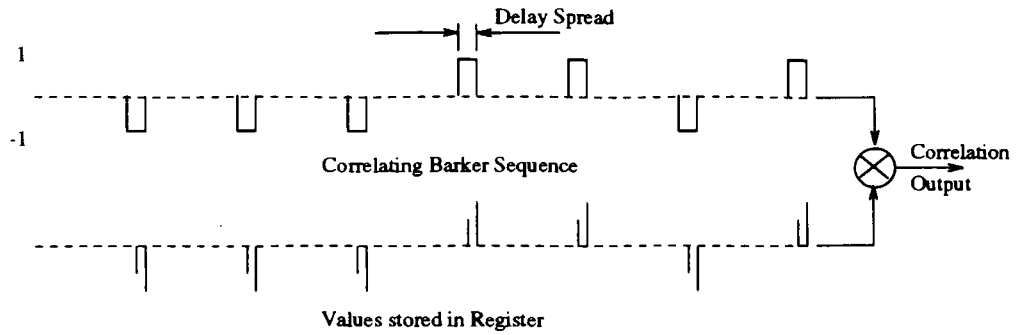

Figure 4.5: Actual Barker Sequence Correlation.

preamble instead. A problem arises when the preamble section has not been decoded completely. Suppose that only the first three bits have been decoded, as shown in figure 4.6, the correlation output will be high enough to cross the threshold. However,

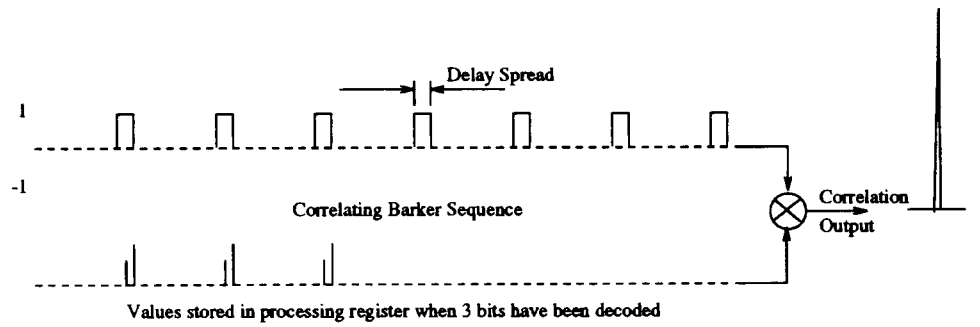

Figure 4.6: Partial Decoding Situation when not using a Barker Sequence.

we cannot achieve frame synchronization in this way. When a Barker sequence is used, the autocorrelation properties of the Barker sequence will keep the value of partial decoding low.

4.4 Two Steps Algorithm

We have assumed in the above sections that we can get alignment of the first ray in a frequency selective channel. In other words, we know when the first ray of the first

decoded symbol reaches the rightmost location in the processing register. To do so, we use a similar scheme as in the on-off keying method: *double threshold detection.* As a preliminary stage, the sum of one tap for each segment is used to find a preliminary correlation output which is tested against a threshold $\tau_{preliminary}$, based on a false alarm rate of 10^{-5}. The tap used is the one on the rightmost of each segment. When $\tau_{preliminary}$ is crossed, a 30 tap correlation for each segment is collected and tested against the actual τ as desired. This serves as a mean to align the first ray of the first symbol to the rightmost position of the processing register, so that the 30 taps cover the delay spread of incoming signal. Besides, it also eases the burden of the processing unit as we only do a 30 taps correlation when necessary.

4.5 False Alarm Rate and Blocking Probability

The false alarm rate is the probability of the Barker correlation output exceeding the threshold τ, when no signal is present. Consider the case when only AWGN of variance $n \sim (0, \sigma^2)$ present in the incoming signal. Due to the differential decoding scheme used, each value $\hat{N}_n$ in the processing register is the multiplication of two random noise values, separated by a difference of one PN code in time,

$$\hat{N}_n = n_n \times n_{n-PN\ length}. \tag{4.5}$$

The first and second moment of $\hat{N}_n$ are given by equations

$$E\{\hat{N}_n\} = E\{n_n\} \times E\{n_{n-PN\ length}\} = 0 \tag{4.6}$$

$$E\{\hat{N}_n^2\} = E\{n_n^2\} \times E\{n_{n-PN\ length}^2\} = \sigma^4. \tag{4.7}$$

The distribution of $\hat{N}_n$, which is the multiplication of two Gaussian random variable is symmetric which does not result in any know distribution. However, when a large number of $\hat{N}_n$ are added, the Central Limit Theorem gets into effect, resulting in a Gaussian distribution. Through Monte Carlo simulation, we have verified that the resultant distribution is Gaussian with variance of $m\sigma^4$ where m is the total number of taps in the Barker correlator and $m = 7 \times$ (taps used in one symbol). We use

this distribution to set the threshold for a desired false alarm rate, which in turn is determined by the blocking probability. When we are considering only the noise effect, the differential decoding process will either increase or decrease the noise effect, depending on whether the SNR is greater than zero or not respectively. We have to stress that only when we are considering the false alarm that the relative noise power can be reduced (for SNR > 0). When symbols are present in the incoming signal, there are other terms (multiplication of signal with noise) that cause a degradation of 3dB in performance when compared to BPSK.

The blocking probability expression for this method is the same as the coincidence detection, as we assume that the receiver will become busy for a period of $L-1$ symbols long. The equations are

$$P_b = \frac{\bar{B}}{\bar{B} + \bar{A}}, \tag{4.8}$$

and

$$\bar{B} = \{P_{fa}[(L-1) + L_D] + (1 - P_{fa})(L-1)\} \times T, \tag{4.9}$$

and the value of $\bar{A}$ is $\frac{T_c}{P_{fa}}$.

4.6 Partial Correlation

Figure 4.7 shows the correlator output (after PN code despreading) for a preamble following a Barker sequence which has passed through a 2-ray channel without noise. We can see that partial correlation interference occurs one symbol before the first bit. Moreover, the same phenomenon occurs between boundary of two symbols of opposite signs. The two effects combined together means a high correlation output within one symbol before the actual acquisition position. In the acquisition scheme using differentially encoded Barker sequence. The partial correlation bears two aspects: 1) partial correlation of the PN sequence, 2) partial correlation of the Barker sequence. Since we use the same PN sequence as in previous chapter, the magnitude of partial correlation is actually the same as before. However, even with the same false alarm, the threshold τ is lower because of the Gaussian distribution characteristic (compared

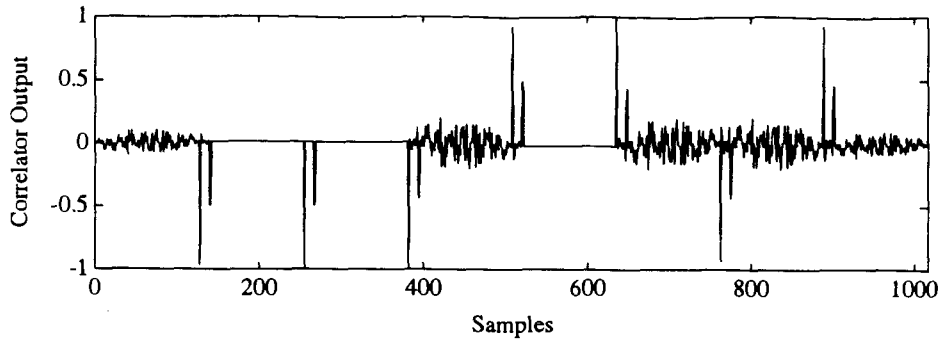

Figure 4.7: Partial Correlation.

to a Gamma distribution) and also the reduction in noise by the differential decoding process when SNR > 0. The lower threshold implies a high chance of crossing threshold by partial correlation, resulting in wrong acquisition. A compromise exists here: when the differential decoding process decreases the noise level (SNR > 0), it also increases the vulnerability to partial correlation of the PN sequence. As a remedy, the $\tau_{preliminary}$ is designed to give a false alarm of 10^{-5}, a lower value than the 10^{-3} as in the previous case. The lower false alarm rate requires a higher threshold and covers up the partial correlation effect.

The choice of a Barker sequence with length 7 gives very desirable partial correlation properties: a value of 0 or -1 when not synchronized. If a Barker sequence of 5 is used instead which gives a output of 1 for $R(\tau = -5)$, we may acquire incorrectly at this position.

Another undesirable effect of using differential detection comes from the additional bit we need to put in front of the Barker sequence. The decoding process will multiply this value of 1 with a noise sample PN code length in front of it. When the noise is high (occasionally happens because of random Gaussian noise process), this multiplication gives a high value. The sign of this multiplication depends on the sign of the noise sample, which has 0.5 probability of being negative or positive. When the multiplication result is positive, we may end up in a wrong acquisition shown in figure 4.8. This effect can be eliminated by using the same windowing technique as in the on-off keying scheme (explained in next section).

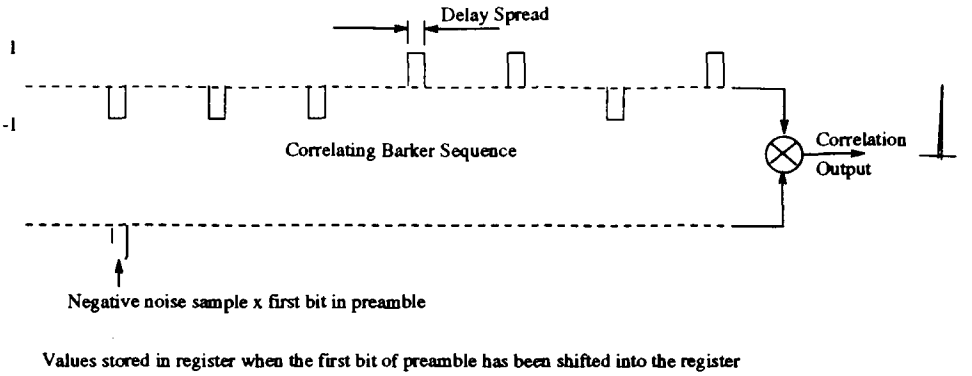

Figure 4.8: Wrong Acquisition due to Additional Symbol Added for Differential Detection.

4.7 Windowing Technique

For this method, we also apply the same windowing technique used in previous chapter here to improve the performance: *once both* $\tau_{preliminary}$ *and* τ *are crossed, we open up a window of length w, and see if any other gives a better correlation.* The windowing technique helps to combat the partial correlation effect and, by making the window size slightly larger than one PN code length (we use [one PN code + 5 taps]), the problem caused by the extra bit added in the beginning of the preamble can be solved too.

4.8 Simulations on a Frequency Selective Fading Channel

We perform simulations on a frequency selective channel for this new acquisition technique using a differentially encoded Barker sequence. A two-ray frequency selective channel is used [32] with a delay spread between the two rays of $10\mu s$, a PN code of length 127 and data rate of 16 kbits/s, same as before. We will compare the

performance of the new method with the on-off keying technique.

Figure 4.9 shows simulation results for a blocking probability of 10^{-5}, a nominal SNR of 20 dB, with varying power distribution among the two paths. The solid line represents the Barker sequence method, and the dotted line is on-off keying technique. We can observe from the graph that the Barker sequence technique gives a higher

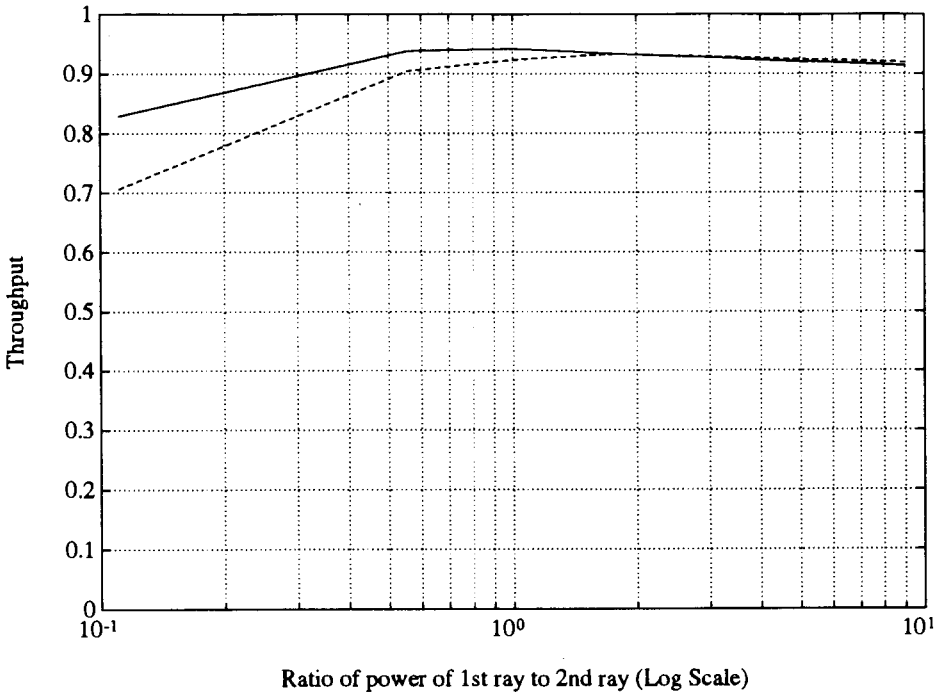

Figure 4.9: Comparisons of Performance between Barker Sequence Method and On-Off keying technique with varying Power Distribution.

output when the ratio is low, and the two graphs merge together when the ratio increases, that is, the case of a flat fading channel. Looking at the exact numbers more closely, we discover that at a ray ratio of 9, the throughput is 0.914 and 0.920 for the Barker sequence and the on-off keying method respectively. The higher the power of the first ray, the higher will be the partial correlation which causes a degradation in the performance of the Barker sequence method. The partial correlation effect will become even more prominent when we consider the performance of varying SNR as shown below in figure 4.10. Again, the solid line is the Barker sequence technique while the dotted line is the on-off keying method. The on-off keying technique gives

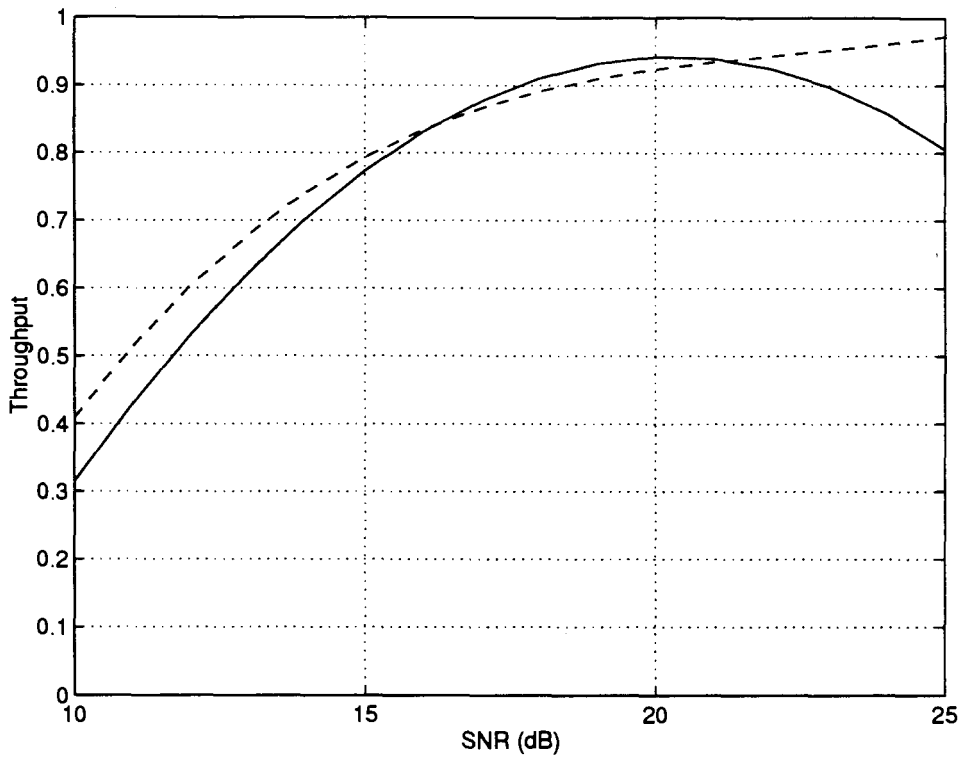

Figure 4.10: Comparisons of Performance between Barker Sequence Method and On-Off keying technique with varying SNR.

slightly higher throughput than the Barker sequence method for SNR ranging from 10dB to $\sim$ 17dB. The Barker sequence technique works better for $\sim$(17-21)dB, but the performance degrades with increasing SNR. The decrease is again due to the partial correlation effect.

4.8.1 Results on a 3-ray Frequency Selective Channel

Similar as the on-off scheme, we also perform studies on a 3-ray frequency selective channel. Figure 4.11 shows the simulation results for a 3-ray distribution of (0dB,$-$3dB,$-$6dB) relative to the first ray. The results are again similar to the 2-ray

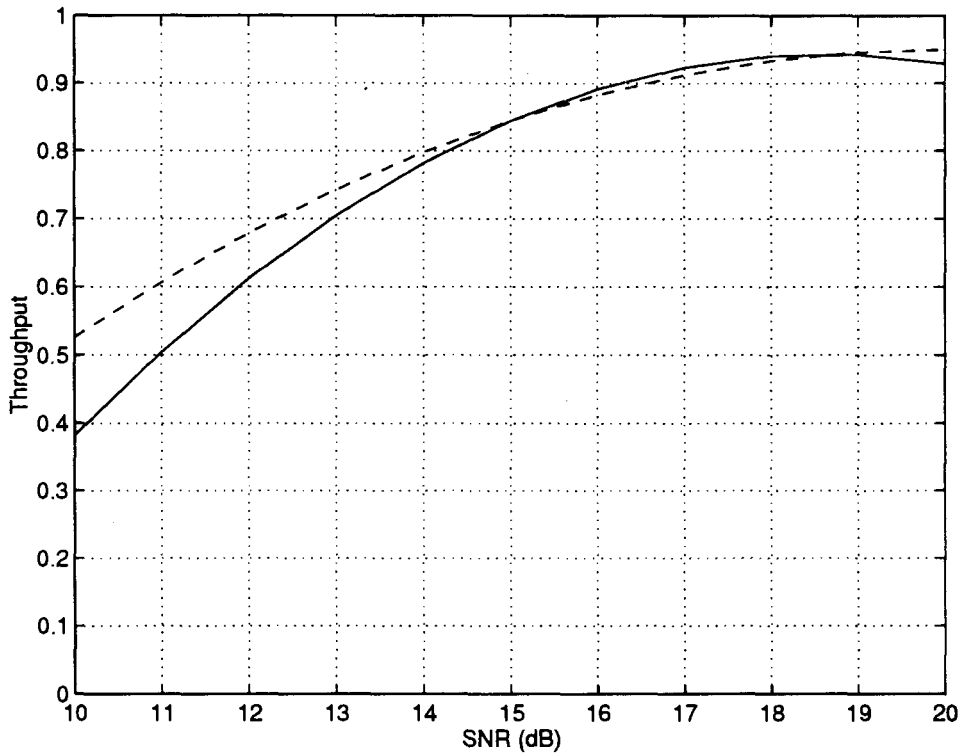

Figure 4.11: Comparisons of Performance between Barker Sequence Method and On-Off keying technique in a 3-ray Frequency Selective Channel.

channel.

4.9 Conclusions

We can observe from the results of previous section that the new method can achieve similar performance to the on-off keying technique. One advantage of the Barker sequence scheme is that it achieve both PN code and frame synchronization at the same time, while in methods described in previous chapter, we still need to search for a marker inside the packet to locate the start of data. In this way, the Barker sequence method will be more efficient in terms of preamble length needed. However, it also requires more hardware and processing power when compared to the on-off keying technique.

Given the same false alarm required, the on-off keying method gives a higher threshold value required which probably covers up the PN sequence partial correlation. The high threshold results from the Gamma distribution of noise output. In the Barker sequence method, the output noise variance is first reduced by the differential decoding process and the distribution is Gaussian. The two effects combined together results in a much lower threshold which may not exceed the partial correlation. Therefore, even though we have applied the same two-level algorithm and windowing techniques in both cases, the partial correlation effect is more prominent in the Barker sequence method. The situation gets even worse when the SNR becomes higher (in contradiction to intuition). We have to note here that we don't mean that the partial correlation effect does not exist in the on-off keying technique, but it just occurs when the SNR becomes really high, for example, over 30dB.

A remedy to the situation of the Barker sequence seems to be simply decrease the false alarm rate. However, when the SNR gets higher, the noise variance decreases and the bell-shaped Gaussian distribution gets compressed on the x-axis. This compression effect happens faster than the increase in threshold caused by lower false alarm rate, making it ineffective. Another method is by increasing the threshold so until it can cover up the partial correlation. This method becomes *ad hoc* as we lose the mathematical background for a constant blocking probability or false alarm rate criteria.

Chapter 5

Power Control in Acquisition

Power control is an *essential* component in any CDMA system. The purpose is to maintain a nominal received signal power. This solves the near-far interferences problem, reduces interference to other mobiles, helps to overcome fading, and conserves battery in portable and mobile units. The nominal power value is designed in a way to maintain the necessary SNR for acceptable error probability. While achieving the above goal, we try to keep SNR as low as possible, so that the power consumption is low and interference to others is minimal. It can be shown that the system capacity is maximized if the transmit power of each user is controlled so that the signal power at the cell receiver is the minimum required to achieve a predetermined signal-to-noise ratio (SNR) [43]. In the ideal situation, when the power control update rate is fast compared to the fade rate, we can eliminate fading completely and the channel is equivalent to an additive white Gaussian (AWGN) channel. Although two kinds of power control are available: *open-loop* and *close-loop*, only open loop power control can be obtained during the preamble section because a close loop configuration implicitly requires PN code despreading. The noise present in the synchronization symbols received, on the other hand, makes the open loop control imperfect. As a result, instead of obtaining a AWGN channel, we will have characteristics in between a AWGN channel and the fading channel.

In this chapter, we will consider the effect of power control on our synchronization algorithms. Simulation results were performed which shows that our acquisition algorithms (on-off keying and Barker sequence method) also perform in a superior manner than the conventional ones under a AWGN channel. After demonstrating superiority in both extremes (AWGN and fading), we can draw the conclusion that our acquisition schemes can perform better in real situations where we have characteristics in between.

5.1 Open and Close Loop Power Control

Power control can be classified as two types: *open-loop* and *close-loop* power control. The difference is the existence of a feed-back mechanism in the latter case.

5.1.1 Open-Loop Power Control

For open-loop power control, the transmitter constantly estimates the channel degradations and updates its transmission power accordingly. As an example, if the transmitter knows that there is a 5dB decrease in signal power from the transmitter to the receiver, then the transmitted power is changed to 5dB higher than the nominal. Under this scenario, the cell site has to transmit synchronization symbols to the mobile between regular intervals. It is from these symbols received that the channel characteristics are estimated. The more frequent these symbols are sent, the better the channel characteristics estimation will be. However, it also means increased bandwidth requirements and power. The degradation in SNR by the channel is simply calculated by the difference between the transmitted power and the received power. In other words, the transmitter power must be fixed, and power control on the synchronization symbols is prohibited because the receiver has no way to know the transmitted power if power control is in effect. In our case, we can either set up

a synchronization channel as in the Qualcomm [1] system, or use pilot symbols[1].

One difficulty in channel estimation is that the forward and the reverse link is usually separated and located in different bandwidth This means that each of them will have independent channel characteristics. In other words, the information provided by the synchronization symbols in the forward link does not convey characteristics of the reverse link, and vice versa.

5.1.2 Closed-Loop Power Control

In closed-loop power control, there is feedback between the receiver and the transmitter. A common closed-loop configuration is shown in figure 5.1. The receiver compares

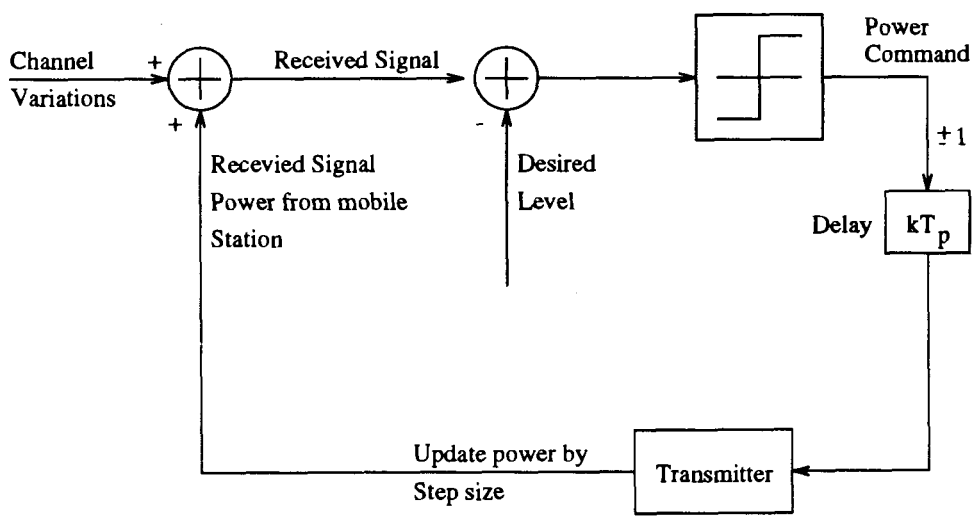

Figure 5.1: Closed Loop Power Control.

the received signal power with the nominal $P_{nominal}$ once every T_p second, where T_p is the power control sampling interval. When the received signal is higher than $P_{nominal}$, a decrease power command is transmitted back from the receiver to the transmitter; otherwise, an increase power command is sent. Upon receiving the power control command from the receiver, the transmitter either increases the transmitted power

[1]If we insert pilot symbols, the symbols must be of fixed SNR also.

by Δp dB (increase power command) or decreases the power by Δp dB. A fixed step update Δp makes it possible for using only one bit in the command from the receiver to the transmitter, thus reducing the link traffic. Moreover, the fixed step update mechanism bears low-pass characteristics to filter out additive noise introduced by the channel. Due to the propagation delay in the closed-loop configuration, when the transmitter receives the power update command, the characteristics of the channel may have altered. This delay, together with the fixed step power control limitation, makes it impossible to provide rapid response in a period of a few microseconds [1]. As a result, a combination of open loop and closed loop control is used in practice, while the former gives quick response, the latter compromises the inaccuracy of channel estimation due to forward/reverse channel bandwidth separation.

5.2 Power Control in PN Code Acquisition

Under the closed-loop configuration, the receiver must be able to despread the PN code and restore the original signal power to compare it with $P_{nominal}$ to determine the power update command. In other words, PN code synchronization is assumed. Since PN code acquisition occurs before any real data communication possible, we cannot have close-loop power control during preamble section. Even if we obtain some form of close-loop control, for example, in the on-off scheme or the search strategy, the base station sends an power update command when it detects the first threshold crossing before even jumping to the verification stage, the propagation delay means that the mobile would have already finished sending the preamble before it receives the power update command. Therefore, we conclude that close-loop control is not possible during acquisition.

We have to resort to open-loop power control during acquisition. As we have mentioned before, the forward and the reverse channels are usually located in different bandwidths. In that way, the two channels will have independent fading processes, which makes the open loop control highly ineffective. The separation of the forward and reverse channel is necessary in the first generation cellular phones where FM

modulation is used and this approach is inherited by many CDMA research groups [1, 39]. However, we believe that in CDMA, we can superimpose a synchronization channel on the same frequency band as the reverse channel. The base station will send out synchronization symbols in this channel at a fixed SNR between regular intervals, T_p. The only difference between the superimposed synchronization channel and the reverse channel is that it uses a different PN code.

Although the base station sends an additional message on the reverse channel, the SNR of the received signal remains unchanged because the base station can subtract the synchronization symbol from the received signal first before any processing. The reverse channel works as if no synchronization symbol is sent by the base station. Now, the synchronization channel and the reverse channel share the same bandwidth, and they should have similar fading characteristics.

Besides the difference in the bandwidth location of the forward and reverse links, another source of wrong estimation is the AWGN noise. When the SNR is low, the synchronization symbols received will be in great discrepancy from the actual fading profile, which makes the open-loop power control based on the information thus provided erroneous. The noise in the synchronization channel makes it impossible to achieve an AWGN channel even when we have perfect open loop power control, especially at low SNR. The fixed step update in the close-loop control, on the hand, processes low-pass characteristics which helps to filter out the noise. We also borrow the idea of fixed step update to open-loop power control so that we gain advantage of noise filtering. The result is a channel with characteristics in between a AWGN and the fading channel investigated.

5.3 Power Update period T_p

The power control update time T_p is very important parameter in eliminating the fading effect. The faster the update rate (shorter T_p), the more the channel approaching a AWGN channel. The update period T_p should be short compared with the average

fade duration. We define the ratio of power update rate to fade rate as the control parameter, called *relative power control rate (RPCR).*

$$\text{Relative Power Control Rate} = \frac{1}{f_D T_p}, \tag{5.1}$$

where f_D is the fade rate. It has been shown in [39] that even with a RPCR of 10 and a fixed update step of 1dB in a closed loop configuration, the residue fade is still very significant. Since open loop control is the only mechanism possible during the preamble section, we will put a closer look into its performance. Again, we use the RPCR as our parameter. We will assume a fade rate of 100 Hz, which is typical for a moving mobile. Moreover, to make the situation more realistic, we simulate a two-way frequency selective channel, instead of a flat fading channel used in [39]. Figure 5.2 and figure 5.3 show the simulation results for various RPCR at SNR of 10dB and 20dB respectively. The solid line represents the original fading profile, while the dotted line is the one after open-loop power control.

For the simulations, we have assumed that the forward and the reverse links share the same bandwidth and therefore has the same fading characteristics. Our simulation results on a RPCR of 10 is in close agreement with those results shown in [39]. We can observe from the figures that, only when the RPCR exceeds a value of 40 will the channel approach a AWGN channel. That in term translate to a data rate of $40 \times 100 = 4$kbits/s in the synchronization channel. Of course, a synchronization bit rate higher than 4kbits/s will provide a better approximation to the AWGN channel. However, too high a synchronization bit rate will impose too high an overhead in terms of processing ability for both the base station and the mobile units.

Looking carefully at the two figures, we can discover that given that same value of RPCR, the one for 20dB is more close to a AWGN channel. This is as expected because for lower SNR, the noise is greater causing more serious errors in channel estimation.

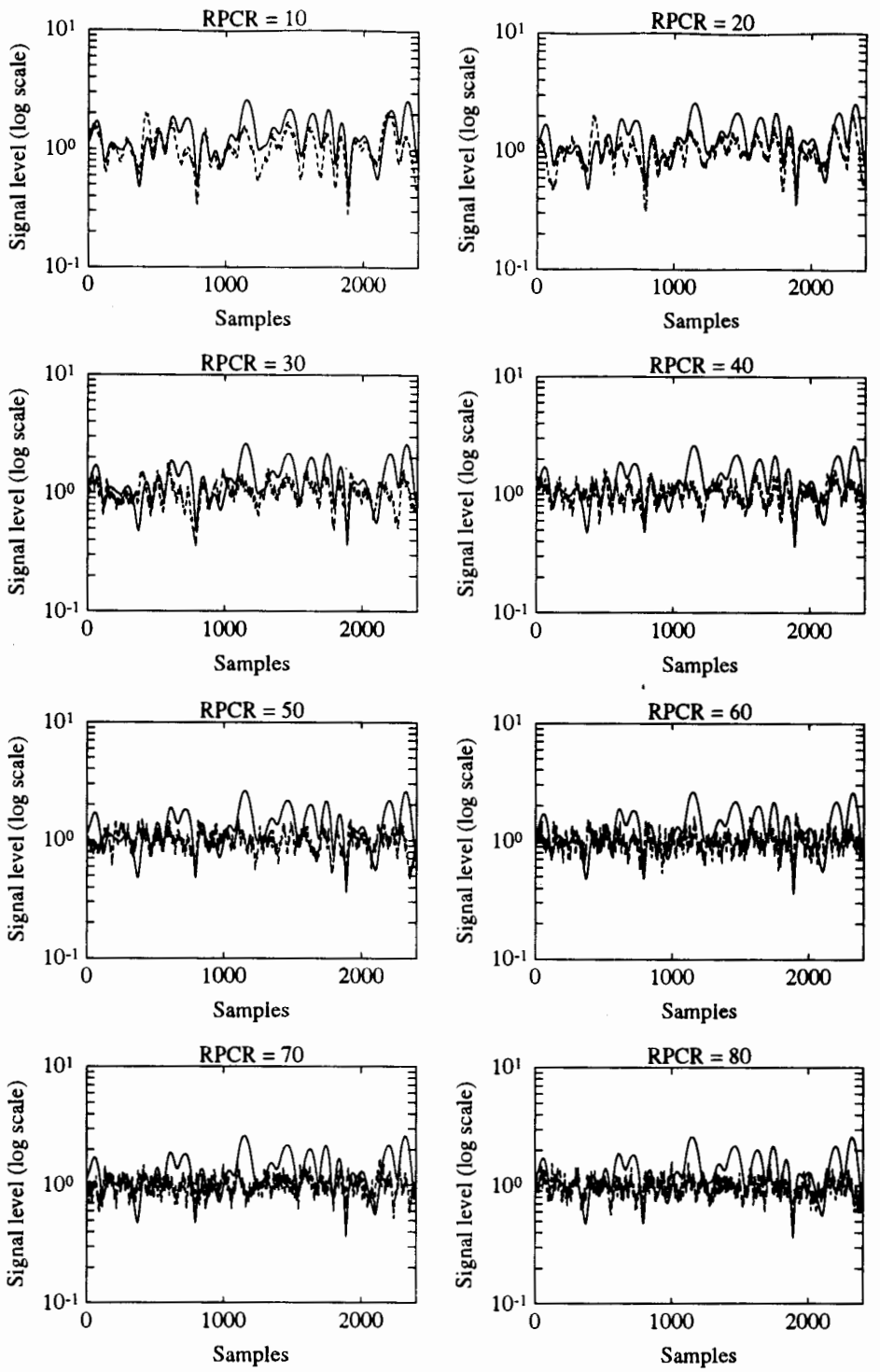

Figure 5.2: Open Loop Power Control Simulation for 10dB.

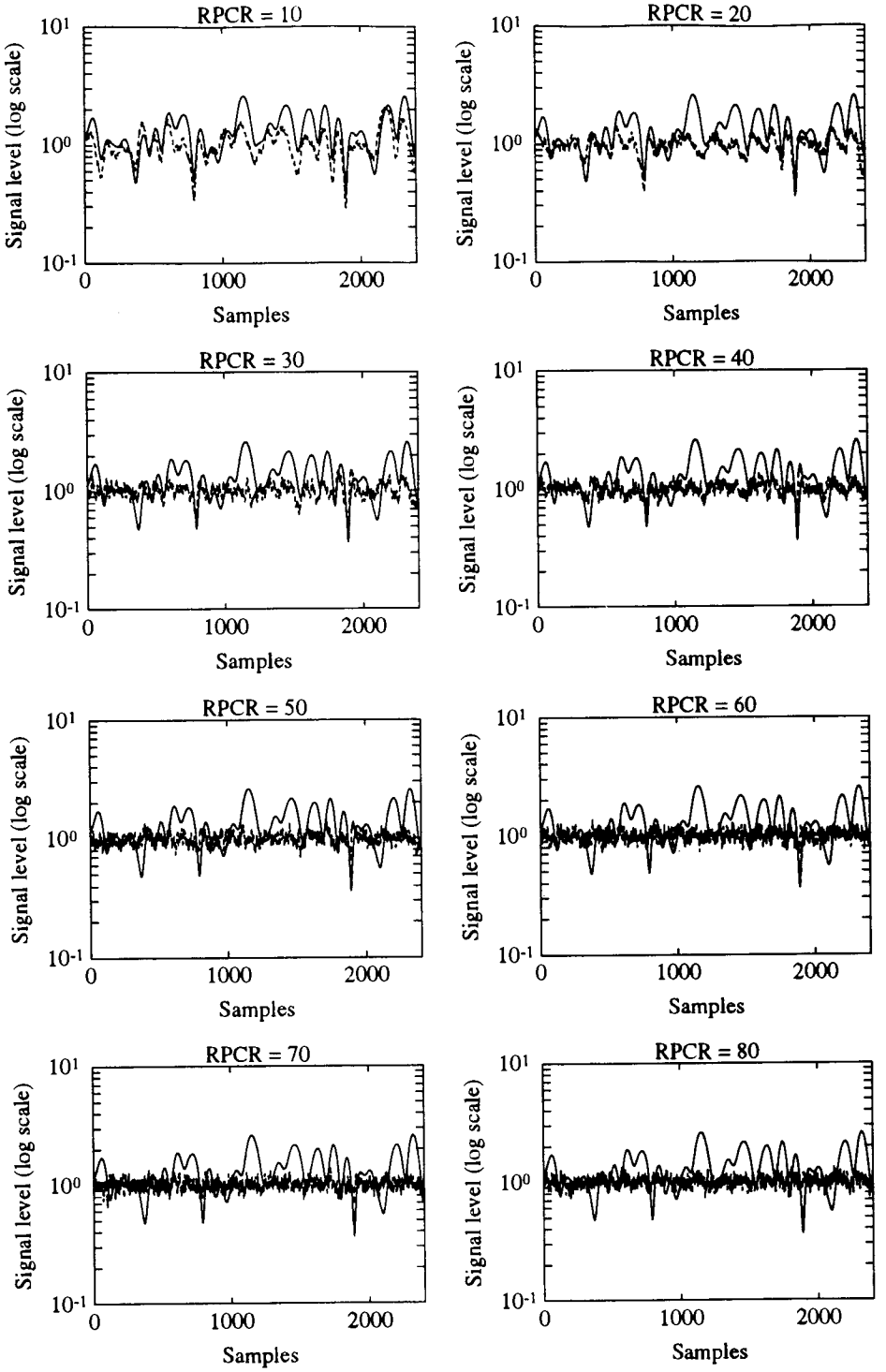

Figure 5.3: Open Loop Power Control Simulation for 20dB.

5.4 Simulation Results of Acquisition Schemes on a AWGN channel

We have demonstrated in the previous section that power control can help to eliminate fading effects, and in the best case, the channel becomes AWGN. However, using open-loop power control to convert a fading channel to a AWGN one will be impractical in real situation because of the followings:

1. The overhead in synchronization channel will be too great because high synchronization symbol rate is needed.

2. Even though the synchronization overhead can be neglected and we send continuous synchronization bits as desired (we pay the price of overhead), the noise component will make channel estimation unreliable. The situation will get worse as the SNR becomes lower (more users in the system).

3. The mobile receives a synchronization bit from the base $T_{propagation}$ after transmission, where $T_{propagation}$ is the one-way propagation delay between the mobile and the base station. If channel is highly dynamic, its characteristics may have changed already after $T_{propagation}$, when the power control command is actually issued by the mobile[2].

Due to the shortcomings mentioned above, it will be highly difficult to obtain a AWGN channel. Instead, we will obtain a channel with characteristics in between a AWGN one and a frequency selective fading channel. We will present some simulation results on a AWGN channel, assuming that perfect power control is capable to eliminate all the fading effects. The significance of the simulation results will be to confirm the effectiveness of our proposed algorithms. We have demonstrated in the last two chapters that our schemes are superior than the conventional ones under a frequency selective fading channel which is one extreme without power control. If we also show that our proposed schemes are better in perfect power control, that is, a

[2]This issue may present no problem when the cell size is comparatively small.

AWGN channel, then it is reasonable conclude that our proposed methods are better in any real situation since the real situation is somewhere in between a fading and a AWGN channel. We believe that demonstrating the two extremes will be better than performing simulations on various values of RPCR because it is simply impossible to cover all the range of RPCR possible in real lives.

Table 5.1 gives a comparison of various acquisition schemes under a AWGN channel. All the results show that our methods are better than the conventional ones.

SNR	Coincidence Detector	Search I	Search II	On-Off	Barker
10dB	~ 0	~ 0	~ 0	0.0323	~ 0
15dB	0.1292	0.2847	0.3229	0.9840	0.9147
20dB	0.9984	0.9990	0.9990	1.0000	1.0000

Table 5.1: Simulation Results of Various Acquisition Schemes in a AWGN Channel.

Compared with the results for a fading channel, as shown in table 5.2, we can ob-

SNR	Coincidence Detector	Search I	Search II	On-Off	Barker
10dB	0.1038	0.1602	0.1707	0.4602	0.3147
15dB	0.6008	0.6669	0.6827	0.8361	0.7733
20dB	0.8797	0.8977	0.8970	0.9549	0.9420

Table 5.2: Simulation Results of Various Acquisition Schemes in a Frequency Selective Fading Channel.

serve one interesting feature: when SNR is low, the performance of various acquisition methods (proposed and the conventional ones) are better in the fading channel than in a AWGN channel. This contradicts common belief as fading is always considered as an impairment on channel performance.

To understand the phenomena, we will look at the situation when SNR is 10 dB, and the case for square law detector. The SNR is defined as $10\log(\frac{A^2}{\sigma^2})$, where A is the carrier magnitude and σ^2 is the variance of white Gaussian noise. Lets normalize the variance σ^2 to be 1. For the SNR of 10dB, we have $A^2 = 10$. By selecting the largest

five of the RAKE receiver, we have a Gamma distribution. Suppose we set a false alarm rate of 10^{-6}, we need to set the threshold at a value of $17.94 \times \sigma^2 = 17.94$, which is already higher than the value of A^2. Therefore, the only possible threshold crossing is by the effect of noise. In fact, when there is no noise, the acquisition probability will be 0. This explains why we get very low values for the case of 10dB. In a fading channel, the output magnitude still has a mean value of $\bar{g^2}\bar{A^2} = 10$, where g^2 is the fading gain, but the distribution of g^2 is exponential and there is probability of it exceeding the value of 17.94. In other words, the fading process occasionally raises the square magnitude and makes the chance of threshold crossing higher. For high SNR, for example 20dB, all acquisition schemes show better performance than the corresponding frequency selective fading channel, as expected.

5.5 Conclusions

In this chapter, we have demonstrated that during the preamble section, only open loop power control is possible, which requires the base station to send synchronization bits constantly for channel estimation purpose. A high synchronization bit rate has high overhead, while a low synchronization bit rate makes channel estimation inaccurate. A compromise is necessary.

Because of the limit in synchronization symbol rate and other open-loop power control imperfections, we have channel characteristics in between a AWGN and a fading channel. By also demonstrating our proposed methods' superior performance over other conventional schemes in a AWGN channel, we draw the conclusion that our proposed method is better in any real situation.

Chapter 6

Conclusions and Future Research

Code Division Multiple Access (CDMA) is a modulation and channel sharing technique which relies on spread spectrum communication. CDMA is a promising technology for future digital cellular and personal communications because of some of its nice features such as: (1) anti-multipath, (2) higher system capacity than TDMA and FDMA, and (3) its flexibility in providing bandwidth on demand. When spread spectrum techniques are utilized, we multiply the data by a pseudorandom noise sequence before transmission so that the power spectrum of the original signal is spreaded to an extent to be hidden under AWGN. At the receiver, the incoming signal is multiplied with a local replica of the PN code which is in synchronization. The synchronization is usually performed in two stages: *acquisition* and *tracking*. The former aims to find a coarse alignment while the latter fine adjusts the phase.

In the thesis, we have considered the PN code acquisition problem under a packet radio system. The packet radio system poses a slightly different situation from traditional spread spectrum communication. In packet radio, there exists a fixed number of bits as the preamble for acquisition. If we cannot achieve acquisition during the preamble section, the corresponding packet will be lost. The price will be either loss of information (eg. video or speech) or a retransmission (eg. file transfer).

Particularly, we propose two new acquisition algorithms: the *on-off keying assisted acquisition scheme* and the *Barker sequence with DPSK acquisition scheme.*

The on-off keying assisted scheme uses an on-off pattern superimposed on the preamble with a Markov search algorithm. Since an on-off pattern is used, we can double the power during the "on" stage while still maintaining the same average power. The advantages are several: first, the double power of the "on" stage makes it more resistant to fading; second, the "off" bit, which consists of noise only, is not subject to any fading; third, we have an extra freedom to set the threshold for the "off" stage.

For the other proposed method, we use a Barker sequence of length 7 as our preamble section and DPSK as the modulation scheme. DPSK is in contrast to energy detection in which we cannot distinguish between a bit 1 or -1. This distinctive characteristic makes decoding the Barker sequence possible. The mechanism involves two levels of correlation, one for the PN code and the other for the Barker sequence. The beauty of this method is that we can achieve both PN code and frame synchronization at the same time.

Because of the fixed preamble nature of a packet radio system. We believe that the acquisition time performance criterion used by many previous researchers is not appropriate. Instead, we adopt the *packet throughput* as our performance measure. With this scenario, the best acquisition method is the one that gives the highest throughput. The throughput consideration also directs us to use a different criterion of setting the threshold, a *fixed blocking probability.* The blocking probability takes into account of various possible busy time encountered by the receiver during the Markov search and is therefore more appropriate[1].

In PN code acquisition, we are facing an abrupt change from silence to having a signal. The partial correlation so generated has a great impact on various algorithms and may cause incorrect acquisition. For our simulation studies, we introduce a windowing technique which we found effective to combat the partial correlation effect.

[1] Although not presented in the thesis, our methods also perform better when a CFAR criterion is used.

We have compared our proposed methods with some existing ones under a two-ray and a three-way frequency selective fading channel. Simulation studies show that our proposed scheme is superior than the others for a wide range of SNR, and also various power distribution among the two rays. Another channel model we have investigated is an AWGN channel. Again, our proposed schemes are better. The AWGN and the frequency selective fading channel are considered as two extremes. In real situations, we will use open-loop power control for the preamble section[2], and because of imperfections of power control, we will end up with channel characteristics in between the extremes. By proving that our systems are better for both extremes, it is possible to conclude that our schemes are superior in real situations. Proving the extremes is more favorable because it is simply impossible to simulate all possible real situations.

It is discovered that the partial correlation effect is more prominent for the Barker sequence method, especially when the SNR is high. When we set the threshold, we need to use the distribution of RAKE receiver output, which is Gaussian for the Barker sequence method, but Gamma for the on-off keying scheme. Given the same false alarm rate, the threshold set for the Barker sequence method will be lower (Gamma vs. Gaussian distribution) which is not possible to cover up the partial correlation. The partial correlation poses a limit on the maximum SNR the Barker sequence method can operate satisfactorily. Therefore, we do not recommend the Barker sequence method for very high SNR, for example > 25dB[3].

Our simulation results have shown that the throughput will not be over 0.8 unless we have a SNR of 20dB. Therefore, we propose to encode the preamble section with a higher SNR than that of the data section in order to achieve good performance, for example, uses 20dB for preamble but 7dB for the data. This results in increased interference to other users temporarily during acquisition. However, since acquisition occurs occasionally, it will be acceptable. Another issue is the packet data length. The preamble is used for synchronization purpose and it does not convey any useful

[2]We have argued that open-loop power control is only one possible during preamble, refer to Chapter 5 for details.

[3]This may not be a problem in real situation because we won't use such a high value of SNR at all!

data information. Therefore, the shorter the preamble, the better the efficiency. In the next generation wireless network, we will have mixed traffic with variable data packet size. For the shorter packets, we will use a shorter preamble (lower overhead), but with a higher preamble SNR, while for the longer data packets, we will use a longer preamble with a lower SNR to reduce interference to other users.

6.1 Discussion

The effect of missing a preamble is not addressed in our study. When a data packet arrives and our system fails to synchronize the preamble section, the algorithm will continuously search through the data portion to declare synchronization which may not be desirable. One method to overcome the difficulty is to use two different PN codes for the preamble and the data respectively. In this way, data in a missed packet will not interfere with the acquisition algorithm.

Under the CDMA approach, we ideally distinguish one user from another by assigning a different code to each to them. When the number of users increases, we will require an increasing number of orthogonal PN codes. The maximum number of orthogonal PN codes, however, is limited. The restriction in orthogonal PN codes availability affects the high level design. We have no choice but to use the same code for different users. When the number of users is small, we may simply allow each of them to start transmission at any time because the probability of collision is low.

However, when the number of users is large, the collision probability will become high and we may need some form of time-division multiplexing in order to distinguish users employing the same PN code. Each user needs to know when to start transmission, for example, by a fixed time t_{start} after its reception of the synchronization symbol. Every two users must be separated by a time gap which equals one delay spread plus maximum propagation delay uncertainty. Each user must listen to find an empty slot and transmit. Collision may occur and a form of collision detection is necessary. The scheme becomes similar to the carrier sense multiple access (CSMA)

in an ethernet network, and very careful planning is necessary. In the above, we have outlined two alternatives in simplified forms, and we must stress that there are many problems that have to be solved. The high-level design is so complex that there is a great number of alternatives possible. Of course, the ideal situation will still be able to find one orthogonal PN code for each user. The ideal situation may not be impossible at all because of the advance in VLSI which makes very long PN code possible (A set of longer PN code will contain a larger subset of orthogonal PN codes).

In the extreme, we will have a highly synchronized system where the base station is responsible for all the timing jobs, like the spread spectrum slotted ALOHA system proposed by some researchers [45, 46].

We state that we can obtain frame synchronization in the encoded Barker sequence method. Actually, some form of frame synchronization is also possible in the on-off keying method by detecting the end of the on-off pattern. A simple strategy will be two (or three) consecutive threshold crossings by signals. We have not addressed this issue for which we believe that will be investigations in the future.

6.2 Future Research

The acquisition system is a portion of the whole packet radio system based on CDMA. As we have seen in chapter 2, various number of techniques exist for the acquisition problem. It would be possible to superimpose other techniques such as the variable dwell or sequential detection on our proposed systems.

Moreover, we have assumed a two-ray/three-ray frequency selective channel with fixed power distribution among the rays. Future research may add the considerations: real-time variation in power distribution among the rays; the time gap between two rays is changing with time. All in all, we may consider a highly dynamic channel in the future.

Another area of interest will be the interaction between our low-level acquisition

problem with the high-level design. A specific high-level design may make a particular acquisition algorithm favorable over the others.

Appendix A

Expected Busy Time Expression

In this appendix, we will demonstrate how can we simplify the expression for the expected busy time in the on-off keying acquisition scheme. Similar techniques can be applied to the coincidence detector, or the search strategies. The expression for the expected busy time is given by

$$\bar{B} = \left\{ P_{fa}[(L-1)+L_D] + (1-P_{fa}) \left[\frac{\sum_{j=1}^{(L-1)/2} P_{01}P_{00}[(1-P_{00})(1-P_{01})]^{j-1} \cdot (2j-1)}{\sum_{j=1}^{(L-1)/2} P_{01}P_{00}[(1-P_{00})(1-P_{01})]^{j-1}} \right] \right\} \times T, \tag{A.1}$$

Consider the expression

$$\left[\frac{\sum_{j=1}^{(L-1)/2} P_{01}P_{00}[(1-P_{00})(1-P_{01})]^{j-1} \cdot (2j-1)}{\sum_{j=1}^{(L-1)/2} P_{01}P_{00}[(1-P_{00})(1-P_{01})]^{j-1}} \right]. \tag{A.2}$$

By eliminating the common factor of $P_{01}P_{00}$, the expression becomes

$$\left[\frac{\sum_{j=1}^{(L-1)/2} [(1-P_{00})(1-P_{01})]^{j-1} \cdot (2j-1)}{\sum_{j=1}^{(L-1)/2} [(1-P_{00})(1-P_{01})]^{j-1}} \right]. \tag{A.3}$$

We will look at the denominator first,

$$\sum_{j=1}^{(L-1)/2} [(1-P_{00})(1-P_{01})]^{j-1} = \sum_{j-1}^{(L-1)/2} x^{j-1} \text{ by letting } x = (1-P_{00})(1-P_{01})$$

$$= \sum_{j=0}^{\frac{L-1}{2}-1} x^j$$
$$= \frac{1-x^{(L-1)/2}}{1-x}, \tag{A.4}$$

with the application of the series equation

$$\sum_{j=0}^{j=n} x^j = 1 + x + 2x + \cdots x^n = \frac{1-x^{n+1}}{1-x}.$$

The numerator, on the other hand, is given by

$$\begin{aligned}\sum_{j=1}^{(L-1)/2} [(1-P_{00})(1-P_{01})]^{j-1}(2j-1) &= \sum_{j=1}^{(L-1)/2} x^{j-1}(2j-1) \\ &= \sum_{j=0}^{\frac{L-1}{2}-1} x^j(2j+1) \\ &= 2x \sum_{j=1}^{\frac{L-1}{2}-1} jx^{j-1} + \sum_{j=0}^{\frac{L-1}{2}-1} x^j \end{aligned} \tag{A.5}$$

By differentiating the series expression shown above, we have

$$\begin{aligned}\sum_{j=1}^{j=n} jx^{j-1} &= 1 + 2x + \cdots + nx^{n-1} \\ &= \frac{(1-x^{n+1}) - (n+1)x^n(1-x)}{(1-x)^2}\end{aligned}$$

Putting the above expression into equation (A.5), we obtain

$$\begin{aligned}\sum_{j=1}^{(L-1)/2} [(1-P_{00})(1-P_{01})]^{j-1}(2j-1) &= 2x\frac{(1-x^{\frac{L-1}{2}}) - \frac{L-1}{2}x^{(\frac{L-1}{2}-1)}(1-x)}{(1-x)^2} + \frac{1-x^{\frac{L-1}{2}}}{1-x} \\ &= \frac{2x(1-x^{\frac{L-1}{2}})}{(1-x)^2} - \frac{(L-1)x^{\frac{L-1}{2}}}{1-x} + \frac{1-x^{\frac{L-1}{2}}}{1-x}. \end{aligned} \tag{A.6}$$

Dividing the numerator by the denominator, we have

$$\left[\frac{\sum_{j=1}^{(L-1)/2}[(1-P_{00})(1-P_{01})]^{j-1} \cdot (2j-1)}{\sum_{j=1}^{(L-1)/2}[(1-P_{00})(1-P_{01})]^{j-1}}\right] = 1 + \frac{2x}{1-x} - \frac{(L-1)x^{\frac{L-2}{2}}}{1-x^{\frac{L-1}{2}}},$$

which can be substituted into equation (A.1) to get the final expresion for $\bar{B}$,

$$\bar{B} = \left\{P_{fa}[(L-1)+L_D] + (1-P_{fa})\left[1 + \frac{2x}{1-x} - \frac{(L-1)x^{\frac{L-1}{2}}}{1-x^{\frac{L-1}{2}}}\right]\right\} \times T. \tag{A.7}$$

REFERENCES

[1] *An Overview of The Application of Code Division Multiple Access (CDMA) to Digital Cellular Systems and Personal Cellular Networks*, Qualcomm, May 1992.

[2] J. G. Proakis, *Digital Communications*, 2nd edition, McGill Hill, 1989.

[3] *PA-100 Spread Spectrum Demodulator Product Information*, UNISYS.

[4] G. M. Comparetto, "A Generalized Analysis for a Dual Threshold Sequential Detection PN Acquisition Receiver", *IEEE Transactions on Communications*, Vol. COM-35, No. 9, pp. 956-960, September 1987.

[5] Y. H. Lee, S. Tantarantana, "Sequential Acquisition of PN Sequences for DS/SS Communications: Design and Performance", *IEEE Journal on Selected Areas in Communications*, Vol. 10, No. 4, pp.750-759, May 1992.

[6] R. B. Ward, *Sequential Analysis*, New York: John Wileyym 1947.

[7] R. B. Ward, "Acquisition of Pseudonoise Signals by Sequential Estimation", *IEEE Transactions on Communications*, COM-13, pp.475-483, December 1965.

[8] A. J. Viterbi, "Spread Spectrum Communications - Myths And Realities", *IEEE Communications Magazine*, May 1979.

[9] R. L. Pickholtz, D. L. Schilling, L. B. Milstein, "Theory of Spread-Spectrum Communications - A Tutorial", *IEEE Transactions on Communications*, Vol. COM-30, No. 5, May 1982.

[10] W. C. Y. Lee, "Overview of Cellular CDMA", *IEEE Transactions on Vehicular Technology*, Vol. 40, No.2, May 1991.

[11] K. S. Gilhousen, I. M. Jacobs, R. Padovani, *el at.*, "On the Capacity of a Cellular CDMA System", *IEEE Transactions on Vehicular Technology*, Vol. 40, No. 2, May 1991.

[12] M. K. Simon, J. K. Omura, R. A. Scholtz, B. K. Levitt, *Spread Spectrum Communications Vol. III*, Computer Science Press Inc., 1985.

[13] P. Lafrance, *Fundamental Concepts in Communication*, Prentice Hall, Englewood Cliffs, New Jersey, 1990.

[14] A. Polydoros, C. L. Weber, "A Unified Approach to Serial Search Spread-Spectrum Code Acquisition - Part I: General Theory", *IEEE Transactions on Communications*, Vol. COM-32, pp.542-549, May 1984.

[15] A. Polydoros, C. L. Weber, "A Unified Approach to Serial Search Spread-Spectrum Code Acquisition - Part II: A Matched-Filter Receiver", *IEEE Transactions on Communications*, Vol. COM-32, pp.550-560, May 1984.

[16] E. Sourour, S. C. Gupta, "Direct-Sequence Spread Spectrum Parallel Acquisition in Nonselective and Frequency-Selective Rician Fading Channels", *IEEE Transactions on Communications*, Vol. 10, pp.535-544, April 1992.

[17] E. Sourour, S. C. Gupta, "Direct-Sequence Spread Spectrum Parallel Acquisition in Fading Mobile Channel", *IEEE Journal on Selected Areas in Communications*, Vol. 38, pp.992-998, July 1990.

[18] P. M. Hopkins, "A Unified Analysis of Pseudonoise Synchronization by Envelope Correlation", *IEEE Transactions on Communications*, Vol. COM-25, pp.770-778, August 1977.

[19] S. M. Pan, D. E. Dodds, S. Kumar, "Acquisition Time Distribution for Spread-Spectrum Receivers", *IEEE Journal on Selected Areas in Communications*, Vol. 8, pp.800-807, June 1990.

[20] J. K. Holmes, C. C. Chen, "Acquisition Time Performance of PN Spread-Spectrum Systems", *IEEE Transactions on Communications*, Vol. COM-25, August 1977.

[21] Y. T. Su, "Rapid Code Acquisition Algorithms Employing PN Matched Filters", *IEEE Transactions on Communications*, Vol.36, June 1988.

[22] L. B. Milstein, J. Gevargiz, P. K. Das, "Rapid Acquisition for Direct Sequence Spread-Spectrum Communications Using Parallel SAW Convolvers", *IEEE Transactions on Communications*, Vol. COM-33, July 1985.

[23] P. F. Driessen, Z. L. Shi, "A New Rapid Acquisition Scheme For Burst Mode DS Spread Spectrum Packet Radio", *MILCOM 91' Proceedings*, pp. 809-813.

[24] Z. L. Shi, P. F. Driessen, "Automatic Threshold Control For Acquisition in Spread Spectrum Packet Radio Communication", *1993*, pp. 478-482.

[25] F. E. Nathanson, *Radar Design Principles*, Sec. Edi., McGraw Hill Inc., 1990.

[26] C. R. Barrett, "Adaptive Thresholding And Automatic Detection", *Chapter 12, Principles of Modern Radar*, Van Nostradn Reinhold Company, New York, 1987.

[27] W. C. Y. Lee, *Mobile Communications Engineering*, New York: McGril Hill, 1982.

[28] A. D. Whalen, *Detection of Signals in Noise*, Academic Press, 1971.

[29] G. L. Turin, "Introduction to Spread-Spectrum Antimultipath Techniques and Their Application to Urban Digital Radio", *Proceedings of the IEEE*, Vol. 68, No. 3, March 1980, 328-352.

[30] U. Grob, A. L. Welti, E. Zollinger, R. Kung, H. Kaufmann, "Microcellular DS/SS Radio System Using N-Path RAKE Receiver", *IEEE Journal on Selected Areas in Communications*, Vol. 8, No. 5, June 1990, pp. 772-779.

[31] C. C. Huang, "Computer Simulation of a DS/SS Cellular Radio Architecture", *IEEE Transactions on Vehicular Technology*, Vol. 41, No. 4, November 1992, pp. 544-550.

[32] T. Chan, P. Ho, "Bit-Error Probability of Uncoded QPSK Transmitted Over a 2-Ray Frequency Selective Rayleigh Fading Channel", *ICC 92' Proceedings*, Vol. 1, pp.311-315.

[33] S. S. Rappaport, D. M. Grieco, "Spread-Spectrum Signal Acquisition: Methods and Technology", *IEEE Communications Magazine*, June 1984.

[34] L. B. Milstein, D. L. Schilling, "Performance of a Spread Spectrum Communication System Operating Over a Frequency-Selective Fading Channel in the Presence of Tone Interference", *IEEE Transactions on Communications*, January 1982, pp. 240-247.

[35] S. S. Rappaport, D. L. Schilling, "A Two-Level Coarse Code Acquisitio Scheme for Spread Spectrum Radio", *IEEE Transactions on Communications*, September 1980, pp. 1734-1742.

[36] A. R. Hambley, *An Introduction to Communication.*

[37] Wiggert, *Codes for Error Control and Synchronization*, Artech House Inc., 1988.

[38] R. M. Balston, R. C. V. Macario, *Cellular Radio Systems*, Artech House, 1993.

[39] S. Ariyavisitakul, I. F. Chang, "Signal and Interference Statistics of a CDMA System with Feedback Power Control", *IEEE Transaction on Communications*, Vol.41, No. 11, pp. 1626-1634, November 1993.

[40] R. L. Pickholtz, L. B. Milstein, D. L. Schilling, "Spread Spectrum for Mobile Communications", *IEEE Transaction on Vehicular Technology*, Vol.40, No. 2, pp.313-321, May 1991.

[41] G. R. Cooper, C. D. Mcgillen, *Modern Communciations and Spread Spectrum*, McGraw-Hill Book Company, 1986.

[42] P. M. Hopkins, "A Unified Analysis of Pseudonoise Synchronization by Envelope Correlation"m *IEEE Transaction on Communications*, COM-25, pp. 770-777, August 1977.

[43] S. Soliman, C. Wheatley, R. Padovani, "CDMA Reverse Link Open Loop Power Control", GlobeComm 92' Proceedings, Vol. 1, pp.69-73.

[44] W. F. Bodtmann, H. W. Arnold, "Fade-Duration of a Rayleigh-Distributed Wave", *IEEE Transactions on Communications*, Vol. COM-30, No. 3, pp. 549-553, March 1982.

[45] R. K. Morrow, J. S. Lehnert, "Packet Throughput in Slotted ALOHA DS/SSMA Radio Systems with Random Signature Sequences", *IEEE Transactions on Communications*, Vol.40, No. 7, pp.1223-1229, July 1992.

[46] R. Prasad, C. A. F. J. Wijffels, "Performance Analysis of a Slotted CDMA System for Indoor Wireless Communication Using a Markov Chain Model", pp.1953-1957, *Globecom 91' Proceedings.*

[47] W. Krzymien, P. Mermelstein, "A Rapid Initial Synchronization Algorithm for CDMA Microcellular Systems", *The Sixth Interference Conference on Wireless Communications, Calgary*, 1994.